Complex Stress States In Structural Birch Plywood

An experimental study on the behaviour of birch plywood in structural applications

Patrik Hedlund

Pontus Persson

Master Thesis

Stockholm, August, 2021

KTH Royal Institute of Technology
School of Architecture and the Built Environment
Department of Civil and Architectural
Engineering Division of Building Materials
SE-100 44 Stockholm, Sweden
TRITA-ABE-MBT-21630

Abstract

For structural engineers, the two most important design criteria are utility and safety. It is about making sure that a structural component is reliable enough not to endanger any of a building's users, while at the same time being as sustainable and efficiently designed as possible. In other words, an element must be safe enough to withstand the improbability and sufficiently cheap to be relevant for the design. Considering this, using a material such as wood instead of metal may prove to be a sustainable alternative for certain building components.

Timber can be designed to sustain high temperatures and fire; it has a high strength relative to its weight and is naturally produced. Furthermore, an engineered wood product such as birch plywood has proven very strong in structural applications, especially when glued. Therefore, birch plywood has great potential as a reliable material in structural components. In this work, a total of 24 specimens with birch plywood connections were tested experimentally.

The specimens were designed to enforce stress states that would occur in actual trusses. Additionally, Specimens were assembled with two different connection methods, one being a dowel-type connection and the other being a glued-type. Each type of connection was tested in both tension and compression, with a total of three repetitions each. For the glued-type specimens, birch plywood plates were investigated in three different angles to the face grain; 0°, 5° and 15°. The load-displacement relationships and the failure modes are of specific interest in this thesis.

Test results showed that failure modes were semi-brittle and distinct, and the tests showed that glued-type connections withstood 37% higher loads than dowelled types. Specimens might withstand even higher loads if gluing were performed in a more controlled environment. The load-to-face-grain angle of plywood also had a significant impact on the capacity of connections. For the 0°-specimens with glued connections tested in compression, no failures occurred in the plywood, and tests reached loads as high as 82 kN. Calculations were made estimating the load capacity as high as 95 kN, but possibly a more realistic approximation would be 85 kN. This would imply that the 0°-specimens are around 20% stronger than the 15°-specimens and approximately 17,7% stronger than the 5°-specimens tested in compression. Birch plywood is promising to be used in connections of timber structures where plates transfer forces between structural elements.

Keywords: large-span-structures, trusses, truss nodes, timber connections, engineered wood products, birch plywood, glued connections, dowelled connections, gusset plates

Sammanfattning

För byggnadsingenjörer är de två viktigaste designkriterierna användbarhet och säkerhet. Det handlar om att se till att ett konstruktionselement är tillräckligt tillförlitlig för att inte äventyra någon utav byggnadens användare, samtidigt som den skall vara så hållbar och effektivt utformad som möjligt. Med andra ord måste den vara tillräckligt säker för att motstå det osannolika men också tillräckligt billig för att vara relevant för designen. Med tanke på detta kan användning av material såsom trä istället för stål visa sig vara ett hållbart alternativ i vissa bärande byggnadsdelar.

Trämaterial kan utformas för att motstå höga temperaturer och eld, samt det har en hög hållfasthet i förhållande till sin vikt och produceras naturligt. Vidare har en ingenjörs-designad träprodukt som till exempel björkplywood visat sig vara mycket starkt i bärande tillämpningar, särskilt om det limmas. Därmed kan just björkplywood ha stor potential som tillförlitligt material-alternativ i bärande byggnadsdelar. I detta arbete testades totalt 24 exemplar med anslutningar av björkplywood experimentellt.

Proverna utformades för att framtvinga spänningstillstånd som skulle uppstå i faktiska takstolar. Prover monterades ihop med två olika anslutningsmetoder, den ena var en anslutning av dymlingstyp och den andra var en av limmad typ. Varje typ av anslutning testades i både draglast och kompressionslast, med totalt tre repetitioner vardera. För limmade prover undersöktes björkplywoodskivor i tre olika relativa fiberriktningar; 0°, 5° och 15°. I denna avhandling var särskilt de olika brotts-typerna och förhållandena av intresse.

Testresultaten visade att brotten som uppstod var halv-spröda och tydliga, samt att infästningar av limmad typ klarade 37 % högre belastningar än dymlingstyper. Proverna kunde förmodligen motstå ännu högre belastningar om limning och montage även hade utförts i en mer kontrollerad miljö. Fiberriktningen hos plywood-skivorna visade sig också ha en betydande inverkan på bärförmågan. För limmade proverna med parallell fiberriktning (0°) i horisontalriktningen inträffade vid kompressions-test inga brott och testerna nådde en belastning så hög som 82 kN. Beräkningar gjordes för att uppskatta lastkapaciteten till så hög som 95 kN, men en mer realistisk uppskattning skulle möjligen vara 85 kN. Detta skulle innebära att 0°-proven var cirka 20 % starkare än de 15°-proven och cirka 17,7 % starkare än de 5°-prover som testats i kompression.

Björkplywood är ett lovande alternativ att användas i alla typer av bärande förband i träkonstruktioner där skivor används för att överföra krafter mellan bärande element.

Nyckelord: stora spännkonstruktioner, fackverk, fackverksnoder, träanslutningar, modifierade träprodukter, björkplywood, limmade anslutningar, dymlings-anslutningar, fästplattor

Preface

This master thesis was carried out between January and June 2021 at KTH Department of Civil and Architectural Engineering, Division of Building Materials, in Stockholm, Sweden. The construction and testing of the test specimens took place at KTH.

First off, we would like to express great gratitude towards supervisors Roberto Crocetti and Magnus Wålinder for providing their expertise on wood science and structural timber engineering and assisting us a great deal throughout the study.

We would also like to give thanks to all the companies who helped provide material for the testing. Moelven- for providing 25 glulam beams, Koskisen- for providing a batch of birch plywood boards, Rothoblaas- for providing fasteners, and Dynea for the supply of MUF glue.

Special thanks also to Lars Blomqvist at RISE-institute for providing knowledge and research-funding through the Kamprad Family Foundation. Great gratitude is also expressed towards p.h.d students Yue Wang and Tianxiang Wang for assisting us with their research on birch-plywood mechanical properties and extensive support and practical help throughout the project. Thanks to Victor Brolund for helping us with any practical issues at the KTH laboratory and workshops. Thanks also to Ronny Bredesen from Dynea for attending our meetings and providing his excellent expertise and technical support on the use of MUF glue. Thanks also to all of the representatives from Moelven SE and Moelven NO that have attended our meetings and provided their knowledge and expertise on their glulam products.

Stockholm, June 2021

Patrik Hedlund & Pontus Persson

Contents

List of figures

List of tables

List of symbols

A	Loaded surface area
b	width perpendicular shear
δ	Displacement
dA	Cross-sectional area
d	Screw diameter
E	Elastic modulus
ε	Strain
ε_{trans}	Transverse strain
ε_{axial}	Axial strain
F	Applied Force
F_M	Force caused by moment
f_t	Ultimate tensile strength
$f_{t.0}$	Tensile strength parallel to grain
$f_{t.90}$	Tensile strength perpendicular to grain
f_c	Ultimate compressive strength
$f_{c.0}$	Compressive strength parallel to grain
$f_{c.90}$	Compressive strength perpendicular to grain
f_v	Shear strength
G	Shear modulus
I_p	Polar moment of inertia
I_x	Area moment of Inertia
I_y	Moment of inertia
k	Stiffness
k_{ser}	Stiffness in serviceability state
k_u	Stiffness in ultimate limit state
L	Reference length
ΔL	Displacement
M	Moment acting on area

M_y	Moment around y axis
N	Axial force
r	Cross sectional coordinate
ρ_m	Mean density
$\rho_{m.1}$	Mean density of material 1
$\rho_{m.1}$	Mean density of material 2
S	Statical moment of inertia
S_{sr}	Statical moment of Inertia
σ_x	Stress in axial direction
τ_{xz}	Shear stress in plane
τ_M	Shear stress in plane
V_Z	Shear force in shear plane
v	Poisson's ratio
W_p	Polar bending resistance
x, y	Local coordinates
y	Cross sectional coordinate
z	Distance from rotational center

List of acronyms

CO2	Carbon-dioxide
EWP	Engineered Wood Product
FEA	Finite-Element Analysis
FEM	Finite-Element Method
GLULAM	Glued-Laminated
IEA	International Energy Agency
KTH	Kungliga Tekniska Högskolan, Royal institute of technology
MUF	Melamine-Urea-Formaldehyde
PF	Phenol-Formaldehyde

1 Introduction

1.1 Background

The amount of energy needed for producing different materials in the construction industry varies by a significant amount. Most common building materials require a high amount of energy to be produced, while at the same time, they also contribute to the release of greenhouse gases into the atmosphere. According to the IEA, the direct CO2 intensity of the steel sector in 2019 was 1.4 tonnes of CO2 per produced tonne steel (IEA, 2020a). Furthermore, as of 2018, cement production contributed 0,54 tonnes of CO2 per produced tonne of cement (IEA, 2020b).

With the ongoing climate change, more and more designers are surveying new ways of constructing buildings using different, more sustainable materials. Modern technology has provided us with several alternative solutions for applications where materials such as concrete and steel have traditionally been used; contrary to concrete and steel, timber materials store around 1,8 tonnes of CO2 per tonne solid mass through its lifetime (Svenskt Trä, 2015).

When designing buildings, the most crucial aspect of the design is a reliable frame system that carries the weight of the building and is strong enough not to endanger any of the users inside. An effective building frame should allow for minimum material usage while controlling the path forces such as weight or wind are transferred safely, all the way from the top of the building down to the ground foundation. A frame system of this type naturally contains many connecting nodes or joints, where forces from several directions are transferred simultaneously. The requirements in such places are higher than in the rest of the building, requiring a higher component quality. Traditionally, steel has been a commonly used material in such joints, often in the form of welded or bolted plates. The reason for this is that steel has high strength. It is also relatively easy to design thanks to its isotropic properties. This report considers birch plywood as a choice of material in this kind of joint, especially timber-to-timber connections in timber structures.

Utilizing birch plywood as material in structural connections is an innovative and sustainable alternative to using steel plates. Birch timber is readily available in most northern countries, and the price is relatively not too high. Tests have indicated that birch plywood has almost twice the strength of ordinary construction lumber. Connecting timber members with plywood connections also have advantages in manufacturing, where steel plates, for example, often need high-precision pre-drilling, especially when holes need to be aligned among all connected timber members. When timber is used instead, more adjustments can occur at the specific building site, thanks to its workability. Another advantage of using more wood instead of steel is the weight saving. For example, in large-span structures, the own weight impacts its overall capacity as a load-bearing structure; using more or only timber could save much weight.

1.2 Objectives

The purpose of this study is to investigate the capacity of birch plywood as a choice of material in timber-to-timber connections. Traditionally, steel has been the most common connector in truss nodes and connections between large timber elements as slotted-in plates. Here birch plywood gusset plates are considered both in glued configurations as well as dowelled configurations.

- How can birch plywood products be used in structural applications?
- What possible solutions could birch plywood provide concerning fastening as well as the assembly?
- What is the s*trength* of birch plywood plates in structural connections subjected to complex stress states?
- What impact does the local load- contra grain- angle direction have on the structural *strength* of the connection?
- What effect does the choice of fastening have on the *structural behavior* of the connection?

1.3 Outline of the Thesis

The mechanical properties of birch plywood are investigated in a parallel, ongoing study at KTH (2020-2021). Research data is used to draw relevant conclusions concerning the strength of birch plywood properties. Experiments conducted in this study are meant to mimic the complex states that would occur in an actual truss while using the mechanical properties investigated. Test specimens are scaled down to a fitting size of the laboratory equipment available at the KTH facilities. Material for constructing test specimens is provided from established actors in the building materials industry, who have also attended meetings and provided technical support on their products throughout the work.

2 Theory

2.1 Materials

2.1.1 Wood

2.1.1.1 Anisotropy

Timber is orthotropic, which means it has different properties in different directions, contrary to steel, which is isotropic and has the same properties in every direction. Hence, defining the local axis system for every structural part when designing timber components is essential. In this report, we define the directions as in the following figure.

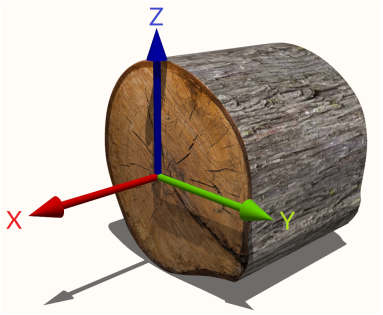

Figure 2.1. Coordinate system of wood

The x-axis runs along the grain, and both the x-axis and y-axis are located in their perpendicular plane. There is also a polar coordinate system to consider when studying the properties of timber. Direction parallel to grain is defined as a longitudinal axis, an axis perpendicular to the grain is defined as a radial direction, and the direction running along the radius of the timber as the tangential direction. The common practice of timber engineering considers the parallel to grain direction and the perpendicular to grain direction, for example, the characteristic compressive strength perpendicular to the grain, denoted as $f_{c.90.k}$.

We set the face-grain fiber direction parallel to the x-axis for plywood and the y axis perpendicular in the board plane. Thus, the angle to grain direction lies relative to the face-grain plane of the plywood.

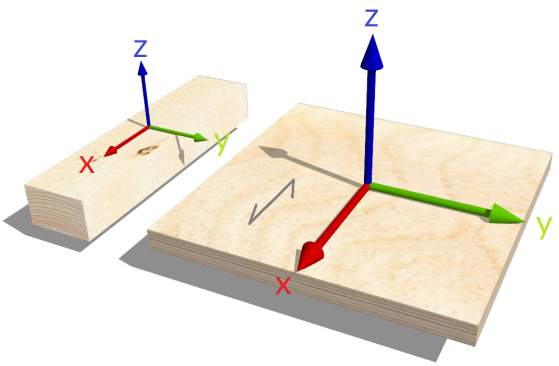

Figure 2.2. Local coordinate system of timber parts

2.1.1.2 Moisture and temperature

Due to its hygroscopicity, timber absorbs and releases water to its surroundings; it constantly adapts its properties depending on the surrounding conditions. The moisture stored in wood affects its properties on a micro-level, meaning pores and fibers behave differently depending on whether they are dry or not. To a certain extent, moisture absorbed by timber pores makes them more ductile and increases their volume. The moisture content of wood affects properties such as strength, density, and even hygroscopicity itself. Additionally, a timber material's ability to be glued or painted is dependent on its current moisture content. Thus, temperature and moisture play a key role in timber material behavior, especially concerning mechanical properties and applications (WoodProducts. 2021a.).

2.1.2.3 Softwoods and hardwoods

The most apparent difference between softwood and hardwood is the shape of its photosynthetic organs. Softwood is a conifer and has needles mostly all year round, while hardwood has leaves that fall off during colder seasons. However, the more structural difference between a hardwood and a softwood is the shape of its cellular structure. Hardwoods are slower growing and have a more dense cellular structure, making them more durable and robust. On the other hand, softwoods are faster-growing and more workable, such as cutting and drilling or fitting on a construction site.

2.1.2.4 Density

Generally, more dense wood is stronger; this is simply because of the compactness of its cellular structure. The longer distance from the marrow of the tree, the denser the timber gets, and therefore also stronger (Wood Products. 2021b).

2.1.2.4 Grading

Because wood is an organic material with living cells feeding on nature itself and dependent on naturally varying weather and surroundings, trees are as unique as any other individual in our nature. Even when we control its environments, making sure they are brought up right, with the right surroundings and conditions, they still come with many imperfections and variations that impact its properties. Imperfections such as knots, insect attacks, rot, cross grain and more influence the timber properties in a way that makes it a challenge to determine its strength (Smith, 2016). Most imperfections are distinguishable by just studying a species appearance, but some of the variations can also be determined by checking its weight or moisture content.

2.1.2 Engineered wood products

2.1.2.1 Melamine Urea Formaldehyde Resin

Formaldehyde is a widely used chemical compound in several different industries. It consists of hydrogen, oxygen, and carbon. Formaldehyde can be reacted with either phenol or urea to form thermosetting polymers such as Urea-Formaldehyde or Phenol-Formaldehyde, which are commonly used resins in composites. The adhesives provide increased strength, increased water and thermal resistance, and bond together engineered wood products such as plywood boards or glulam beams. Substituting or adding melamine to urea in urea-formaldehyde resins increases the moisture resisting properties further and seems to make the resin less susceptible to formaldehyde release (Conner, 2001).

Application with a string applicator is the most common method for bonding laminated beams, and the glue lines obtained are light-colored and will not darken over time. Moreover, they give water- and weather-proof bonds, conforming to Adhesive Type 1 of the European standards for adhesives for load-bearing timber structures (EN 301:2006) (Dynea, 2021).

2.1.2.2 Glulam

A common type of structural timber material is Glulam. Glulam is an engineered wood product that consists of laminated pieces of timber. Small rectangular pieces of timber are glued together with both the long shape and the grain direction parallel to the length of the tree. This lamination technique strengthens the tree and reduces the timber structural variations. The material is typically more robust than ordinary structural lumber because of the lamination effect. In practice, it dictates that the more a wood product is sawn up and reassembled, the stronger it gets, as long as the grain or fibers are oriented in a similar direction. The effect works by reducing the material's imperfections and controlling the orientation of local grain directions of each glued-together lamination.

2.1.2.3 Plywood

Plywood is a material made of cross-laminated timber veneers. The cross-lamination of timber veneers gives the material multiple valuable characteristics that can be utilized in timber connections. The lamination of the veneers increases the strength parallel to the member's direction and increases its stiffness (Wang et al., 2021).

The cross-lamination of veneers in plywood boards eliminates the natural cleavage plane that naturally exists in wooden boards perpendicular to the grain direction. Another favorable characteristic that is obtained by this is the increased shear strength for in plane loads.

2.2 Structural timber applications

2.2.1 Trusses

Trusses are made up of axially loaded chords connected in the shape of triangles. It consists of top-and-bottom chords connected with web members. The top chord often acts in compression and the bottom chord in tension, while the web members can vary in both tension and compression depending on the truss design.

Trusses can be made in many different shapes, depending on their usage. For example, parallel chord trusses can be compared to regular beams. They have higher material utilization as their design is engineered to place large proportions of the material at the edges, i.e., tension and compression zones. Thus, webs in I-beams have internal stresses resembling that of a truss.

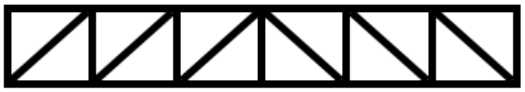

Figure 2.3. Parallel chord truss shape

If we focus on creating trusses that can span large distances, it is more common to see pitched trusses where the top and bottom chords are no longer mounted parallel to each other. When truss-shapes resemble bending moment diagrams, higher proportions of their loads are carried in each member's axial direction—often contributing to a more optimized structural system.

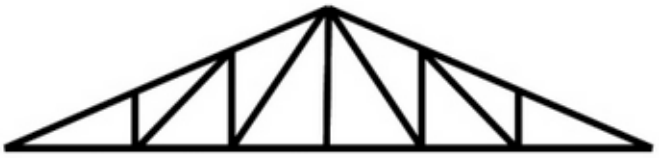

Figure 2.4. Pitched truss shape

A connection between members in a truss is called a node or joint and is usually calculated as freely rotating, meaning that they carry no bending moment. In reality, however, this is not usually the case; wooden connections are usually either glued or connected with plates and dowels/screws. As a result, these connections become rather stiff and can no longer be considered hinged joints because of the local eccentricities of the fastening. To minimize bending moments developed in such connections, it is recommended that the centerlines of all such members align; however, few actual joints can be considered purely ideally hinged like theoretical trusses.

2.2.1.1 Gusset plates

To connect members in a truss or corners in a frame, gusset plates are attached on the sides of the connecting members. They are either glued onto the adjacent surfaces of the connecting elements or attached with several fasteners in different patterns.

2.2.1.2 Examples of timber trusses

Because of the mechanical properties of timber, truss systems are exceptionally efficient to consider when designing large-span structures. Thanks to the relatively high strength-to-weight ratio, large spans are efficiently constructed without becoming too heavy. As early as the 18th century, members of the Swiss family Grubenmann developed timber bridge structures that allowed for vast spans, up to 67m. The system was designed with arch-frames alongside truss systems and allowed for high material efficiency. Unfortunately, many of their bridges were burnt or destroyed, and nowadays, only a few bridges that span up to 30 meters have survived.

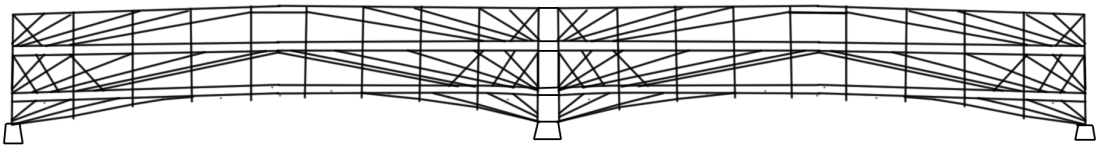

Figure 2.5. Truss/arch system of a Grubenmann Bridge

2.2.2 Truss proposal

The following truss geometry was proposed for a large-span timber structure spanning up to 60 meters. Because of erection and on-site assembly issues, the supports were designed as simple pin and roller support at each end. This would allow for a more safe and efficient assembly of the truss in its actual application.

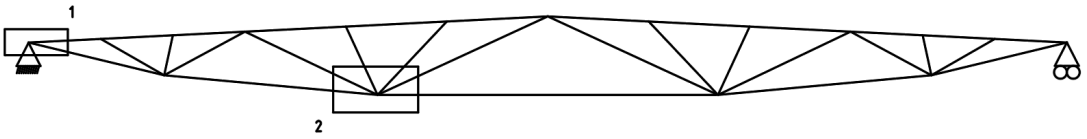

Figure 2.6. Truss system of a proposed large span timber structure

Especially at two nodes in this truss, critical load transferring connections could be designed with birch plywood plates in mind. If the truss were to be loaded with an evenly distributed load along its length, large axial forces would develop in these members. Consequently, complex stress states would develop wherever these axial forces are to be transferred in different directions.

2.2.2.1 Node 1

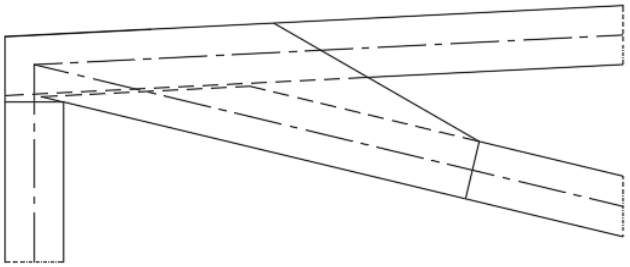

Figure 2.7. Node 1 in the proposed truss system, see figure 2.6

At node 1 the truss is pinned on a support that could represent any pillar or frame. The support would be designed to brace against lateral and horizontal displacements. High compressive axial forces would develop in the top member and tensile forces in the bottom member during loading.

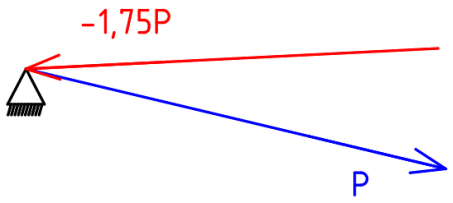

Figure 2.8. Axial forces transferred at node 1 in the proposed truss system

How these forces would be transferred in such a connection is the leading research topic for this thesis. The test specimens were designed with this proposed truss-geometry in mind.

2.2.2.2 *Node 2*

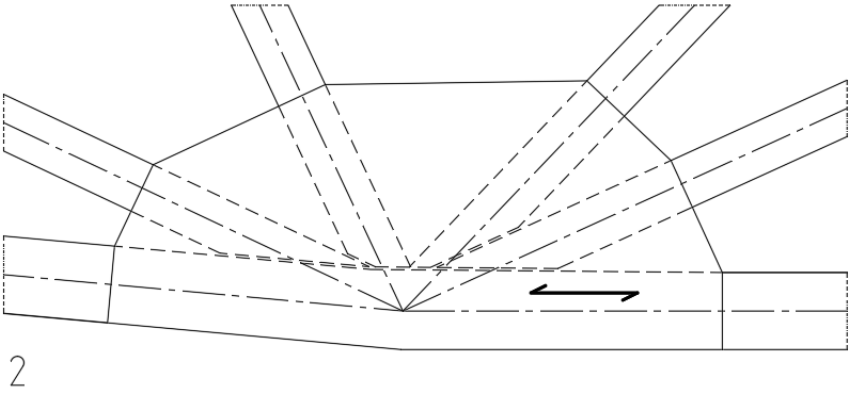

Figure 2.9. Node 2 in the proposed truss system, see figure 2.6

At node 2 in the proposed truss geometry high tensile forces would be transferred in the bottom members. Considering the direction of these forces relative to the face-grain of the plywood plates, a good design would be to consider orienting the face-grain parallel with the highest axial force of the truss node since the highest strength of plywood is along its face-grain direction.

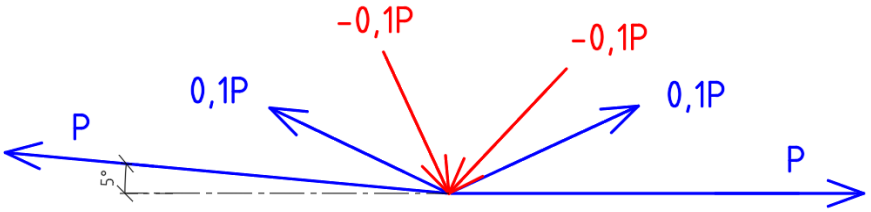

Figure 2.10. Axial forces transferred at node 2 in the proposed truss system

However, small angle-variations between the top two members at node 2 could occur, making it interesting to investigate what difference minor angle variations would make regarding the strength of the connection. Therefore the test specimens were constructed with minor variations in the plywood's face-grain angle to investigate the influence from angle variation (Wang et al., 2020).

2.2.3 Design proposal of truss node connection

A connection was proposed for a large span timber structure spanning up to sixty meters, with axial forces up to 1500 kN. The connection would feature birch plywood plates milled into the ends of groups of members, joined together with screws and glue, as shown in *Figure 2.11*. Groups of members would then be attached, adding up to a sufficient width of the truss node. In theory, this solution would be scalable to whatever load or design is needed.

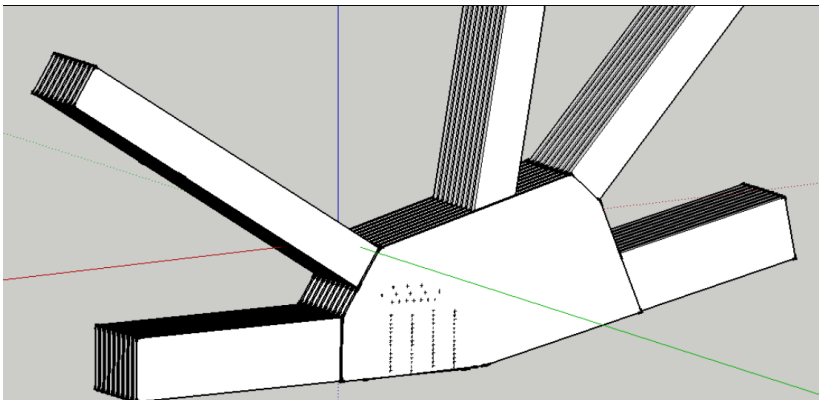

Figure 2.11. Birch plywood connection proposal

2.2.3.1 Assembly

Birch plywood plates with a thickness of 21 mm would be attached to pre-milled glulam beams with a thickness of 115 mm. Plates would be screw-glued with MUF glue and added together to increase the total thickness of joined beams. In *Figure 2.12* an example of this can be seen where a beam is created with a width of 460 mm.

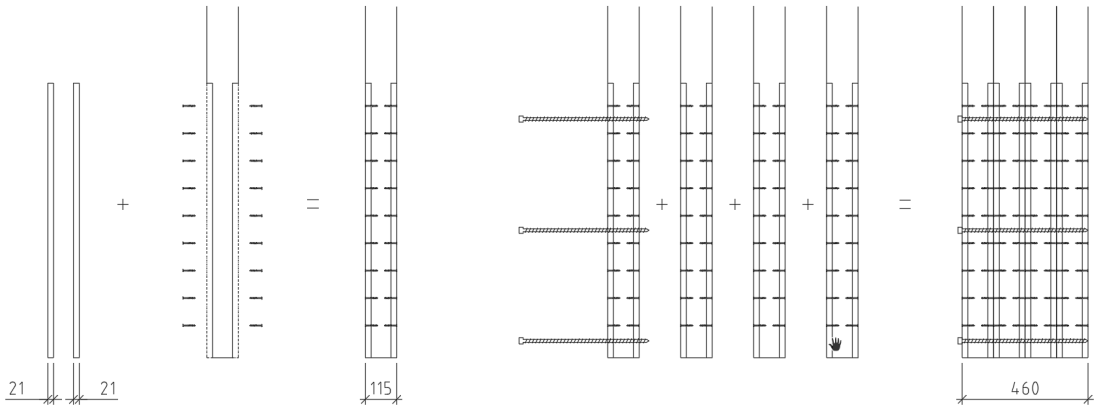

Figure 2.12. Assembly proposal of birch plywood connection

2.3 Computer software

Computer models were made to investigate the stress distributions in the proposed test specimen design.

2.3.1 AutoCAD

AutoCAD is computer-aided design software for computers that produce drawings and models in 2D and 3D environments. The workspace is based on units, and lines are drawn as vectors. In this project, the drawing line weights and patterns we used were based on a Swedish standard called Ritning Definition BH90 (SIS, 2021).

2.3.2 RFEM

The testing subject was modeled with finite elements in the FEA software Dlubal RFEM. RFEM is a 3d finite element analysis software. It can be used for the design of steel, concrete, and timber structures in structural analysis. The model used in this report features solid elements with orthotropic materials in 3D. The geometry and the mechanical properties were the same as the test specimens, and the corresponding load situations were also replicated.

2.4 Theoretical models

2.4.1 Formulas

2.4.1.1 Statistical tools

Mean

$$\bar{x} = \frac{x_1 + x_2 + \ldots + x_n}{n} = \frac{1}{n}\sum_{i=1}^{n} x_i \tag{1.1}$$

$\bar{x}$	Mean	-
x_1, x_2	Observations	-
n	Number of observations	-
x_i	Observation number i	-

Standard deviation

$$s^2 = \frac{1}{n-1}\sum_{i=1}^{n}\left(x_i - \bar{x}\right)^2 \tag{1.2}$$

s	Standard deviation	-
$\bar{x}$	Mean	-
x_1, x_2	Observations	-
n	Number of observations	-
x_i	Observation number i	-

2.4.1.2 Geometry

Area moment of Inertia

The second moment of inertia, also known as Area moment of Inertia, is used to predict deflection, bending and stresses in structural elements

$$I_x = \iint y^2 dxdy \tag{2.1}$$

I_x	Area moment of Inertia	mm^4
y	Cross sectional coordinate	mm

Polar moment of Inertia

A beam's ability to resist torsion which is required to calculate the twist of a beam subjected to torque

$$I_p = \iint r^2 dA = \iint x^2 + y^2 dxdy = I_{xx} + I_{yy} \tag{2.2}$$

I_x	Polar moment of Inertia	mm^4
r	Cross sectional coordinate	mm
dA	Cross-sectional area	mm^2

Polar bending resistance

$$W_p = \int r\, dA = \frac{I_p}{r} = \iint r\, dxdy \tag{2.3}$$

W_p	Polar bending resistance	mm^3
r	Cross sectional coordinate	mm
dA	Cross-sectional area	mm^2

Bolt pattern moment of inertia

$$S_{sr} = \sum \left({x_i}^2 + {y_i}^2 \right) \tag{2.4}$$

S_{sr}	Statical moment of Inertia	mm^2
x, y	Local coordinates	mm

Forces caused by moment

$$F_M = \frac{M \cdot r_i}{S_{sr}} \tag{2.5}$$

F_M	Force caused by moment	N
M	Moment acting on area	kNm
S_{sr}	Statical moment of Inertia	mm^2

2.4.1.3 Stress

Internal forces inside a structural part develop when it is subjected to external forces. Stresses develop on the planes on which these forces act

Stress caused by axial load

$$\sigma_x = \frac{N}{A} \tag{3.1}$$

σ_x	Stress in axial direction	N/mm^2
N	Axial force	N
A	Loaded surface area	mm^2

Stress caused by moment

$$\tau_M = \frac{M_y}{I_p} \cdot r \tag{3.2}$$

τ_M	Shear stress in plane	N/mm^2
M	Moment around y	kNm
r	dist. from center of stress surface	mm
I_p	Polar moment of inertia	mm^4

2.4.1.4 Elasticity

Elastic strain

Strain is a unitless relation between a target reference length and its displacement when subjected to a stress. It is most commonly described as

$$\varepsilon = \frac{\Delta L}{L} \tag{4.1}$$

ε	Strain	%
ΔL	Displacement	m
L	Reference length	m

Poisson's ratio

Poisson's ratio describes relative geometry change of a material, it usually lies between 0 and 0.5 and is in its simplest form dependent of compression in only one axis and one transverse direction

$$\upsilon = -\frac{d\varepsilon_{trans}}{d\varepsilon_{axial}} = -\frac{d\varepsilon_{y}}{d\varepsilon_{x}} = -\frac{d\varepsilon_{z}}{d\varepsilon_{x}} \tag{4.2}$$

v	Poisson's ratio	-
ε_{trans}	Transverse strain	%
ε_{axial}	Axial strain	%

Elastic modulus

The elastic modulus is defined as the stress divided by strain and basically represents the linear slope of a stress-strain curve. The expression is normally expressed as

$$E = \frac{\sigma}{\varepsilon} \tag{4.3}$$

E	Elastic modulus	MPa
σ	Stress	MPa
ε	Strain	%

Shear modulus

The shear modulus is the shear-deformation of a material when subjected to a force

$$G = \frac{\sigma_v}{\varepsilon_v} \tag{4.4}$$

G	Shear modulus	MPa
σ_v	Stress	MPa
ε_v	Strain	%

2.4.1.5 *Failure criterions*

1. Linear interaction equation

$$\frac{\sigma_x}{f_x} + \frac{\sigma_y}{f_y} + \frac{\tau_{xy}}{f_v} = 1 \tag{5.1}$$

2. Linear quadratic criterion

$$\left(\frac{\sigma_x}{f_x}\right)^2 + \left(\frac{\sigma_y}{f_y}\right)^2 + \left(\frac{\tau_{xy}}{f_v}\right)^2 = 1 \tag{5.2}$$

3. Invariant of Von Mises criterion

$$\left(\frac{\sigma_x}{f_x}\right)^2 + \left(\frac{\sigma_y}{f_y}\right)^2 - \frac{\sigma_x}{f_x}\frac{\sigma_y}{f_y} + 3\left(\frac{\tau_{xy}}{f_v}\right)^2 = 1 \tag{5.3}$$

4. Tsai-Wu criterion

$$\sigma_x\left(\frac{1}{f_{t,x}} - \frac{1}{f_{c,x}}\right) + \sigma_y\left(\frac{1}{f_{t,y}} - \frac{1}{f_{c,y}}\right) + \frac{\sigma_x{}^2}{f_{t,x}f_{c,x}} + \frac{\sigma_y{}^2}{f_{t,y}f_{c,y}} + 2\alpha_{x,y}\sqrt{\frac{\sigma_x\sigma_y}{f_{t,x}f_{c,x}f_{t,y}f_{c,y}}} + \frac{\tau_{xy}{}^2}{f_v{}^2} \tag{5.4}$$

Where

σ_x	Stress in x-axial direction	MPa
f_x	Ultimate x-axial strength	MPa
σ_y	Stress in y-axial direction	MPa
f_y	Ultimate y-axial strength	MPa
τ_{xy}	Shear stress in xy-plane	MPa
f_v	Ultimate shear strength	MPa
$f_{t.x}$	Char. tensile strength parallel grain	MPa
$f_{c.x}$	Char. compressive strength parallel grain	MPa
$f_{t.y}$	Char. tensile strength perpendicular grain	MPa
$f_{t.y}$	Char. compressive strength perpendicular grain	MPa

2.4.2 Evaluation of failure criterions

A study was made comparing different failure criteria for predicting off-axis tensile strength of oriented strand board (OSB) panels. In it, they compared the linear failure criterion (eq. 6.1) used for Hankinson's formula with three quadratic criteria (Cabrero,2010).

The three quadratic criteria compared were;

1. A quadratic failure criterion, see formula (5.2)
2. An invariant of Von Mises criterion, which is very similar to Norris criterion, see formula (5.3)
3. Tsai-Wu criterion, see formula (5.4)

Quadratic failure criterion

Concerning failure criteria, a simple one could be written as a formula (5.1), where we can differentiate a general critical difference contrary to the linear-quadratic one (5.2). For example, in the quadratic one, the angle alpha to the on-axis direction of each stress plays a significant role. At the same time, extreme values may also be located at the boundaries of the angle range.

Tsai-Wu failure criterion

Contrary to the Linear (5.1) and quadratic (5.2) failure criteria, Tsai-Wu allows mixed positive and negative signs of the normal stresses. If the tension and compression strength in the x- and y- directions are set equal, the criterion becomes the same as the quadratic one stated above. Hence, the quadratic failure criterion may be perceived as a particular case of the Tsai-Wu tensor polynomial approach (Aicher, 2001).

Von mises failure criterion

A problem with Von Mises failure criterion is that it is made for isotropic materials where objects are assumed to have the same uni-axial properties in all directions. Wood is anisotropic, which makes it more complex to calculate. Because of its anisotropy, Von Mises' failure criterion is not as suitable. Failures often occur in tension perpendicular to grain or in axial stresses in places where the wood specimen has an irregular internal structure, such as a knot. Furthermore, wood has a significant difference in strength depending on the uniaxial sign direction, whether or not the stress is tensile or compressive. Failure criteria used to evaluate the properties of wood need to take several other properties into account that isotropic failure conditions do not.

The failure conditions in criteria considering wood need to

1. be orthotropic

2. allow mixed positive and negative signs of normal stresses

There exists some models specifically developed for wood, such as Norris, 1950; or van der put, 2005. However, the more common but more complex criterion is the Tsai-wu criterion based on distortion energy theory and takes sign convention into account.

An evaluation of the failure criteria in wood members was performed by (Cabrero, 2010) that showed that Norris, Von Mises, and Tsai-Wu models performed better than all others for on-axis loading. For biaxial testing Tsai Wu and Norris, models received the most accurate results; for pure bi-axial testing and with combined tension and compression, the best results were given by van der Put and Tsai-Wu. It may seem as if best results are always obtained using the Tsai-Wu model, which is true, but this is partly because the model contains a correlation factor for the stresses, which means it can be better adjusted to suit each load case. In *Figure 2.13* a graph is shown where the different failure criteria have been plotted together with experimental data.

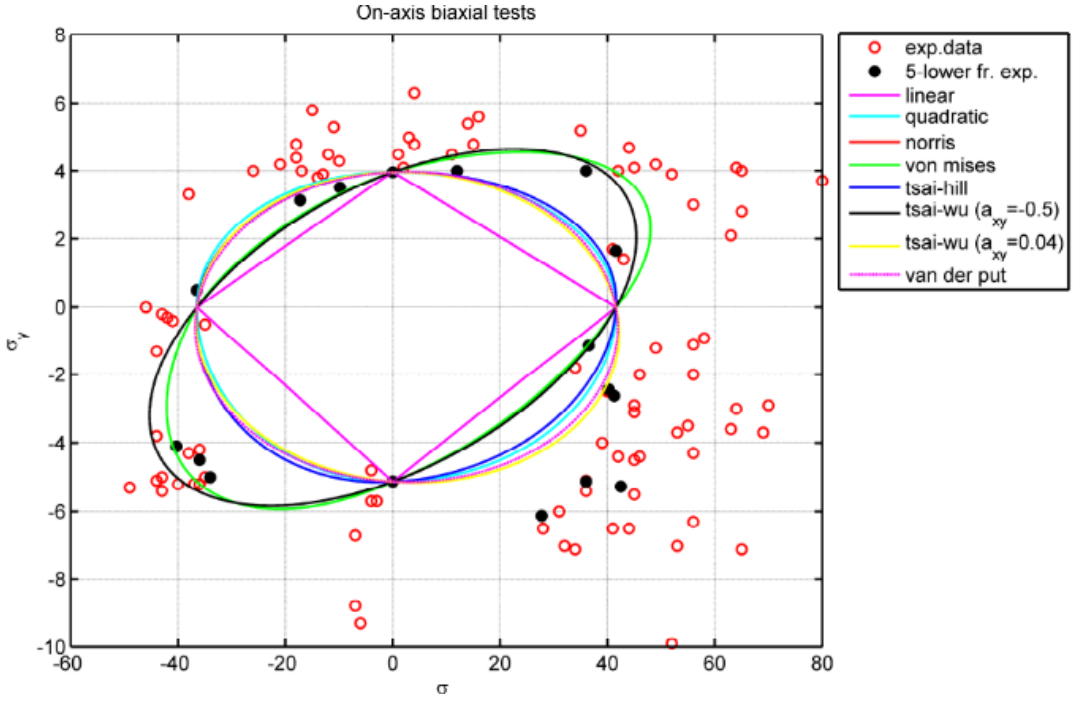

Figure 2.13. Plot of failure criteria with experimental data (Eberhardsteiner, J. 2002)

This report primarily considers the Tsai-wu criterion for evaluating failures in birch plywood plates subjected to complex stress states in truss nodes.

2.4.3 Yield theory

Johansens' yield theory was developed in 1949 (Johansen, 1949) and is used to predict fasteners' failure modes and deformations in timber connections. This has been implemented into the Eurocode, where timber-to-timber joints in double shear are described to fail in four different ways.

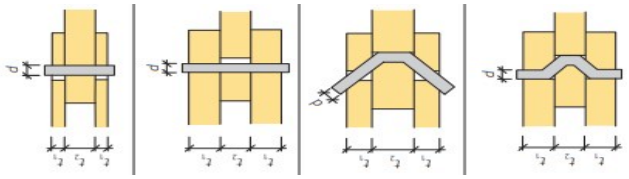

Figure 2.14: Failure modes for a timber connection in double shear (Svenskt trä, 2016)

To calculate the load-bearing capacity for each shear plane according to Johansens' yield theory, the following equations are presented in the Eurocode:

$$F_{v,Rk} = f_{h,1,k} t_1 d \tag{6.1}$$

$$F_{v,Rk} = 0,5 f_{h,2,k} t_2 d \tag{6.2}$$

$$F_{v,Rk} = 1,05 \frac{f_{h,1,k} t_1 d}{2+\beta} \left(\sqrt{2\beta(1+\beta) + \frac{4\beta(2+\beta) M_{y,Rk}}{f_{h,1,k} d t_1^2}} - \beta \right) + \frac{F_{ax,Rk}}{4} \tag{6.3}$$

$$F_{v,Rk} = 1,15 \sqrt{\frac{2\beta}{1+\beta}} \sqrt{2 M_{y,Rk} f_{h,1,k} d} + \frac{F_{ax,Rk}}{4} \tag{6.4}$$

$F_{v,Rk}$	Capacity per shear plane	kN
$f_{h,1,k}$	Embedment strength	N
$M_{y,Rk}$	Yield moment for fastener	mm
β	Relative embedment factor $f_{h,2,k}/f_{h,1,k}$	-

Johansens' yield theory assumes that the nails and timber have perfect elastic behavior. However, failure of the joint might occur before the embedment strength is reached, for example, by splitting of timber members. To account for this, the Eurocode also governs the distance between each fastener and edge distances.

In our design, failure mode 2 in *Figure 2.14* had significantly less capacity than the others due to the thin dimensions of the plywood plates. Together with the fact that we weren't able to stay within the recommended dowel spacing, the calculations made it so that our predicted failure mode was very brittle. Either the nails would be torn out of the plywood, the plywood fails or a combination of both.

3 Method

Experimental tests, analytical calculations, and numerical simulations have been conducted to analyze complex stress states in truss nodes connected with birch plywood plates. Our goal is to evaluate the potential of birch plywood connections and how it behaves in complex stress states. Variables in this experiment include angle-to-face-grain variation of plywood plates, type of fasteners (glued or dowelled), and loading directions.

3.1 Experiment

3.1.1 Margin of error

Specimens were manufactured at KTH using materials sent directly from each material manufacturer. Representatives from material manufacturers Dynea and Moelven were present during meetings and provided expertise and support on assembly and other subjects throughout the process. The testing specimens manufacturing quality was determined partly from previous working experience in the field and knowledge attained during studies at KTH with help from assistants and supervisors. The precision of cut boards and members were determined by hand with a tolerance of ±3mm. Angles of plates were also calculated by hand with a tolerance of ±2°. The humidity of wood materials was checked both with oven tests and a calibrated moisture measuring pin device. Finally, the density was deduced by weighting every part of each specimen and dividing it with the nominal drawing measurements.

3.1.1.1 Measurements and drawings

Drawings were designed in CAD software Autodesk AutoCAD and manufacturing of specimens was made after that. Measurements when manufacturing was made with simple hand tools and calculations. A jig was constructed with the exact general dimensions of the test specimens. The specimens were assembled layer by layer from starting at the bottom.

Figure 3.1. Miter of glulam and template for mounting of specimen parts

Connection details were printed in 1:1 scale drawings and used for making drilling templates. The drawings were then used to increase precision and speed up the manufacturing process.

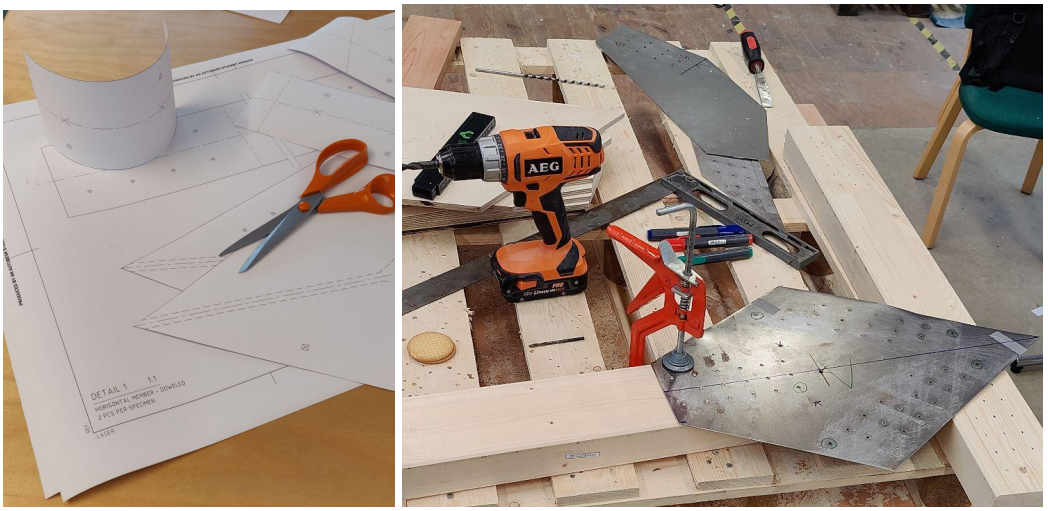

Figure 3.2. Printed out drawings in 1:1 scale (to the left) and drilling template (to the right)

3.1.1.2 Moisture content

Moisture content was measured in glulam members with a resistance-based moisture meter of the brand Gann called “Hydromette HT 85” (see Figure 3.3). The measurement was performed according to the provided equipment instructions. The measurement resulted in mean moisture content of 12,6% for glulam beams, with a standard deviation of 1,1%. In addition, moisture in plywood plates was measured with the oven method. For plywood, the measurement resulted in mean moisture content of 8,9%, with a standard deviation of 0,4%.

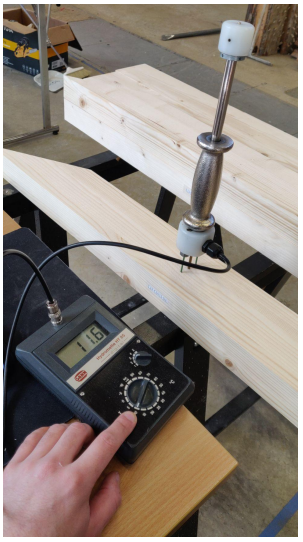

Figure 3.3. Moisture measuring device

3.1.1.3 Density

The density of all parts was calculated by dividing each part's nominal volume with its respective weight. For glulam beams, the measurement resulted in a mean density of 463 kg/m^3, with a standard deviation of 17 kg/m^3. For plywood, the measurements resulted in a mean density of 714 kg/m^3, with a standard deviation of 29 kg/m^3.

Figure 3.4. Weigh and measuring station, with scale and computer

3.1.2 Control group design

The main focus of the experimental study was to analyze failure modes of plywood in complex stress states. Complex stress states occcur when a part is simultaneously loaded in several different directions at the same time. Resembling complex stress states was achieved by designing test specimens similar to real truss-nodes, where loads were applied on the top of each specimen. In addition, its structural design distributed the loads throughout the specimens similar to that of a real-world application.

3.1.2.1 Geometry

The test specimens were designed to promote the highest axial force in their horizontal members. Therefore, when tests were carried out with tensile load, the specimen diagonal members would be subjected to compressive stresses. When specimens were loaded in compression, the horizontal members would be subjected to tensile stresses.

3.1.2.2 Perfect truss

A perfect truss is hinged at all of its nodes, meaning only axial forces are submitted throughout the structure. However, in reality, connections are made stiff by fasteners, and no actual load is ideally distributed over the length of constructions. Furthermore, the shape of fasteners also influences how forces are transmitted through connections. This adds to eccentricity that contributes to moments developing that influence the axial forces and normal stresses at each part. In our particular test-specimen design, members were relatively short and fastened connections rather stiff; this meant moments developed in areas that could influence the results and induce stress concentrations at unpredicted points.

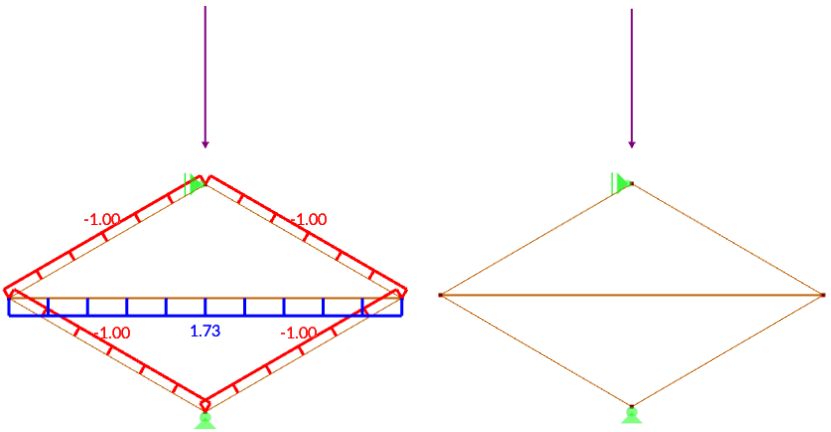

Figure 3.5. Frame analysis of truss with hinged joints. Axial force (kN) (left) and moment distribution (kNm) (right)

The frame analysis in *Figure 3.5* was designed with the same geometry as test specimens. Because of the specimen in this case acting as an ideally perfect truss, no moments are transferred into the timber members. Instead, pure axial forces are transferred with equilibrium.

If each timber connection is modelled as stiff with beam elements instead, moments are distributed throughout the diagonal members and through each node (see *Figure 3.6*).

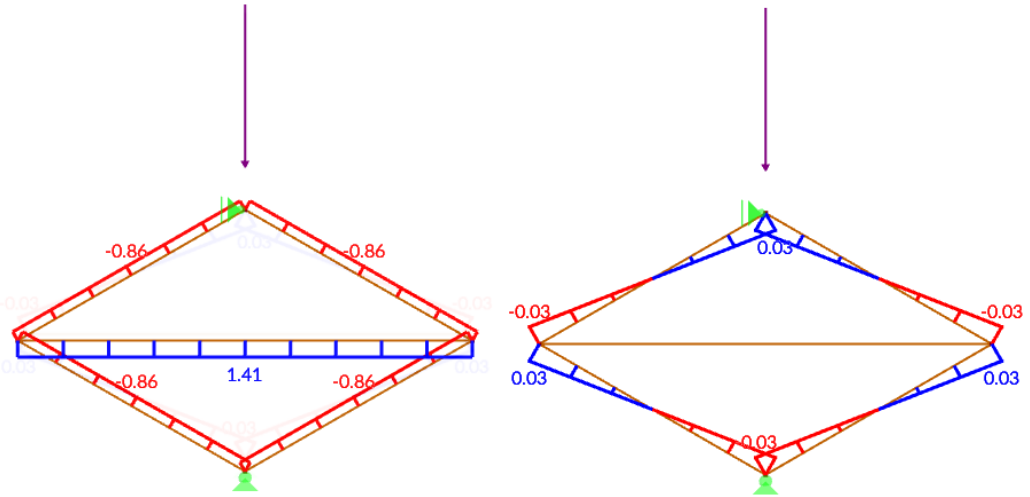

Figure 3.6. Frame analysis of a truss with stiff joints. Axial force (kN) (left) and moment distribution (kNm) (right)

This moment distribution also invokes shear forces throughout the diagonal members, according to the picture below.

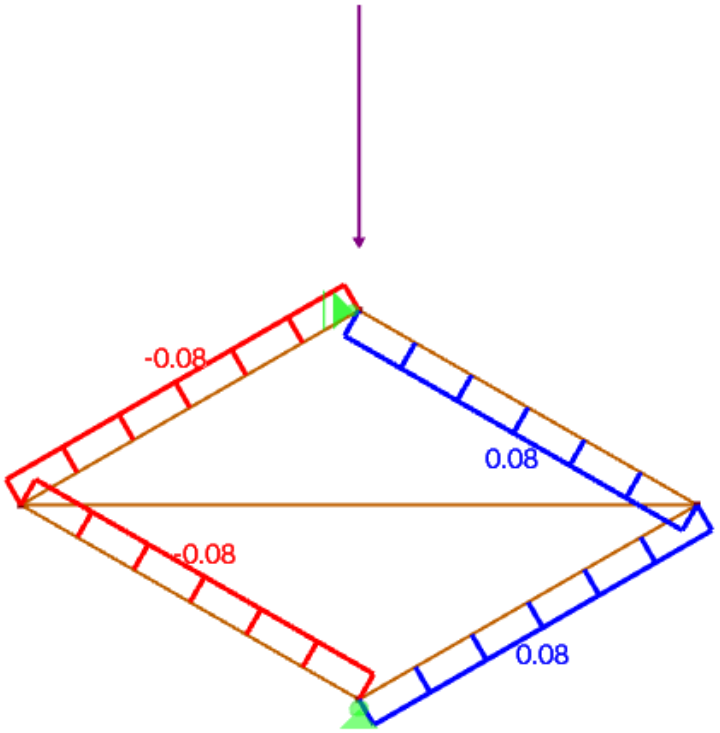

Figure 3.7. Frame analysis of a truss with stiff joints. Shear force distribution (kN)

3.1.2.3 Dimensions and material

Initial testing and calculations showed stress concentrations developing in timber members and top/bottom plates that were disadvantageous for our intended study. The experiment design aimed to promote failure modes in the middle plywood plate B (see picture below). In order to promote this, the dimensions of the timber beams were over-designed, and glulam were used instead of ordinary construction lumber since glulam is easier to work with and has a slightly higher strength than ordinary construction lumber. Another challenge was not to break the top and bottom birch plywood plates; this was prohibited by adding additional side plates at both the top and bottom and wedges in between the diagonal members for any compressive tests.

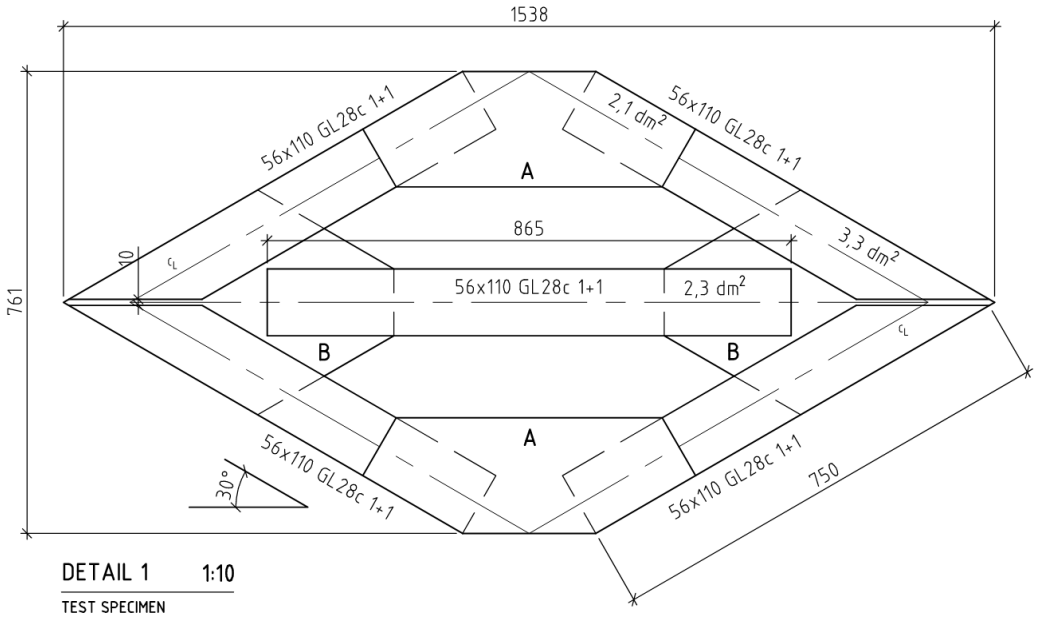

Figure 3.8. General geometry of all test specimens, see drawing K-20-2-1001, Appendix D

An initial assumption to maximize the plywood strength was to have the face-angle-to-grain of the middle plywood plate parallel with the largest developed normal stress, i.e., orienting the face grain of middle plates with the horizontal members subjected to the highest normal stress. As a result, 0-degree face-grain-orientation was the configuration of choice for all dowel-type control groups, while minor variations in the angle-to-grain configuration were carried out for the glued control groups.

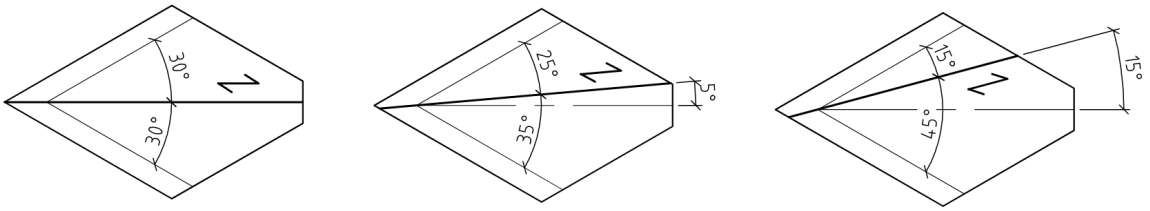

Figure 3.9. Angle to grain variations in plywood-plates of control groups, see drawing K-20-2-1001, Appendix D

The variation in angle-to-grain of the plywood plates was made to study what impact it would have on the specimen strength and possibly stiffness, resembling situations in a truss similar to the one in section 2.2.2.

3.1.2.4 Materials used

Materials were provided from several companies interested in the research. Birch plywood manufacturer Koskisen sent us birch plywood boards with thicknesses of 9 mm. Moelven provided us with glulam beams in quality GL28c that we cut ourselves in workshops at KTH. Dynea in Norway sent us Melamine-Urea-Formaldehyde two-component glue that we mixed ourselves according to technical data sheets and applied to the specimens. Rothoblaas provided us with screws that were used in the assembly of screw-glued specimens. Gunnebo carpentry nails with a dimension of 5.1x150 were used in dowel-type specimens as dowels after pre-drilling holes with a simple screwdriver and wooden drill.

Table 3.1. Materials used

Name	Type	Specification	Company
Gusset plates	Birch plywood	9 mm	Koskisen
Timber members	Glulam GL28c	56 x 110 mm	Moelven
Glue	MUF 2-Component	-	Dynea
Fastener	HBS Cts	3,2 x 50 mm	Rothoblaas
Fastener	VGZ	5,6 x 140	Rothoblaas
Dowels	Blank Trådspik	5,1 x 150	Gunnebo

3.1.2.5 Testing scheme

Testing was carried out in four different control group configurations, tested in both tension and compression. Angle to grain variations were only carried out for screw-glued specimens. During ongoing testing, decisions were made that influenced the original testing scheme, changing the number of repetitions for tensile respective compressive tests. Compression tests provided a higher success rate and, therefore, higher numbers of viable testing data.

Table 3.2. Control groups and repetitions

α	$n_{compressive}$	$n_{tensile}$	$t_{plywood\_plate}$	Fastener	∑n
0°	3	3	9 mm	Doweled	6
0°	5	1	9 mm	Screw-Glued	6
5°	4	2	9 mm	Screw-Glued	6
15°	5	1	9 mm	Screw-Glued	6
					24

3.1.3 Manufacturing of specimens

3.1.3.1 Waste minimizing

Cutting pattern proposals were prepared in Autodesk AutoCAD for all plywood boards and glulam beams to ensure that waste material was minimized and that the right amount of materials was ordered from each manufacturer.

Figure 3.10. Cutting pattern for glulam, see drawing K-20-2-1002, Appendix D

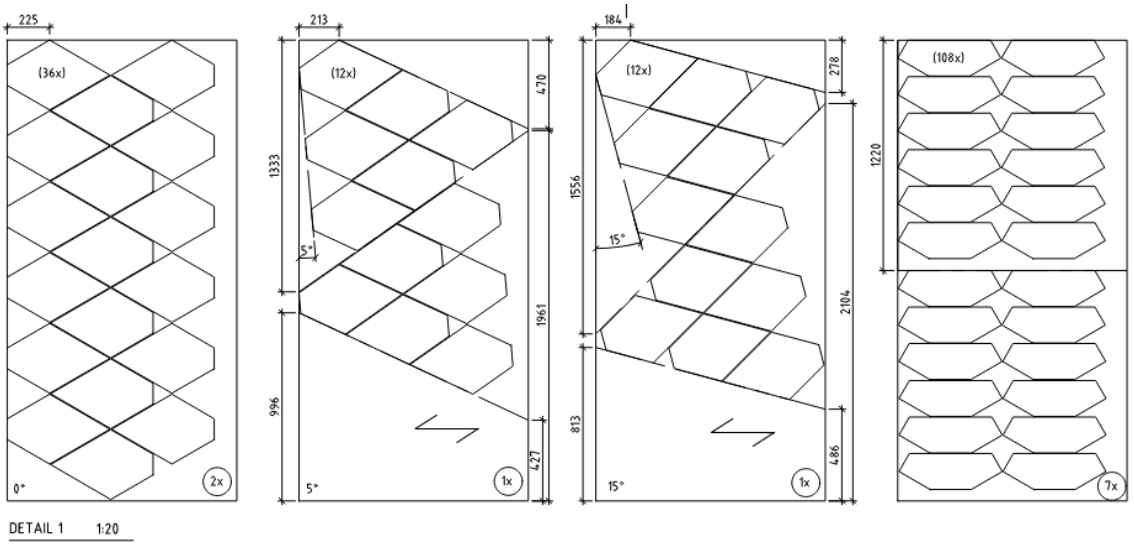

Figure 3.11. Cutting pattern for plywood plates, see drawing K-20-2-1002, Appendix D

NUMBER OF SPECIMENS		1	3	6	18	24
HORISONTAL MEM.	56x110 GL28c	2	4	12	36	**48**
DIAGONAL MEM.	56x110 GL28c	8	24	48	144	**192**
PLATE A	BIRCH PLYWOOD	6	18	36	108	**144**
PLATE B	BIRCH PLYWOOD	2	6	12	36	**48**
GLUED AREA (m2)	DYNEA MUF	0,7	2,1	4,2	**12,6**	16,8
SMALL SCREWS	HBS 3,2x50	40	120	240	**720**	960
LARGE SCREWS	VGZ 5,6x140	20	40	120	**360**	480
DOWELS (NAILS)	BLANKSPIK 5,1x150	80	240	**480**		

Figure 3.12. Table of parts needed (bold), see drawing K-20-2-1002, Appendix D

3.1.3.2 Littera

Littera for each part and each specimen were created to quantify the material, speed up the manufacturing, and keep better track of failures and properties of each test. Even numbers of part-littera were positioned in the bottom, and the parts were numbered, increasing from left-to-right, front-to-back. Specimen littera was also named according to load type, connection type, and angle-to-grain variant.

Part letters were named D- for Diagonal timber member, H- Horizontal timber member, A- Plywood plate A and B- Plywood plate B.

For example, **01** - **C1G0** - **A1** is
Specimen **01** - **C**ompression, Repetition **1** (of 3), **G**lued type, **0** Degree - Plate **A1**.

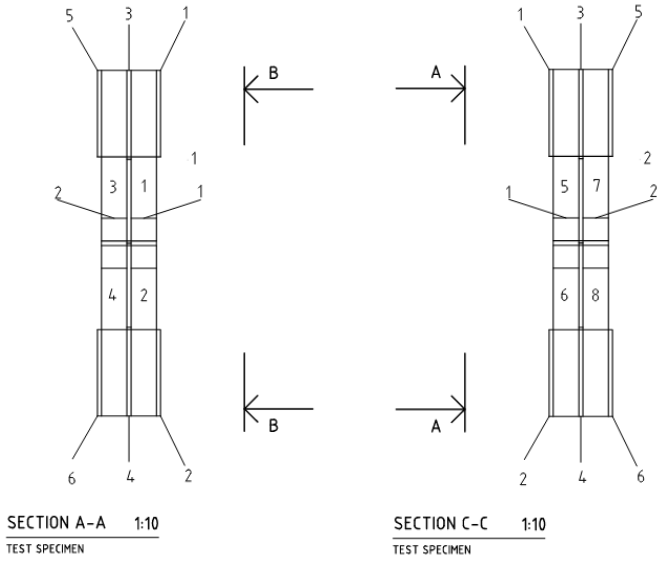

Figure 3.13. Littera numbering for specimen parts, see drawing K-20-2-1003, Appendix D

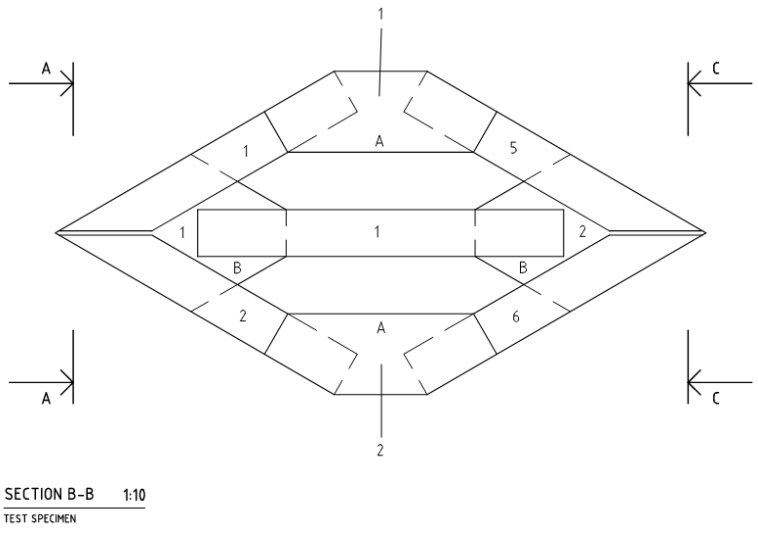

Figure 3.14. Littera numbering for specimen parts, see drawing K-20-2-1003, Appendix D

3.1.3.3 Cutting of timber

The plywood plates were first cut in respective angular shapes with a smaller circular saw to speed up the manufacturing and ensure the right angle-to-grain was achieved. Angular sawed plates were then sawed in the format saw according to detailed drawings. Next, glulam beams were pre-cut with a smaller miter saw before being cut in the larger format saw.

Figure 3.15. Miter saw used (to the left), and format saw used (to the right)

3.1.3.4 Gluing of glue-type specimens

Glued parts were first sanded at adjacent surfaces and then glued with a MUF glue provided by Dynea. The glue was mixed in a ratio of one part hardener and ten parts glue. (1:10). Parts were then attached with small screws according to figure 3.16 and 3.17. Procedure for glued assembly

1. Timber was pre-drilled about 2 cm deep with 4 mm holes
2. Adjacent surfaces were roughened with a sanding machine
3. Glue was applied on both surfaces
4. Clamps were tightened
5. Small 3,5x50 screws were inserted into timber and plywood plate
6. Clamps were removed

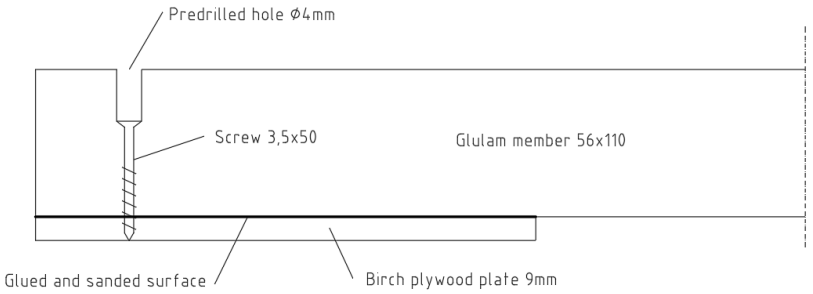

Figure 3.16. Glulam member to the plywood plate assembly

7. Plywood plates were pre-drilled with 4 mm holes
8. Adjacent surfaces were roughened with a sanding machine
9. Glue was applied on both surfaces
10. Small 3,5x50 screws were inserted into plates and timber member level with the plate surface.

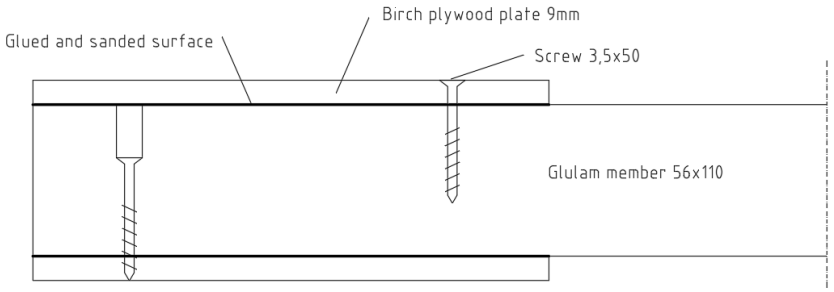

Figure 3.17. Plywood plate to glulam member assembly

Figure 3.18. Glued surface (to the left), first layer of glued plate and member assembly with small screws (to the right)

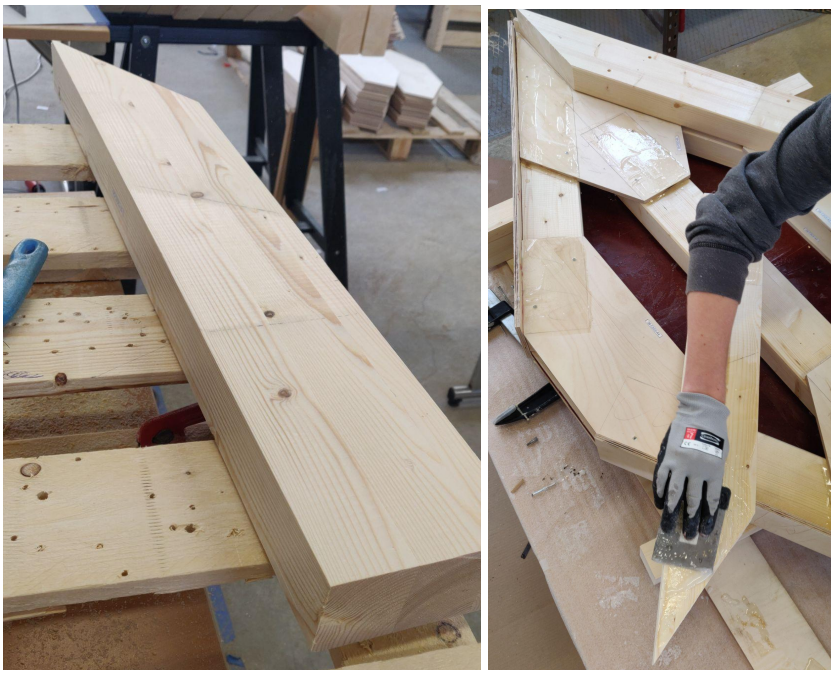

Figure 3.19. Sanded surfaces (to the left), glueing of adjacent surfaces (to the right)

The quality of glue lines bonded with MUF was determined by:

Glue-mix
MUF 2-Component glue system was mixed at a ratio of 1:10 Hardener/Resin

Temperature
The temperature at the facility of manufacturing and curing were around 10℃

Bonding pressure
Clamps were mounted at bonded surfaces and tightened by hand

Pressing time
Clamps were left on specimens for 24 hrs then removed

Curing time
Specimens were left untouched, curing for about 1-2 weeks

Bonded materials
Glulam beams were bonded together with birch-plywood, and adjacent surfaces were sanded with a sanding machine before the bond

3.1.3.5 Nailing of dowel-type specimens

The template used for gluing was also used in assembly for nailed specimens. Timber parts were placed into the template and clamped together to form a rigid frame with the correct geometry. Holes were then drilled through, ensuring a correct alignment of the holes. Instead of round-shaped dowels, we used square nails with a square cross-section of 5,1mm sides and 150mm long. Holes drilled were 6 mm in diameter. Hole positions were positioned according to 1:1 scale drawings; see, for example, K-20-6-1002 in Appendix D.

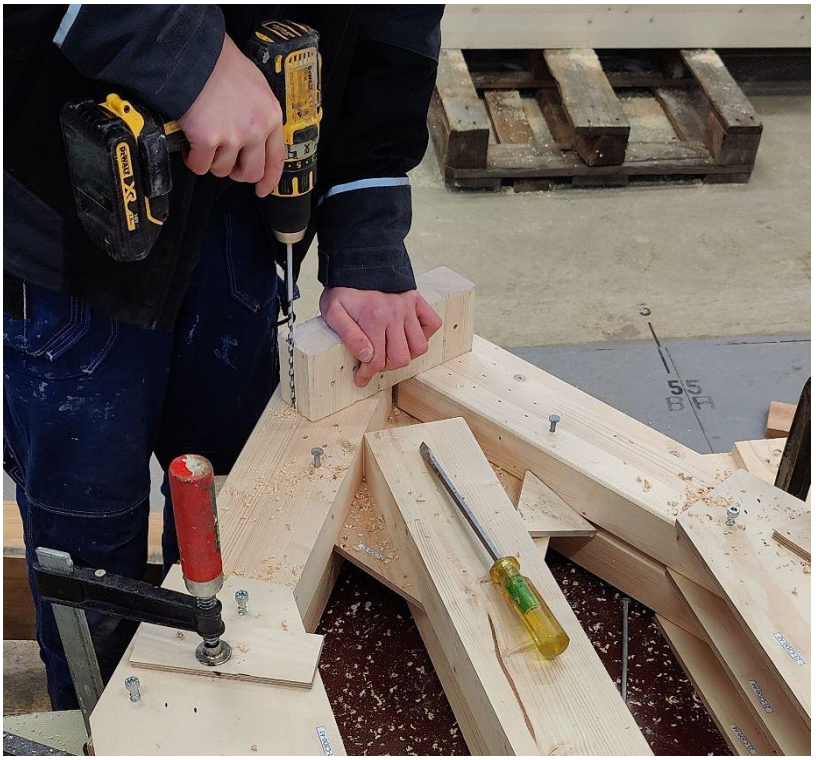

Figure 3.20. Predrilling during assembly of dowelled specimens

3.1.4 Testing

Testing was carried out in a hydraulic universal testing machine MTS 810 that recorded load and displacement. The machine could test up to 100 kN loads on specimens with a maximum height of around 1100 mm.

3.1.4.1 Compressive testing

In compressive testing, loads were applied on the top of each specimen while resting flat on the bottom supports. Forces were evenly transferred through the diagonal members with wedges cut out of glulam and fitted between the top and bottom members.

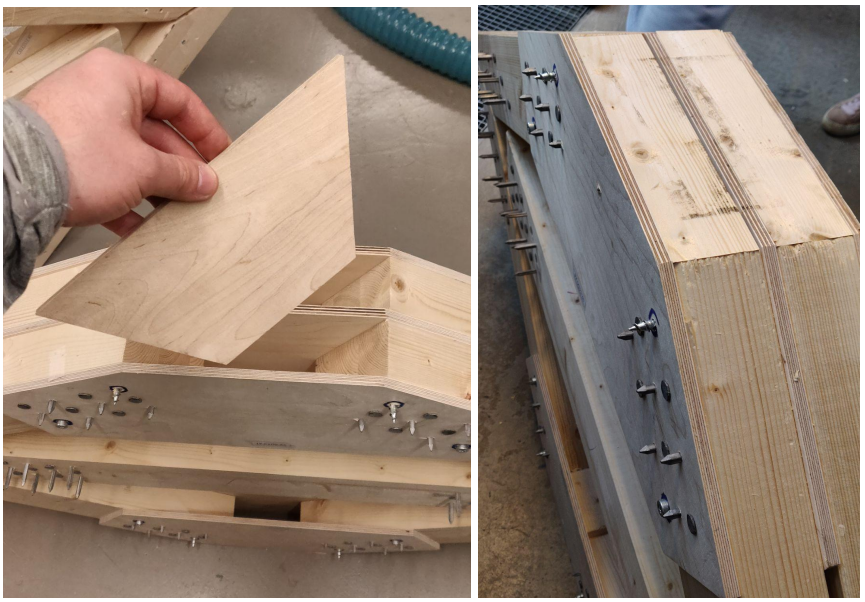

Figure 3.21. Wedges put into top and bottom of each specimen

Lateral movements were prohibited, with bars inserted into both the top and bottom supports.

Figure 3.22. Bottom support of compressive test setup

3.1.4.2 Tensile testing

In tensile testing, steel plates were cut out and connected to the inward-facing edges of the outer plates, transferring tensile forces through the top and bottom plates to the diagonal members.

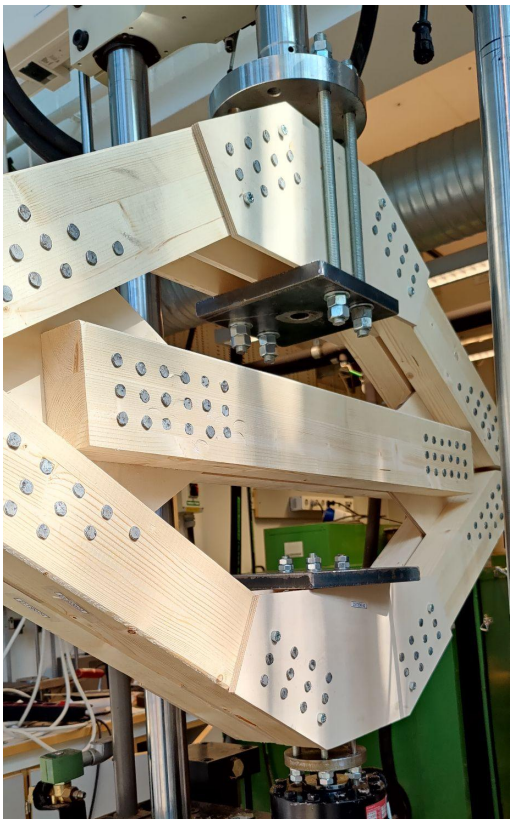

Figure 3.23. Tensile mounting supports made out of steel rods and metal plates

3.2 Simulation and Calculations

3.2.1 *Mechanical properties*

Mechanical characteristic properties of glulam are taken from Eurocode EN-1995-1-1. In addition, some mean mechanical properties of birch plywood are taken from ongoing tests at KTH, others from literature (Handbook Of Finnish Plywood, 2002; Wang et al., 2021).

Table 3.3. Mechanical properties used in the calculations and simulations

Material constants			Glulam 28c	Birch Plywood
			Characteristic	Mean test value
E-modulus	E_x	[MPa]	11 000	9399*
	E_y	[MPa]	370	6657*
	E_z	[MPa]	370	1110
Shear modulus	G_{yz}	[MPa]	69	186
	G_{xz}	[MPa]	690	206
	G_{xy}	[MPa]	690	620
Poisson's ratio	υ_{yz}	-	0	0,427
	υ_{xz}	-	0	0,443
	υ_{xy}	-	0	0,036
Material strengths			Glulam 28c	Birch Plywood
Ultimate tensile strength	$f_{t,x}$	[MPa]	14,5	62.49*
	$f_{t,y}$	[MPa]	0,4	56.69*
	$f_{t,z}$	[MPa]	0,4	56.69*
Ultimate comp. strength	$f_{c,x}$	[MPa]	21	31.32*
	$f_{c,y}$	[MPa]	2,5	23.93*
	$f_{c,z}$	[MPa]	2,5	23.93*
Ultimate shear strength	$f_{v,yz}$	[MPa]	0,9	11,98*
	$f_{v,xz}$	[MPa]	4,0	11,98*
	$f_{v,xy}$	[MPa]	4,0	11,98*

*Mean values from tests performed at KTH, 2020-2021

3.2.2 RFEM

Finite element models were made to investigate the stress distributions in the proposed test specimen designs.

The geometry and the mechanical properties programmed were the same as the test specimens, and the corresponding load situations were also replicated.

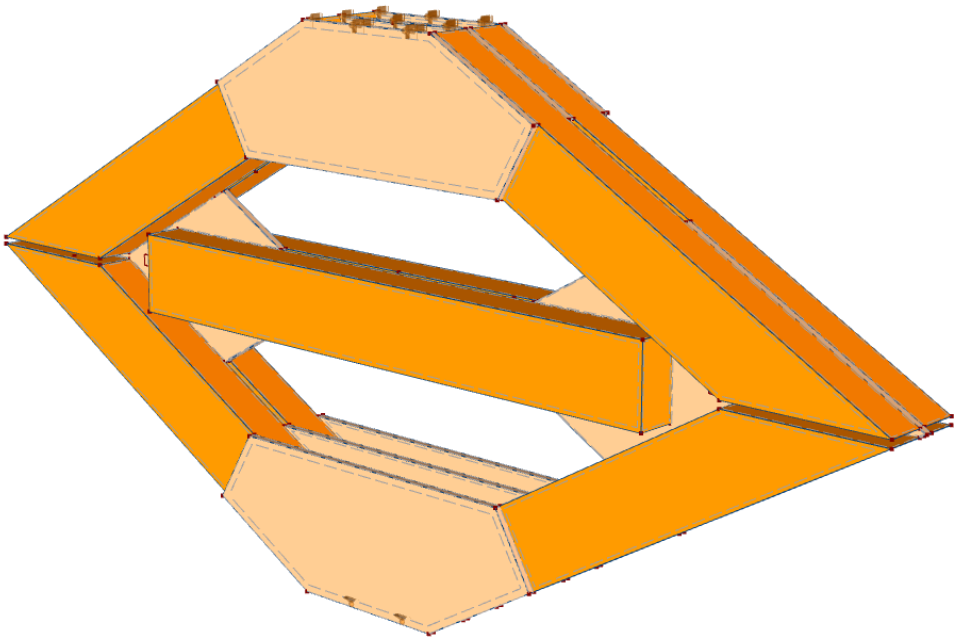

Figure 3.24. Specimen model in FEA software RFEM

3.2.2.1 Simulation input

Stresses relative to the face grain of the plywood plates were simulated by locating local axis systems with their x-axis parallel to grain and material properties in respective directions. Tests were performed on both 0° and 15° configurations, both in a compressive and tensile load setup.

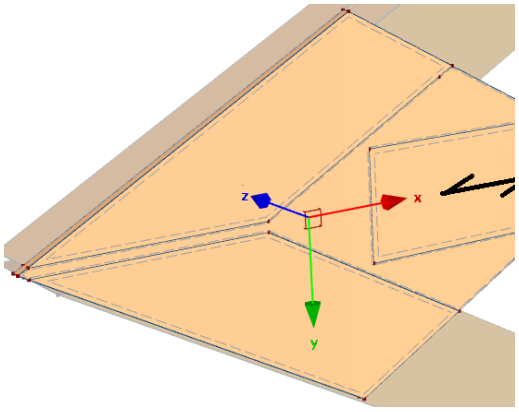

Figure 3.25. Local coordinate system for 0° plywood plate B

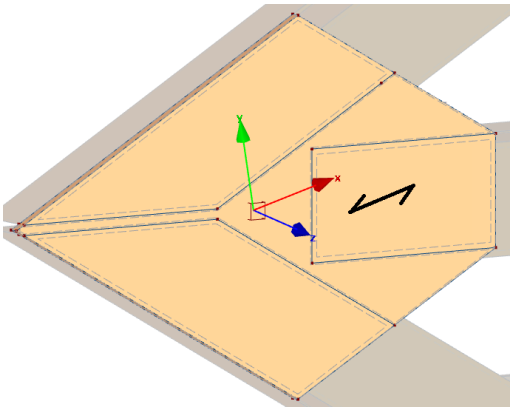

Figure 3.26.Local coordinate system for 15° plywood plate B

In compressive setups, loads were distributed on the outer surface of the top plywood solids, with hinged support on the outer surface of the bottom plywood solids.

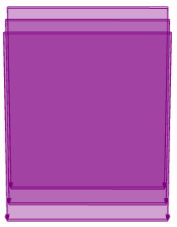

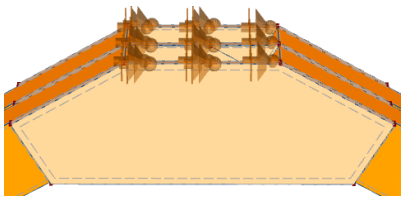

Figure 3.27. Top Surface support and surface load compressive model

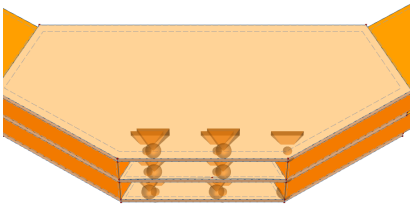

Figure 3.28. Bottom Surface support

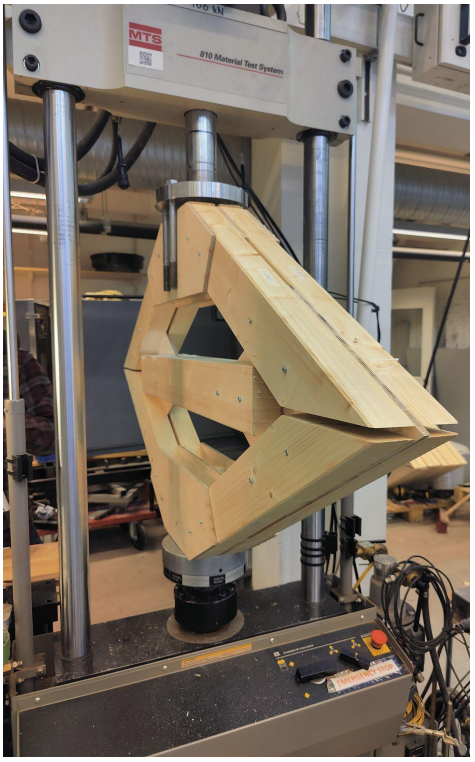

Figure 3.29. Compressive mounting supports

In tensile setups, loads were distributed on the inner surface of the top plywood solids, with hinged support on the inner surface of the bottom plywood solids.

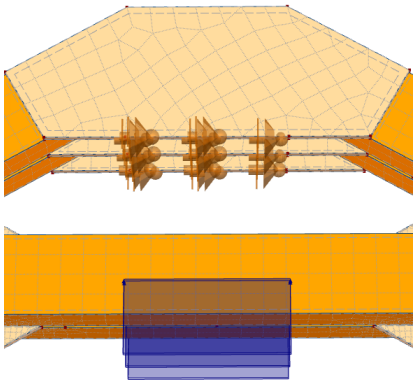

Figure 3.30. Top Surface support and surface load tensile model

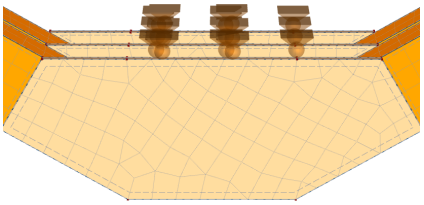

Figure 3.31. Bottom Surface support

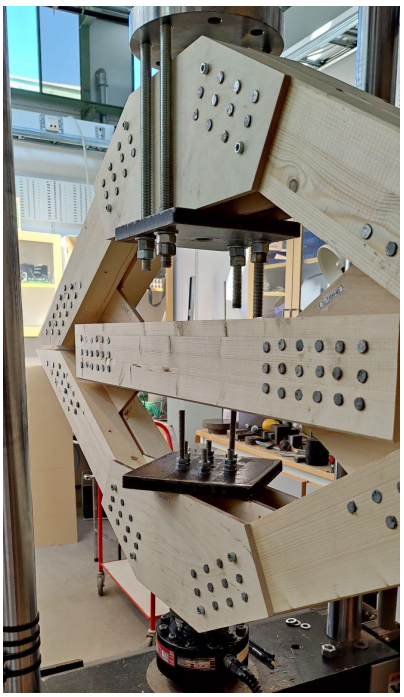

Figure 3.32. Tensile mounting supports made out of steel rods and metal plates

The model was designed as a solid with finite element lengths of 0,03m throughout the whole specimen except at the plywood plates in the middle, which had a mesh refinement set to 0,008m. The shapes of the finite elements were triangular and quadratic. The connected surfaces were shared between every solid member in the model, assuming no slip.

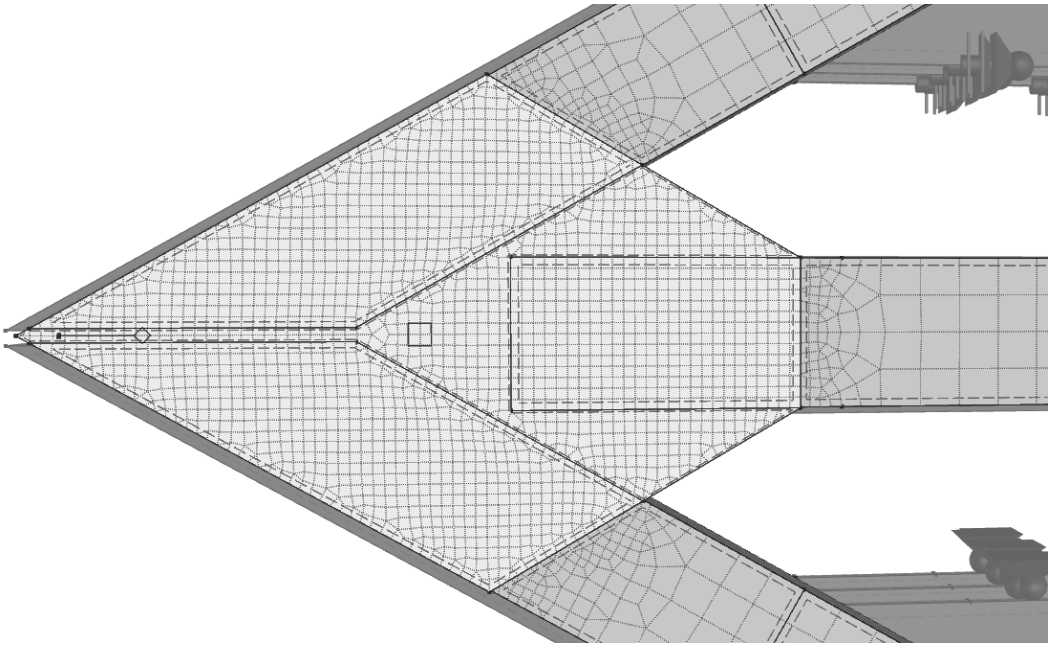

Figure 3.33. Finite element mesh

4 Results

4.1 Experiments

4.1.1 Test groups

See appendix for diagrams and individual specimen results

4.1.1.1 Test group A

Test type	Connection type	Angle to-grain
Compressive	Glued	0°

Minimum failure load	Mean 1st failure load	Mean 2nd failure load
-68,9 kN	-71,07 kN	-77,50 kN

Comment
For this configuration, no failures occurred in plywood plate A, but we did reach high loads, which indicates that the plywood probably had higher capacity than test results. Failures occurred in the glue line, probably due to compromised conditions during curing.
77,5 kN < Plywood capacity

4.1.1.2 Test group B

Test type	Connection type	Angle to-grain
Compressive	Glued	5°

Minimum failure load	Mean 1st failure load	Mean 2nd failure load	Mean plywood failure load
-70,20 kN	-73,88 kN	-81,87 kN	-78,15 kN

Comment

Two failures occurred in the plywood in this configuration, indicating plywood capacity probably was around the same levels as the test indicates. Glue line failure before plywood failure in specimen 08 could contribute to an eccentricity of stress distribution at the horizontal connection.

The failure mode in the plywood was tensile failure originating close to the end of the horizontal bars following a vertical line towards the diagonal members. At the edge of the diagonal beams the failure started following the direction of the beams as shown in Figure 4.1 and 4.2

74,5 kN < Plywood capacity < 85 kN

Photos from experiments; see appendix for better resolution.

Figure 4.1. Plywood failure mode of specimen 08

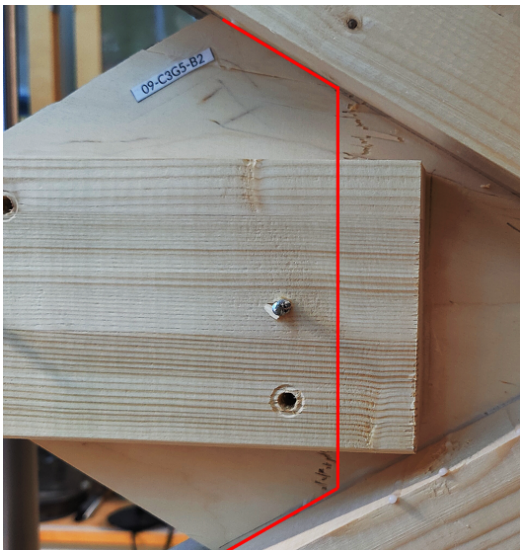

Figure 4.2. Plywood failure mode of specimen 09

4.1.1.3 *Test group C*

Test type	Connection type	Angle to-grain
Compressive	Glued	15°

Minimum failure load	Mean 1st failure load	Mean 2nd failure load	Mean plywood failure load
-56,2 kN	-70,53 kN	-74,30 kN	-74,80 kN

Comment

In this configuration, four failures occurred in plywood, which means plywood capacity should be around the same as the test results indicate. However, glue line failing before the plywood could induce an eccentricity at the horizontal connection contributing to the plywood failure.

The failure modes for the plywood plates with a 15 degree face-grain angle differ from the zero degree samples by not always being completely vertical and not always going all the way to the diagonal member. For two of the specimens the failure started in tension at the horizontal member and propagated towards the edge of the plywood plate following its face-grain angle where a more complex state exists, this can be seen in Figure 4.5 and 4.6.

74,5 kN < Plywood capacity < 85 kN

Photos from experiments; see appendix for better resolution.

Figure 4.3. Plywood failure mode of specimen 14

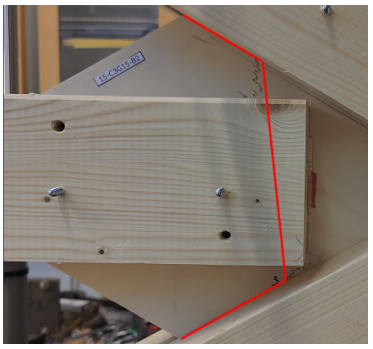

Figure 4.4. Plywood failure mode of specimen 15

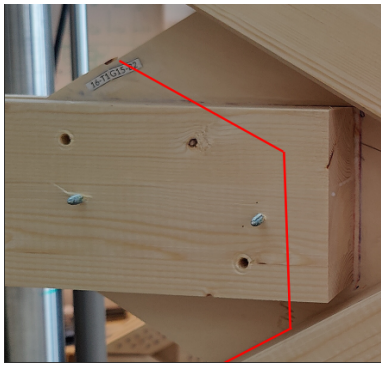

Figure 4.5. Plywood failure mode of specimen 16

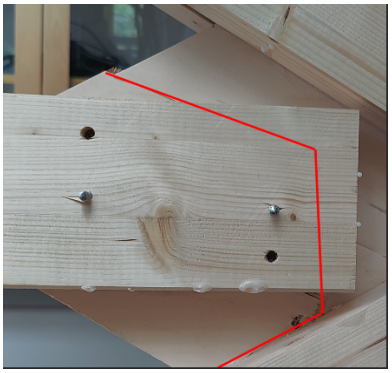

Figure 4.6. Plywood failure mode of specimen 17

4.1.1.4 Test group D

Test type	Connection type	Angle to-grain
Tensile	Glued	0°

Minimum failure load	Mean 1st failure load	Mean 2nd failure load
72,20 kN	75,20 kN	72,20 kN

Comment
In this configuration, no failures occurred in plywood, which means plywood capacity is higher than test results

75,2 kN < Plywood capacity

4.1.1.5 Test group E

Test type	Connection type	Angle to-grain
Tensile	Glued	5°

Minimum failure load	Mean 1st failure load	Mean 2nd failure load
69,60 kN	73,10 kN	76,20 kN

Comment
In this configuration, no failures occurred in plywood, which means plywood capacity is higher than test results

76,2 kN < Plywood capacity

4.1.1.6 Test group F

Test type	Connection type	Angle to-grain
Tensile	Glued	15°

Minimum failure load	Mean 1st failure load	Mean 2nd failure load
71,50 kN	74,30 kN	71,50 kN

Comment
In this configuration, no failures occurred in plywood, which means plywood capacity is higher than test results.

74,3 kN < Plywood capacity

4.1.1.7 Test group G

Test type	Connection type	Angle to-grain
Compressive	Doweled	0°

Minimum failure load	Mean 1st failure load	Mean 2nd failure load
-46,00 kN	-49,23 kN	-49,23 kN

Comment

In this configuration, three failures occurred in plywood, which means plywood capacity is around the same as test results

The failure mode for the doweled specimens followed a completely vertical line starting at the end of the central nail group for the horizontal member. The failure then propagated out towards the edge and passed the last nail hole for the diagonal members as shown in Figure 4.7-4.9.

46 kN < Plywood capacity < 52 kN

Photos from experiments; see appendix for better resolution.

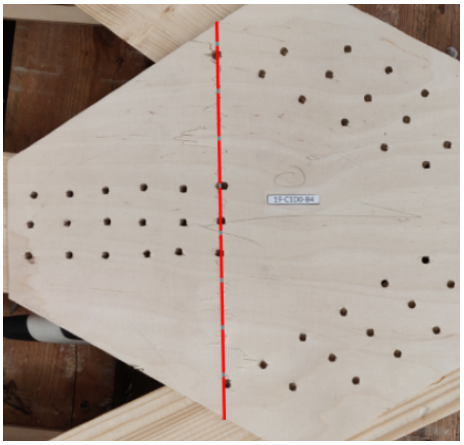

Figure 4.7. Plywood failure mode of specimen 19

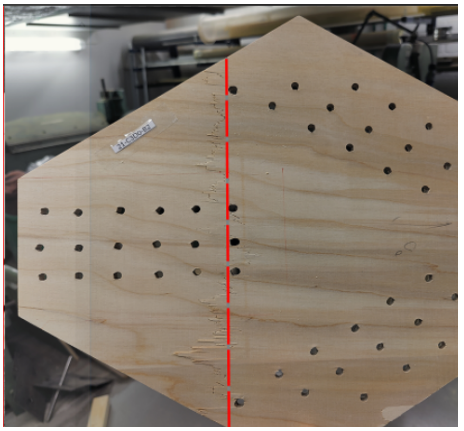

Figure 4.8. Plywood failure mode of specimen 21

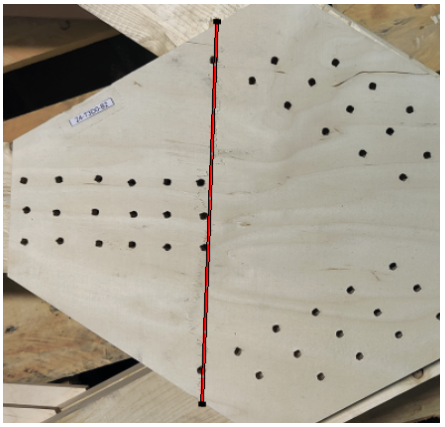

Figure 4.9. Plywood failure mode of specimen 24

4.1.8 Test group H

Test type	Connection type	Angle to-grain
Tensile	Doweled	0°

Minimum failure load	Mean 1st failure load	Mean 2nd failure load	Mean plywood failure load
-57,10 kN	-58,30 kN	-64,20 kN	-58,35 kN

Comment

Two failures occurred in plywood in this configuration, indicating plywood capacity could be around the same as test results; local compressive buckling in plywood occurred at the horizontal dowels before failure occurred in the diagonal.

The failure in the horizontal member consists of two parts that both will contribute to the strength of the connection. At the end of the horizontal member failure will occur in the form of local buckling, along the top and bottom of the nail group shear failure takes place following a horizontal line along the nails. This can be seen in Figure 10.

The other failure mode that was seen during testing was along the diagonal members, this failure occurs in a complex stress state when the diagonal members are in tension. The failure starts with the nails starting to be pulled through the plywood and continues following the inner line of the nail group in a mixture of shear and tension. This failure will result in the plywood getting completely separated from the rest of the specimen, as seen in Figure 4.11-4.13. For the specimens where this type of failure occured it should be noted that local buckling already can be seen at the end of the horizontal members.

57,1 kN < Plywood capacity < 64,2 kN

Photos from experiments; see appendix for better resolution.

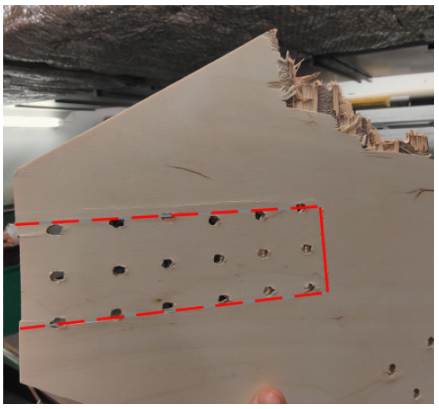

Figure 4.10. Plywood compression of specimen 22

Figure 4.11. Plywood failure mode of specimen 22

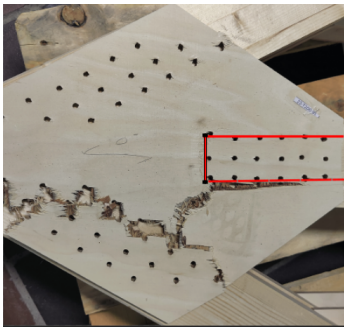

Figure 4.12. Plywood compression of specimen 23

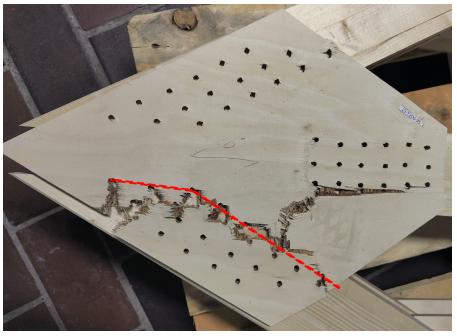

Figure 4.13. Plywood failure mode of specimen 23

4.1.2 Test group summary

Table 4.1. Summary of test results

Group	n	Type	Config.	Min fail	Mean 1	Mean 2	Mean Ply
	#			kN	kN	kN	kN
A	3	Comp.	Glued 0°	-68,9	-71,07	-77,5	-
B	4	Comp.	Glued 5°	-70,2	-73,88	-81,87	-78,15
C	4	Comp.	Glued 15°	-56,2	-70,53	-74,3	-74,8
D	1	Tens.	Glued 0°	-72,2	-75,2	-72,2	-
E	2	Tens.	Glued 5°	-69,6	-73,1	-76,2	-
F	1	Tens.	Glued 15°	-71,5	-74,3	-71,5	-
G	3	Comp.	Doweled 0°	-46,0	-49,23	-	-49,23
H	3	Tens.	Doweled 0°	-57,1	-58,3	-64,2	-58,35

For 0° specimens, no failures occurred in the plywood, and tests reached loads as high as 82 kN. Calculations were instead made estimating the load capacity as high as 95 kN, but possibly, a more realistic estimation would be 85 kN. This would imply that 0° specimens are around 20% stronger than the 15° specimens and around 17,7% stronger than the 5° specimens tested in compression. Testing results indicate 5° specimens are around 4-5% stronger than the 15° specimens when tested in compression.

Not all failures occurred in plywood plates. Probably due to low temperatures in the manufacturing facility, curing conditions of MUF-glue were compromised. Most testing specimens failed at glue lines before they failed in the plywood. Any test specimen that did not fail in Plywood plate B had more potential load-bearing-wise. Despite the gluing being compromised, glued specimens were around 37% stronger than dowelled ones. This raised some questions considering the use of glue-fasteners instead of dowels in structural timber-to-timber connections. It is undoubtedly stronger, but at the same time, there are many uncertainties concerning curing conditions. In addition, Glueing must be performed in a controlled environment. Tensile timber failures are always very brittle, but dowelled connections could behave in a ductile manner if either the nails are designed to yield or local compressive buckling occurs at dowel groups. Compressive local deformations could also occur at glue connections but have not been present during this testing as other failure modes are more likely to occur before.

4.2 Calculations

4.2.1 Nailed connections

4.2.1.1 Johansen Theory

The behavior of the nailed connection was first studied using Johansens' yield theory, where the capacity for each nail was calculated according to *formulas 6.1-6.4*. We could see that the plywood will fail before we start to see any deformations in the nails. According to Johansens Theory, we get the second failure mode in *Figure 2.14* with a capacity of 1.7 kN per shear plane or 3.3 kN per nail.

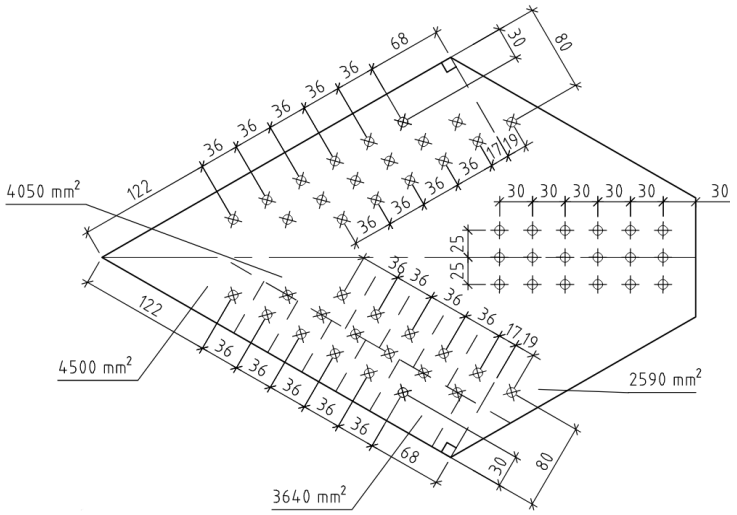

Figure 4.14: Dowel groups checked with Johansen theory, see drawing, K-20-6-1002, Appendix D

4.2.1.2 Failure from the diagonal members

During the tests we saw failure in the plywood in between the diagonal members. To calculate this, an assumption was made that the force can be linearly distributed along the two failure lines in *Figure 4.24* concerning the horizontal direction. The normal force from the diagonal beams could then be transferred to parallel and perpendicular components relative to the face grain angle in the plywood.

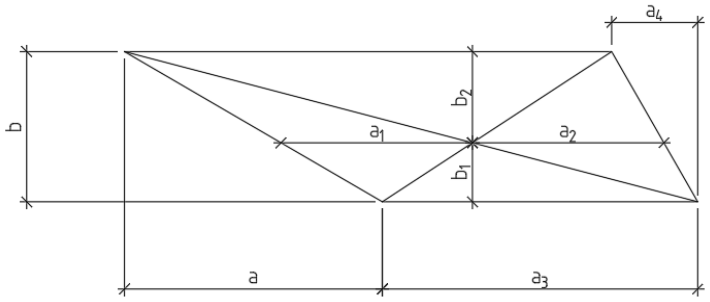

Figure 4.15. Area geometry at diagonal member

The distances l_1 and l_2 are calculated as the average distance between the two most outer nails along the line and half of the distance to the plywood edge. This calculation model becomes very sensitive to changes in these lengths; if using this model for design applications, the distance between the nails can therefore be used for a design on the safe side.

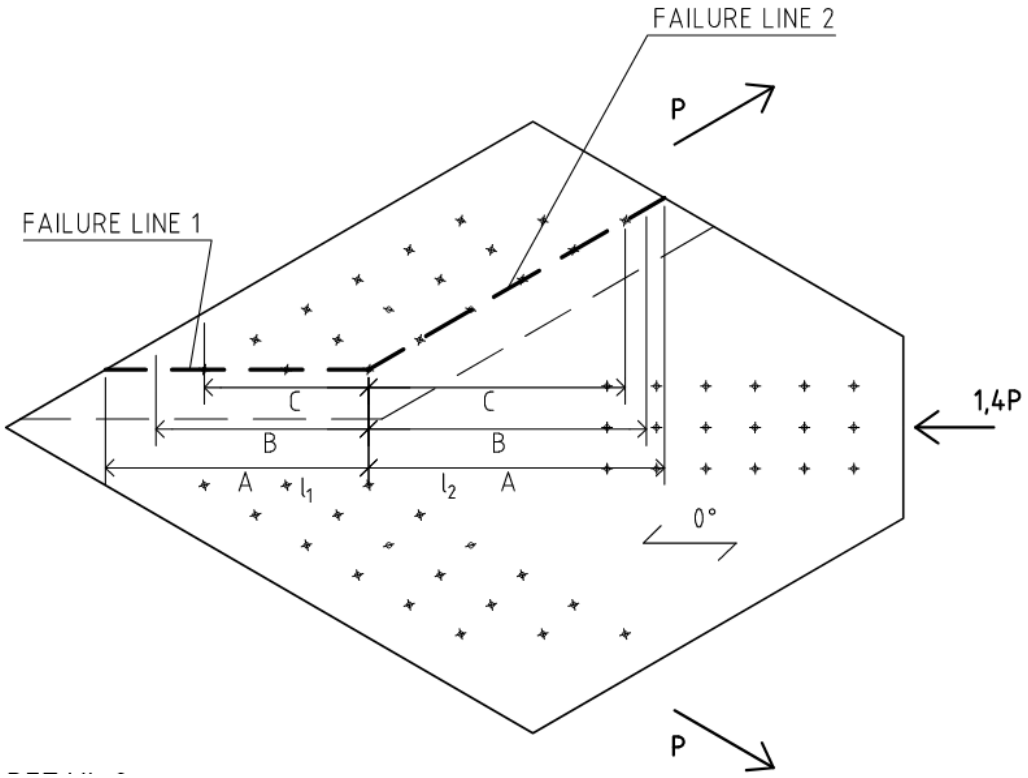

Figure 4.16. Failure lines from the diagonal tensile test

The shear force is calculated as the average between the two ends of each fracture line with regard to the distance to the center of the nail group. Stresses within the plywood can be calculated when all the forces are calculated and be compared to the Tsai Wu failure criteria.

In *Table 4.2* the results are presented for three different scenarios regarding the lengths l_1 and l_2. The first one considers the entire distance between the nails and the edge of the plywood, the second one takes the average between the nails and the plywood edge, and the third is only the distance between the nails.

Table 4.2: Calculated failure loads for different configurations

Mode	Failure Line	l_1 mm	l_2 mm	Force kN
A	1 or 2	142	143	77
B	2	112	131	58
C	2	82	118	39

4.2.1.3 Compressive failure from horizontal member

Before the tensile failure described in 4.2.1.2, a compressive deformation occurred at the horizontal connection along the nail group in the figure below. Local shear failures started to form along the failure line and local buckling phenomena at one end of the failure. During the test of specimen 23, this compressive failure possibly weakened the connection and made it fail at a lower load. A failure like this is relatively ductile and safe; in our case, other failure modes are more likely to happen before. Calculations made for this type of failure that considers the combination of shear and compressive deformation were not made. Only considering the failure to be in compression appears to be inaccurate and no better models have been evaluated.

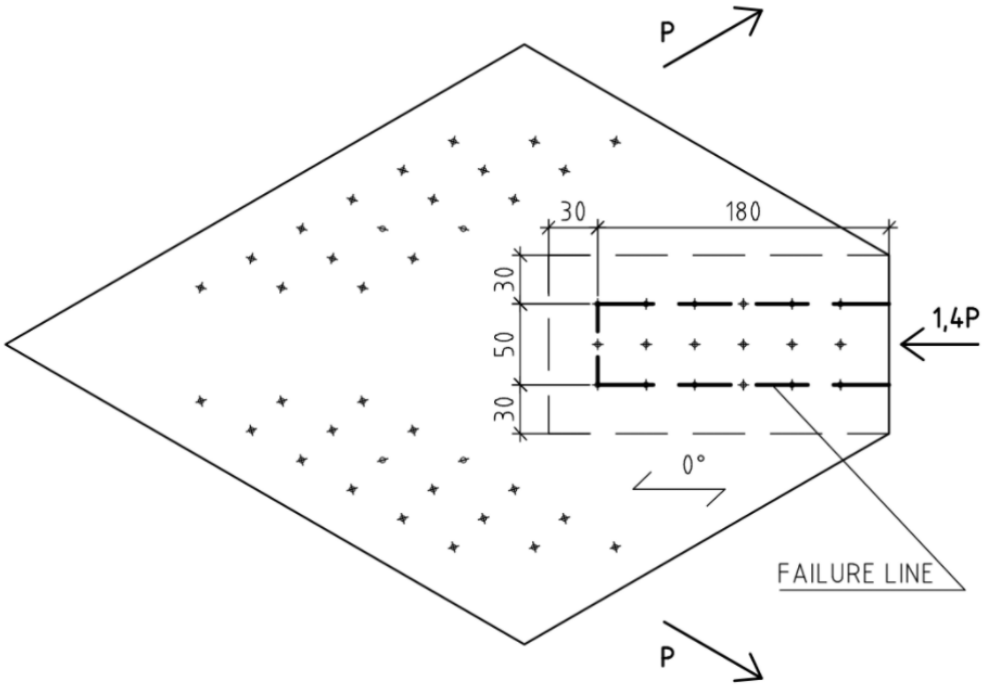

Figure 4.17: Nail group and edge distances beneath the horizontal timber member

4.2.1.4 *Tensile failure from horizontal member*

When the test specimens are loaded with compressive tensile force, stresses develop in the plywood origination from the horizontal member. Pure tensile stresses will develop for plywood with zero degree face grain angle in relation to the horizontal timber member. These stresses are only compared to the tensile strength of the plywood, and no failure criteria are used.

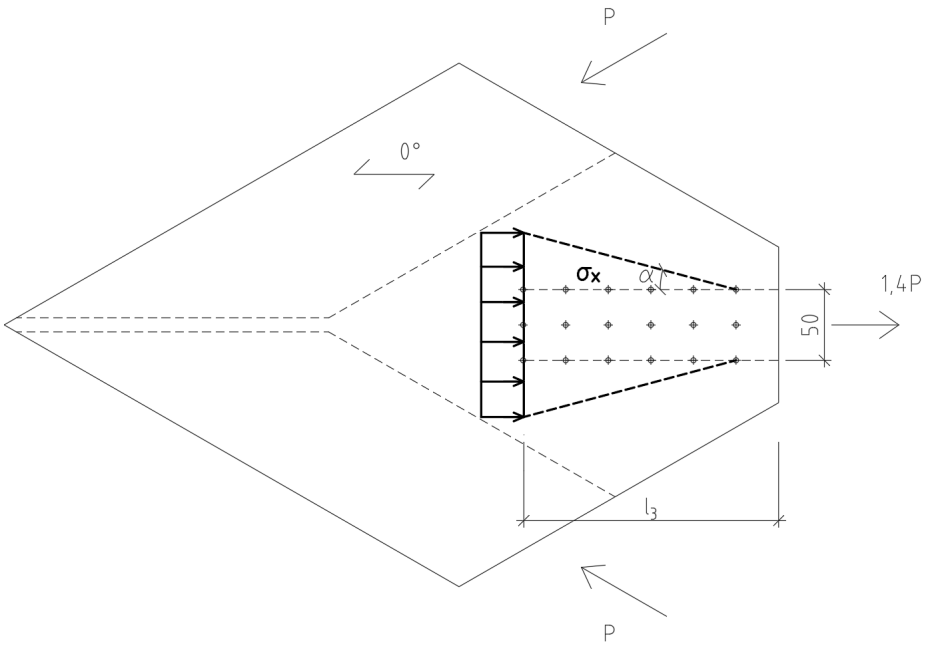

Figure 4.18. Axial stress distribution at the horizontal timber member

In *Table 4.3* three different failure loads are calculated with regard to the angle that the stresses spread at within the range of 10-20 degrees. In addition, two different loads are also presented; one regards the net height where the nail holes are removed, the second one is the brutto height where no regard was taken to the nails.

Table 4.3. Calculated failure loads and angle variations

α **°**	F_{brutto} **kN**	F_{netto} **kN**
10	41	34
15	52	45
20	64	57

4.2.2 Glued connections

In the glued connection, the only failure modes observed in the plywood originated from the horizontal member. The same calculation for the diagonals was conducted for the glued connection but was not close to showing any failure for the loads we were able to achieve during the testing. Therefore, the calculations will focus on the different face grain angles for tensile failure originating from the horizontal member.

4.2.2.1 Tensile failure from horizontal member

These calculations assume that the failure starts with a straight line originating perpendicular to the horizontal timber member. However, for the glued connection, a more complex stress state will develop in the plywood as the forces from all the members will be transferred closer to each other within the plywood.

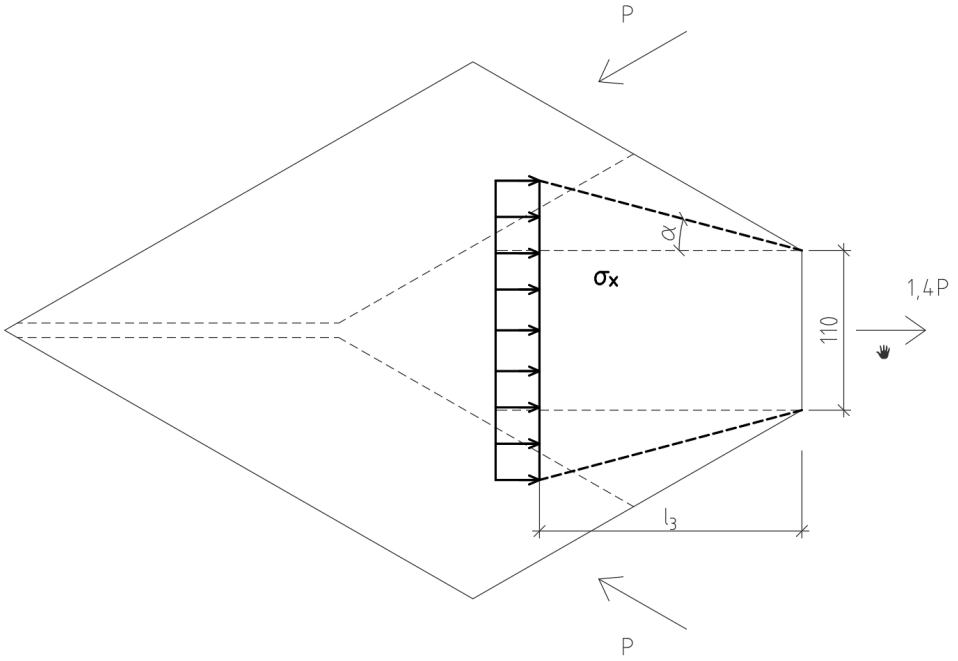

Figure 4.19. Stress distribution at the horizontal timber member, glued

4.2.2.2 Tensile failure from horizontal member, 0° face-grain angle

In *Table 4.4* results are presented from the calculations where the angle at which the stresses spread is varied between 10-20 degrees, as well as the distance to when the failure originates.

Table 4.4. Failure loads in different stress angle variations

l_3 **mm**	**α °**	**F kN**
	10	86
160	15	102
	20	117
	10	83
170	15	98
	20	114
	10	80
180	15	95
	20	111

4.2.2.3 Tensile failure from horizontal member, 5° face-grain angle

For the plywood plates with 5-degree face-grain angle in relation to the horizontal timber member, the tensile force is converted to have a component parallel to grain and one perpendicular. These forces can then be used to calculate the internal stresses and inserted into the Tsai-Wu failure criteria. In *Table 4.5* the results are presented with the same variations as in the zero degrees face-grain setup.

Table 4.5. Failure loads in different stress angle variations

l_3 **mm**	**α °**	**F kN**
	10	78
160	15	91
	20	105
	10	75
170	15	88
	20	102
	10	72
180	15	85
	20	100

4.2.2.4 Tensile failure from horizontal member, 15° face-grain angle

The calculations for the 15 degree face-grain plywood were conducted in the same way as for the five degree setup. The results are presented in *Table 4.6*

Table 4.6: Failure loads in different stress-angle variations

l_3 **mm**	**α °**	**F kN**
	10	61
160	15	71
	20	83
	10	58
170	15	69
	20	80
	10	56
180	15	67
	20	78

4.2.2.5 Comparison between face-grain angles

In *Figure 4.20,* a comparison is made between the previously calculated data. Each data set presented in the graph is from the tables above with the length $l_3 = 170mm$. One can see that the failure load is linearly dependent on the stress distribution angle that is used and that it decreases when the face-grain angle increases.

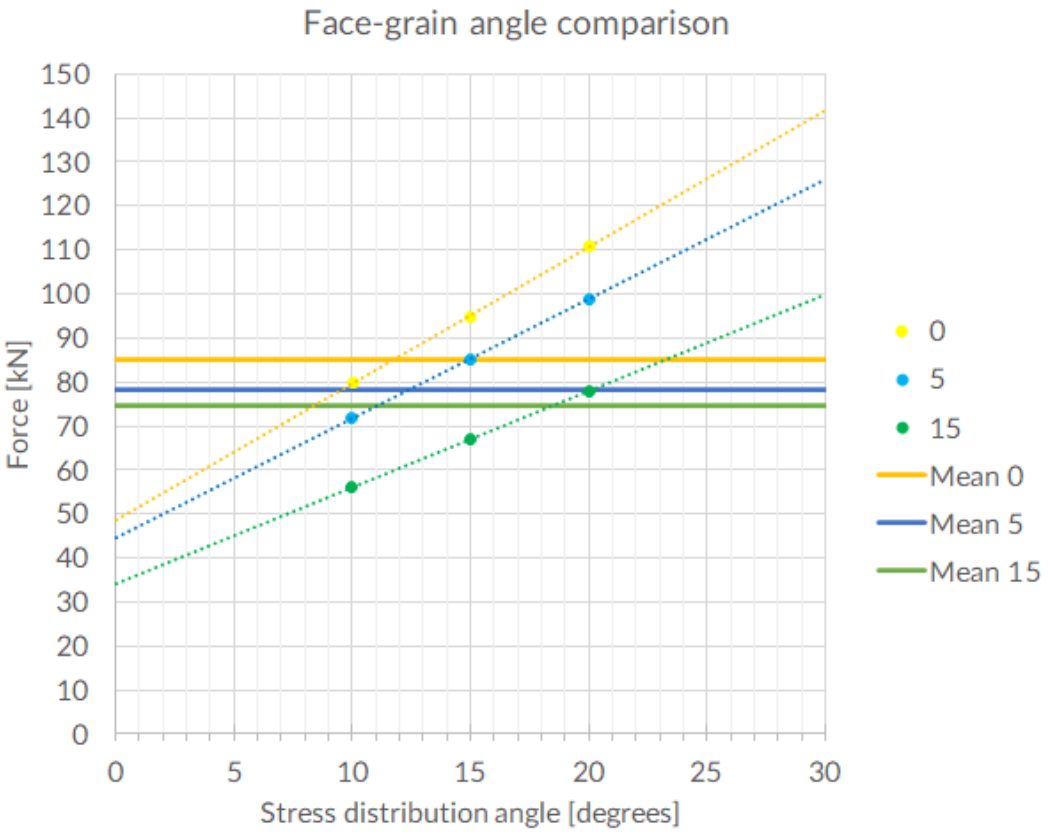

Figure 4.20. Failure loads for different stress distribution angles (x-axis) contra face-grain orientation (y-axis)

4.2.3 Calculations summary

Calculations performed for the failure modes above have the potential to be further developed to offer a higher precision for determining the capacity for gusset plates made of birch plywood. There are multiple variables in the models that have to be decided in order for the calculations to be in line with the test results.

The failure load can be approximated within a relatively small interval for the tensile plywood failures at the horizontal members. To increase the precision of the calculations, the stress spread angle has to be further studied. The calculations in this report ignore the fact that there are complex stress states where the diagonals in compression would increase the shear stresses and counter the tensile stresses. This is simply regarded by moving the failure line from the edge of the beam closer to the specimen center; this was done after studying the failures that occurred during the testing. If this method were to be used in design applications, a safe way to approximate this distance would have to be developed, or the entire length of the tensile zone would have to be used, which would decrease the capacity of the connection.

What can be seen is that linear and quadratic failure criteria are not flexible enough to consider the complex stress states that will develop in parallel connections where the face-grain angle of the plywood is rotated even small angles in relation to the acting force. Therefore, for birch plywood in pure tension with small-angle variations (<30 degrees), the Tsai Wu failure criteria is recommended, which can be seen in the appendix where the quadratic failure criteria differ and more as the face-grain angle increases.

4.3 Simulations

The following simulations were made in RFEM

Only 0° and 15° angle-to-grain variant tests were performed

Table 4.7. Simulations performed in RFEM

Group	Type	Config.	Load
A	Comp.	0°	-80 kN
C	Comp.	15°	-80 kN
D	Tens.	0°	80 kN
F	Tens.	15°	80 kN

4.3.1 Simulation summary

The stress distribution and levels are in line with calculations and test results. For the compressive tests where tensile stresses develop around the horizontal timber member, decreasing the load that the failure according to the Tsai-Wu criterion starts at the end of the timber member. In the tests, the failure occurred further in. In *Figure 4.21* and *Figure 4.23,* this is close to the area where the red area at the top/bottom intersects with the glulam. Therefore, if only small areas in the FEM analysis results in Tsai Wu stresses above, one failure should occur. However, when compared to the test results, it seems as if the failure in the RFEM has to develop between two edges of the plywood to give a capacity similar to that of the test results.

Compressive

Tensile

0°

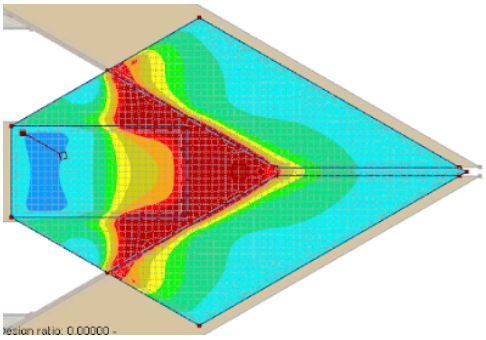

Figure 4.21. Tsai-Wu Critereon simulation A

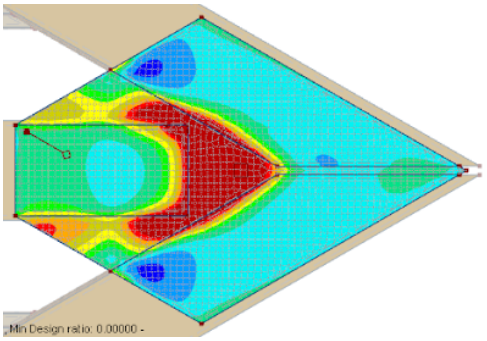

Figure 4.22. Tsai-wu Criterion simulation D

15°

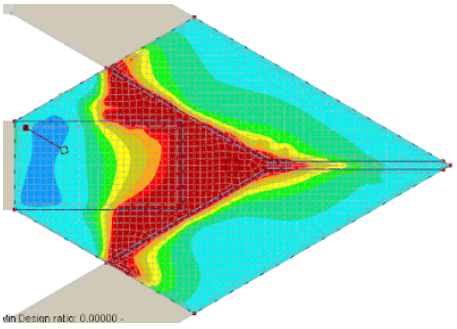

Figure 4.23. Tsai-Wu criterion simulation C

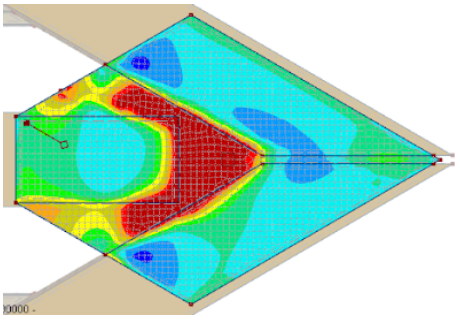

Figure 4.24. Tsai-wu critereon simulation F

In RFEM the simulations where the face-grain angle was rotated 15 degrees, the resulting Tsai Wu stresses were marginally higher in the top of the plate. At the same time, the failure would most likely be assumed to be similar to that of the zero-degree plywood plates. From the tests we could see that the failure started with tensile failure at the bottom of the plate and developing into a combination of tension and shear where the plywood split along the face-grain angle at the top of the plate. To see this fully developed in RFEM the load would have to be increased to around 90 kN leaving us far beyond the values obtained during testing.

Predicting failure in birch plywood under complex stress states is to some extent possible using computer simulations. It is possible to relatively safely predict a range between which the members will start to fail. However, it does not seem to be possible to predict the exact failure lines that would occur.

5 Conclusion

Utilized in timber-to-timber connections, birch plywood has a very high potential as an alternative choice of material compared to steel. Thanks to its workability, many applications and adjustments can be made directly at the construction site, instead of first having to be prepared at a metal workshop.

Thanks to high strength in shear, birch plywood is especially capable of being efficiently designed in structural components subjected to complex stress states. In our tests, we reached tensile stresses very close to that of the mean tensile strength while at the same time being subjected to high shear forces caused by moments. For example, in ordinary structural lumber, where the shear capacity is relatively low, moments and eccentricity would have most likely made the component fail before reaching the axial strength.

What could be seen during the tests is that the relation between the load and face grain angle has an impact. Oversimplified, it could be said that the capacity of the connection decreases by 0.5-1 % for each degree that the load angle differs from the face-grain angle. Therefore, the differences are pretty slight, and for small-angle variations, this alone would not be reason enough to deter anyone from using birch plywood as a material in a connection.

Birch plywood can either be fastened with metal fasteners such as dowels, or it can be glued with a resin such as MUF. Metal fasteners have the advantage of being able to be installed on-site, while glued connections need to be assembled in a more controlled environment regarding temperature, application pressure, and moisture. Timber-to-metal connections also have the advantage of being more ductile, in some cases being a more safe alternative. The main disadvantage of metal fasteners is their price, especially compared to the glued connection. In addition, metal parts need higher precision manufacturing.

Compared to dowel tests, glued specimens were about 37% stronger than dowelled ones, although curing conditions during specimen manufacturing were compromised. MUF Glue is brittle depending on its hardener/resin ratio. It is, however, stronger if more resin is used. This means a trade-off has to be made between its ductility and strength. In many cases during this work, tests failed one horizontal glue-line at a time. Surprisingly enough, almost all of the second glue-line failures of each test failed at a higher load than the first one. This means; first, the weakest glue-line fails, then all of the load is held up by the second glue-line. This means to some extent that the glue lines are stiff enough not to transfer forces between each other. More ductile behavior of the glue can make them work more coherently.
Depending on the design, metal fasteners can provide a more ductile behavior of the connection. To some extent, this can be considered safer. However, since the strength is 37% lower than glued ones, this may not necessarily be an effective trade-off, especially when considering the other advantages of using more wood in a connection.

6 Future work

To further develop the area of timber-to-timber connections, a few other topics are also of interest. These include different aspects concerning manufacturing, behavior of fasteners, calculation models;

- Further research concerning adhesion properties of glue between hardwood/softwood, specifically birch plywood and glulam made of spruce or pine.
- Fastening group behavior such as block shear effects, but in compression, i.e., interaction formula between shear and compressive stresses.

7 References

Aicher, S and W. Klöck. (2001). Linear versus quadratic failure criteria for in-plane loaded wood based panels. *Otto-Graff-Journal*. 12: 187-199

A.H. Conner. Wood: Adhesives. Encyclopedia of Materials: Science and Technology. *Elsevier*. (2001). Pages 9583-9599. [online] Available at: https://www.sciencedirect.com/science/article/pii/B0080431526017344/ [Accessed 1 June 2021].

Cabrero, M and Gebremedhin, K. (2010). Evaluation Of Failure Criteria In Wood Members. [Conference Paper]. *World Conference On Timber Engineering*. Trento. Italy.

Dynea. (2021). Melamine-urea adhesives. [online] Available at: https://dynea.com/products/product-technology/melamine-urea/ [Accessed 5 June 2021].

Eberhardsteiner, J. (2002). Mechanisches Verhalten von Fichtenholz. Vienna, Austria: Springer.

Falk, R. and Colling, F. (1995). Laminating Effects in Glued-Laminated Timber Beams. *Journal of Structural Engineering*, 121(12).

Finnish Forest Industries Federation. (2002). Handbook Of Finnish Plywood.

Hallqvist, A. (1978). Energy consumption: Manufacture of building materials and building construction. *Habitat International*. [online] Available at: http://www.sciencedirect.com/science/article/pii/0197397578900188/ [Accessed 1 June 2021].

IEA. 2020a. Iron and Steel Technology Roadmap, IEA, Paris. [online] Available at: https://www.iea.org/reports/iron-and-steel-technology-roadmap [Accessed 1 June 2021].

IEA. 2020b. Cement, IEA, Paris. [online] Available at: https://www.iea.org/reports/cement [Accessed 1 June 2021].

Johansen, K.W. (1949). Theory of timber connections. *IABSE publications = Mémoires AIPC = IVBH Abhandlungen*.

Smith, R. (2016). Understanding & working with wood defects | Woodworking Network. [online] Woodworking Network. Available at: https://www.woodworkingnetwork.com/best-practices-guide/solid-wood-machining/understanding-working-wood-defects [Accessed 10 June 2021].

Svenska institutet för standarder, SIS. (2021). Bygghandlingar 90. [online] Available at:

https://www.sis.se/konstruktionochtillverkning/bygg/bygghandlingar-90-ritningar/ [Accessed 8 June 2021].

Svenskt trä. (2015). Träprodukter lagrar kol. [online] Available at: https://www.traguiden.se/om-tra/miljo/miljoeffekter/miljoeffekter/traprodukter-lagrar-kol/
[Accessed 1 June 2021].

Svenskt trä. (2016). Design of timber structures. 2nd ed. Stockholm: Swedish Forest Industries Federation, p.41.

Vegard Kilde, Kjell Helge Solli, Birte Pitzner, Per Lind and Jan Bramming. (2006). Björk i synlige konstruksjoner. *Norsk Treteknisk Institutt*

Wang, T., Wang, Y., Crocetti, R., & Wålinder, M. (2020). Prediction of the tensile strength of birch plywood at varying angles to grain. In 16th Annual Meeting of the Northern European Network for Wood Science and Engineering (pp. 80-82).

Wang, Y., Wang, T., Crocetti, R., & Wålinder, M. (2021). Mechanical properties of acetylated birch plywood loaded parallel to the face grain. World Conference on Timber Engineering WCTE2021,

Wang, T., Wang, Y., Crocetti, R., & Wålinder, M. (2021). Multiple shear plane timber connections with birch plywood and dowel-type fasteners. 17th Annual Meeting of the Northern European Network for Wood Science and Engineering,

WoodProducts. (2021a). Moisture properties of wood. [online] Available at: https://www.woodproducts.fi/content/moisture-properties-wood/
[Accessed 7 June 2021].

Wood Products. (2021b). Strength properties of wood. [online] Available at: https://www.woodproducts.fi/content/wood-a-material-1/
[Accessed 7 June 2021].

8 Appendix

8.1 Appendix A - Testing results

8.1.1 Specimen results

8.1.1.1 Specimen 01

Test type	Compressive
Connection type	Screw-Glued
Angle-to-grain	0
Failure	Diagonally both horizontal glue-lines

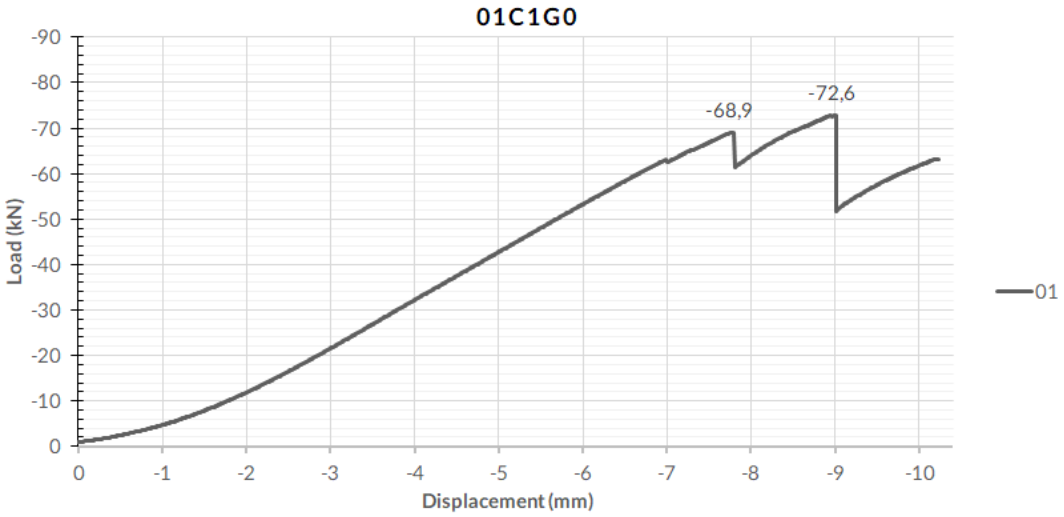

Figure A1.1.1. Testing diagram of specimen 01

Figure A1.1.2 .Specimen 01

Figure A1.1.3. Where failures occured

Figure A1.1.4. Glueline failure horizontal member 1

Figure A1.1.5. Glueline failure horizontal member 2

8.1.1.2 Specimen 02

Test type	Compressive
Connection type	Screw-Glued
Angle-to-grain	0
Failure	Horizontal glue line failure

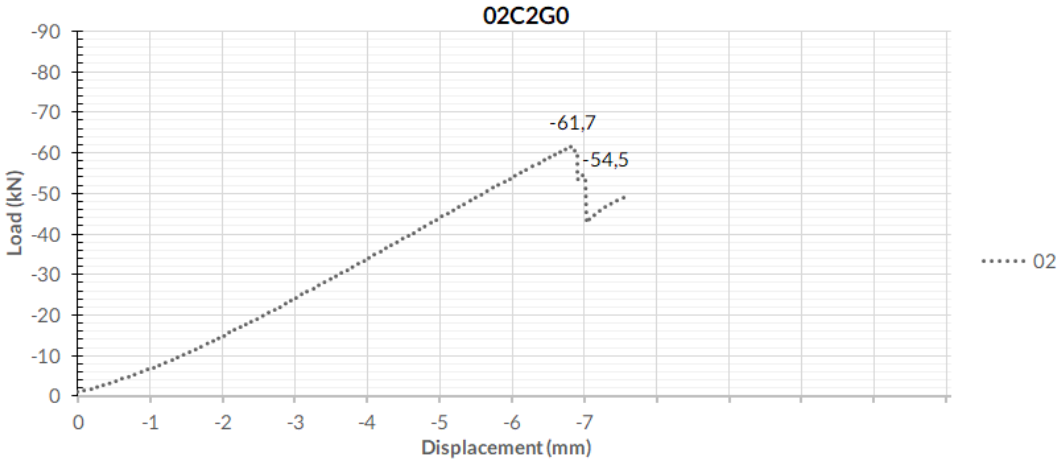

Figure A1.2.1 Testing diagram of specimen 02

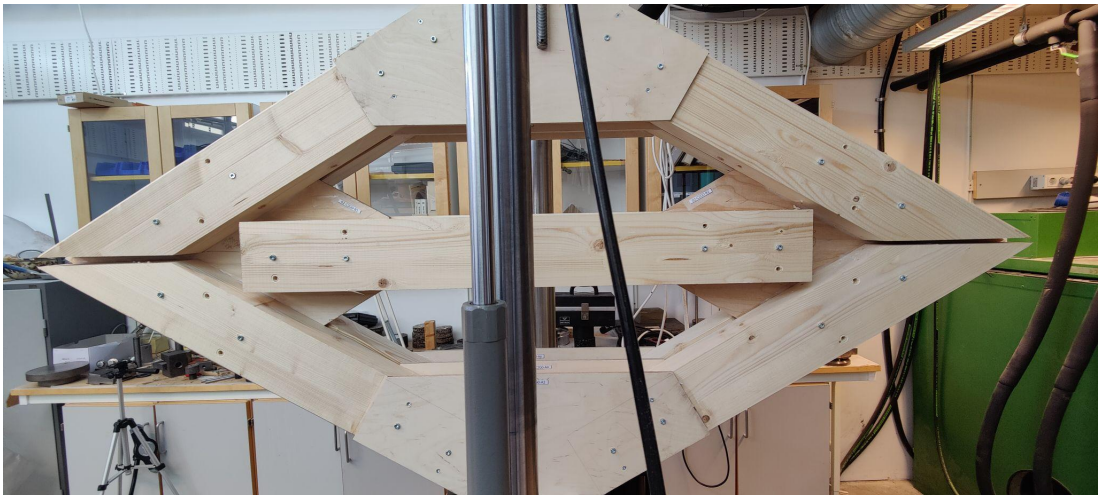

Figure A1.2.2. Specimen 02

Figure A1.2.3. Location of failue 1 (glueline horizontal)

Figure A1.2.4. Location of failure 2 (glueline horizontal)

8.1.1.3 Specimen 03

Test type	Compressive
Connection type	Screw-Glued
Angle-to-grain	0
Failure	Horizontal glue-line failure

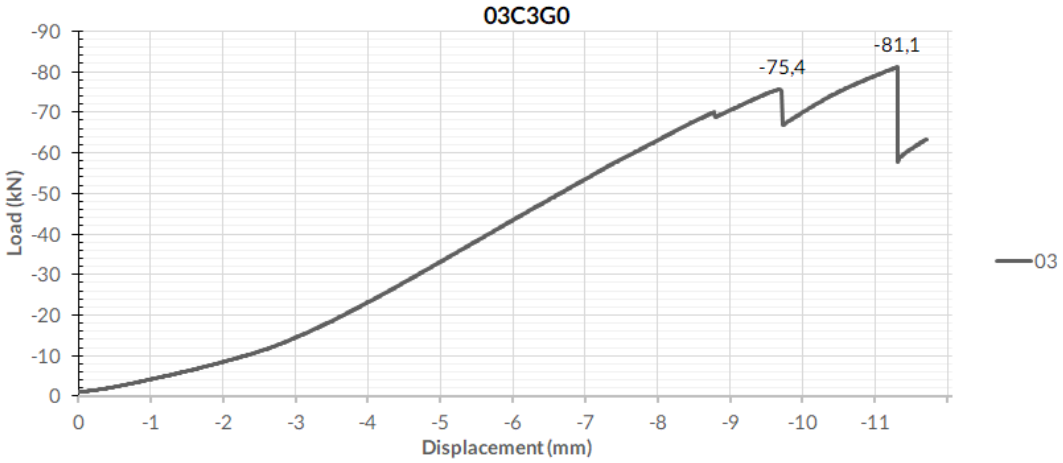

Figure A1.3.1. Testing diagram of specimen 03

Figure A1.3.2. Specimen 03

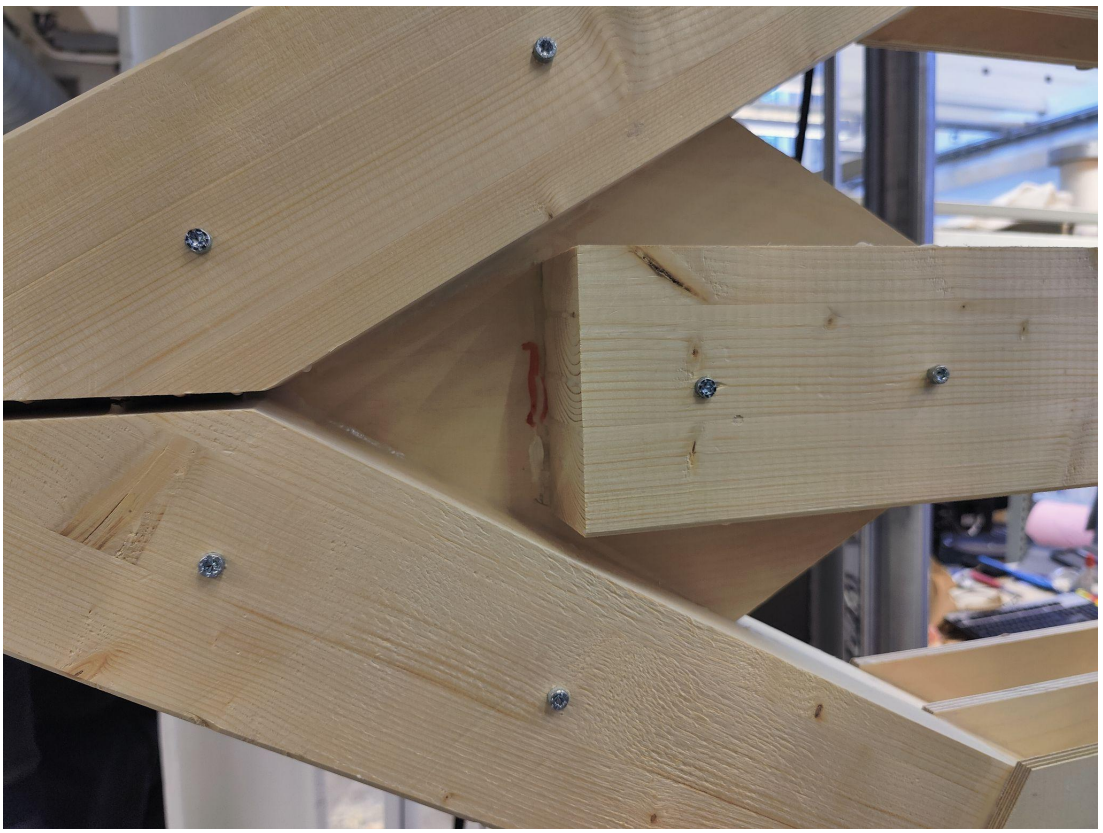

Figure A1.3.3. Location of failue 1 (glueline horizontal)

Figure A1.3.4. Location of failue 2 (glueline horizontal)

8.1.1.4 Specimen 04

Test type	Compressive
Connection type	Screw-Glued
Angle-to-grain	0
Failure	Horizontal glue-line/timber failure

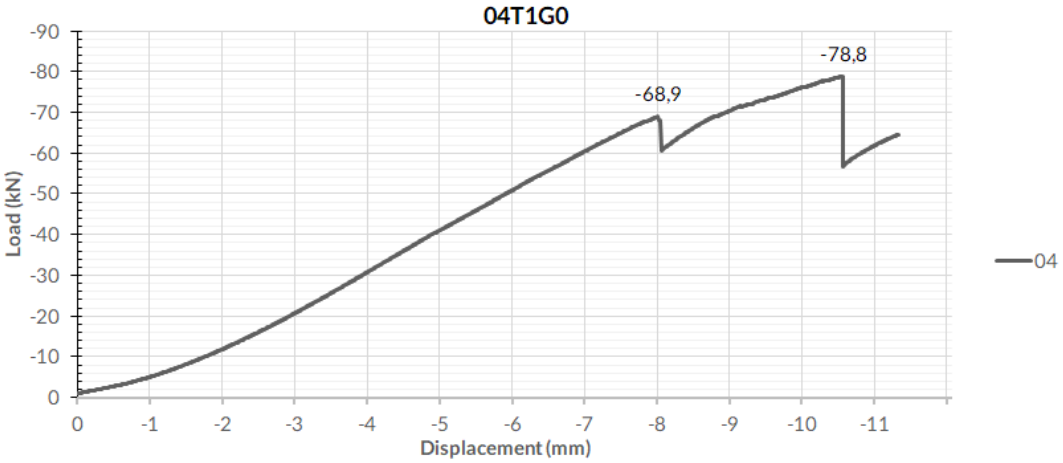

Figure A1.4.1. Testing diagram of specimen 04

Figure A1.4.2. Specimen 04

Figure A1.4.3. Glueline failure

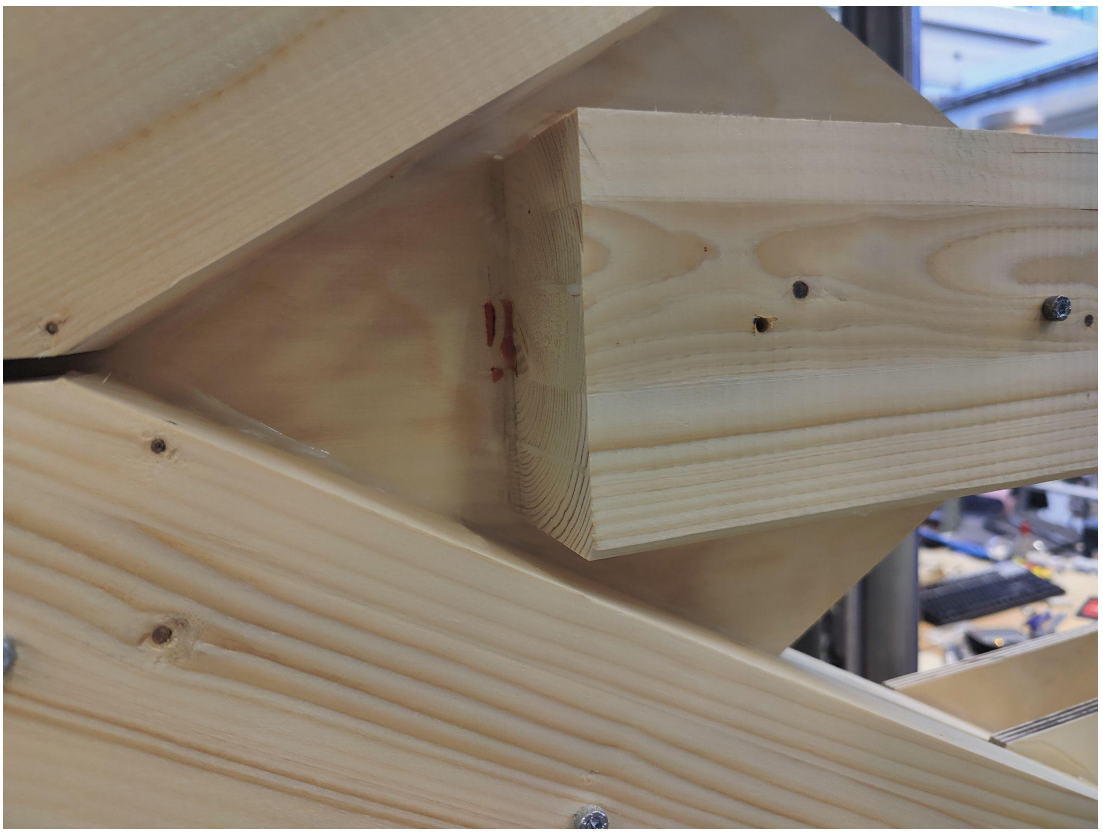

Figure A1.4.4. Glueline failure

8.1.1.5 Specimen 05

Test type	Compressive
Connection type	Screw-Glued
Angle-to-grain	0
Failure	Horizontal glue-line failure at 65,5 kN
	Then failure at 85,2 kN

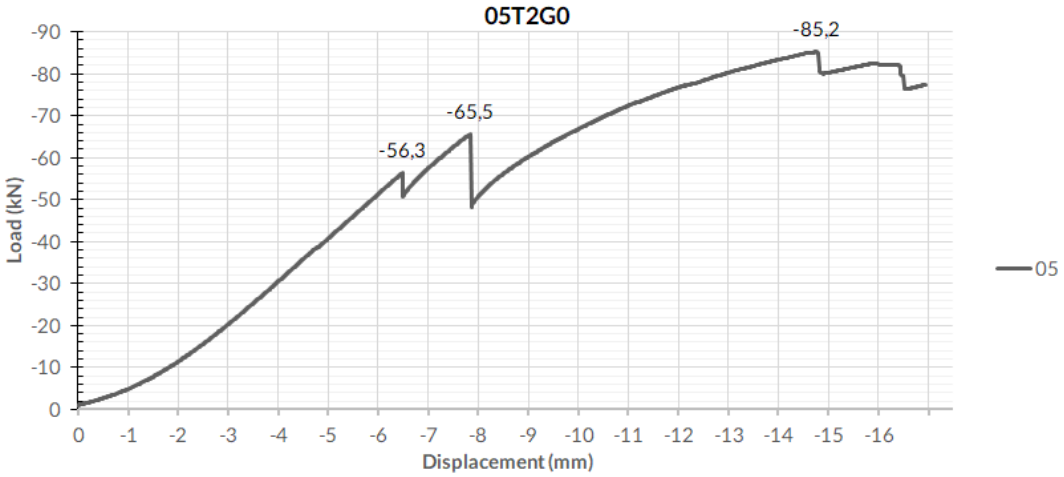

Figure A1.5.1. Testing diagram of Specimen 05

Figure A1.5.2. Specimen 05

Figure A1.5.3. Especially bad glue-line

8.1.1.6 Specimen 06

Test type	Tensile
Connection type	Screw-Glued
Angle-to-grain	0
Failure	Various timber failures

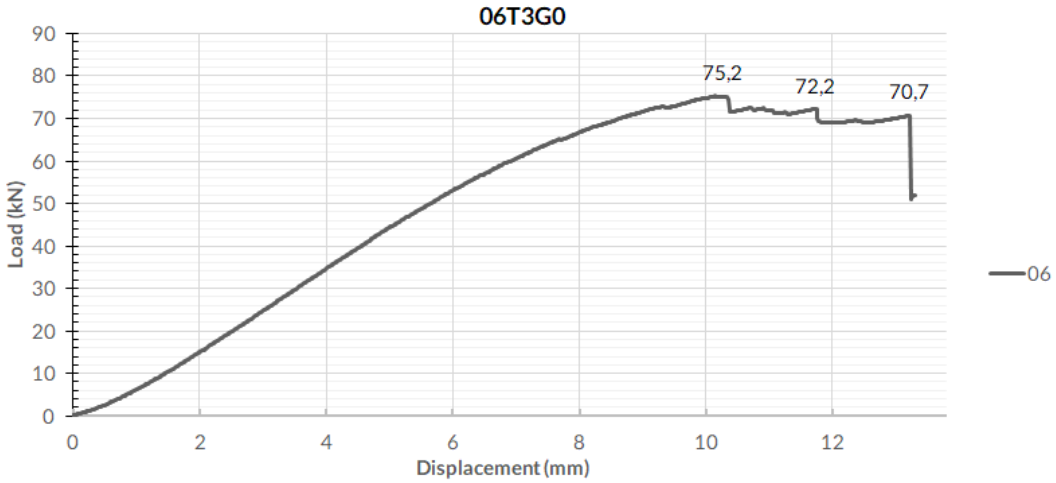

Figure A1.6.1. Testing diagram of specimen 06

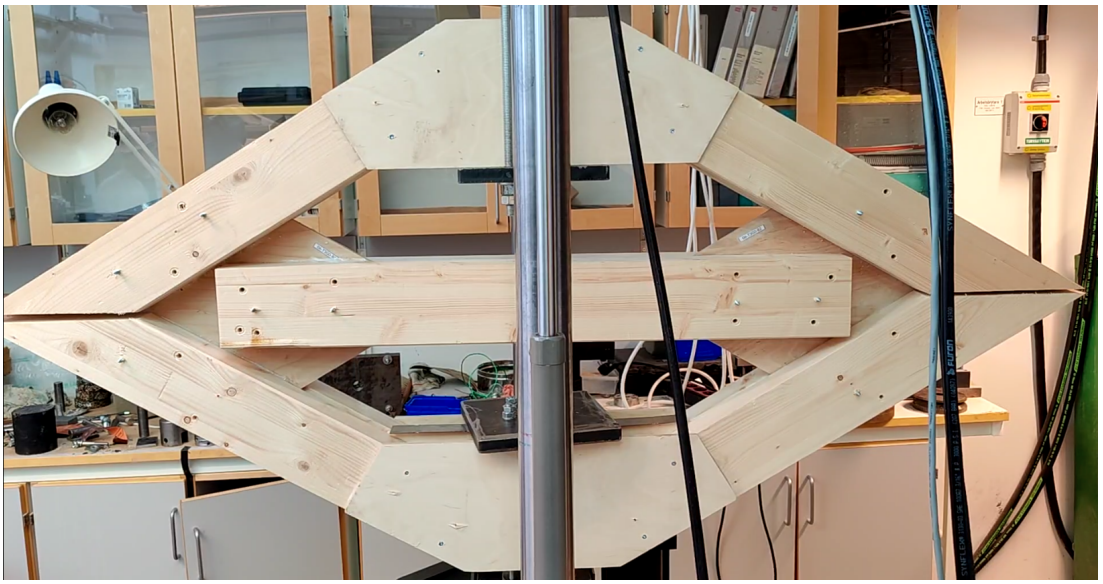

Figure A1.6.2. Specimen 06

Figure A1.6.3. Timber failure in diagonal of specimen 6

Figure A1.6.4. Timber failure in horizontal of specimen 6

Figure A1.6.5. Timber failure in diagonal of specimen 6

8.1.1.7 Specimen 07

Test type	Compressive
Connection type	Screw-Glued
Angle-to-grain	5
Failure	First horizontal glue-line failure at 80,1 kN
	Then failure at 85,2 kN

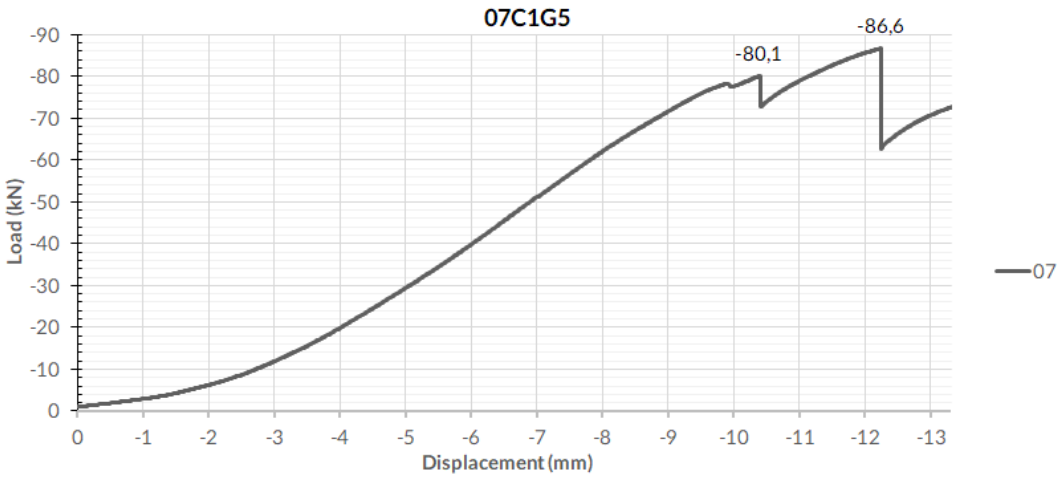

Figure A1.7.1. Testing diagram of specimen 7

Figure A1.7.2 Specimen 07 before testing

Figure A1.7.3 Glue-line failure

Figure A1.7.4 Deformation of nail

Figure A1.7.5 Glue-line failure

8.1.1.8 Specimen 08

Test type	Compressive
Connection type	Screw-Glued
Angle-to-grain	5
Failure	Horizontal glue-line failure at 70,7 kN
	Then plywood failure at 81,8 kN

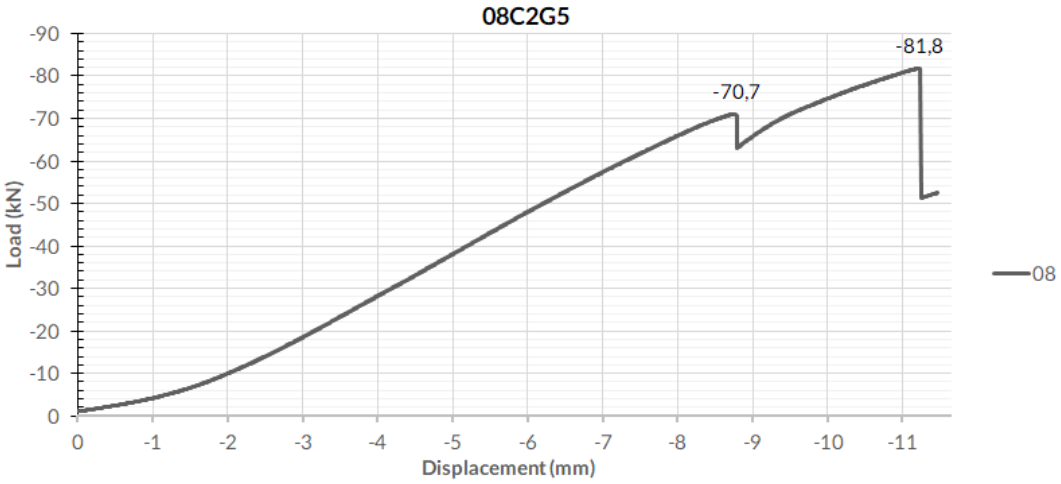

Figure A1.8.1 Testing diagram of specimen eight

Figure A1.8.2 Specimen before testing

Figure A1.8.3 Tensile failure in plywood

Figure A1.8.4 Tensile failure in plywood

8.1.1.9 Specimen 09

Test type	Compressive
Connection type	Screw-Glued
Angle-to-grain	5
Failure	Tensile failure in plywood

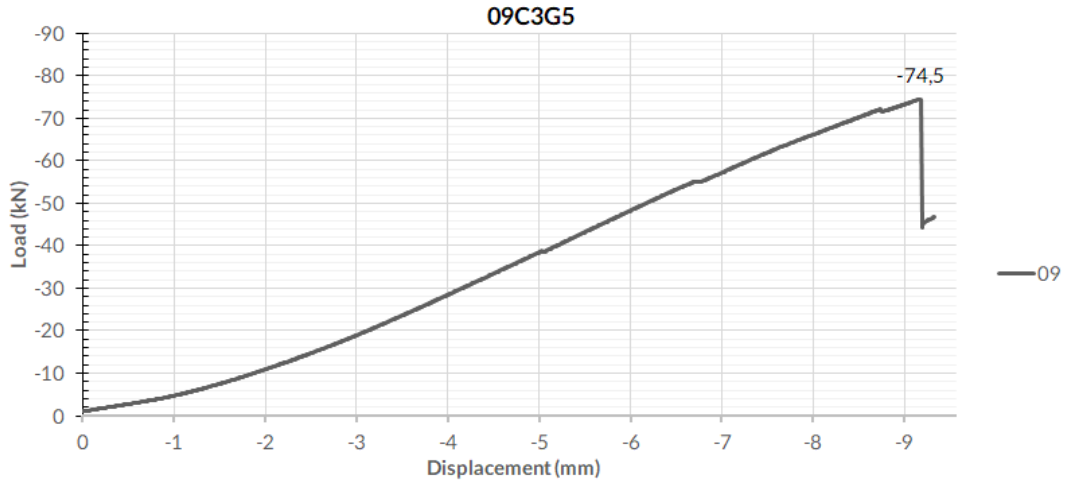

Figure A1.9.1 Testing diagram of specimen nine

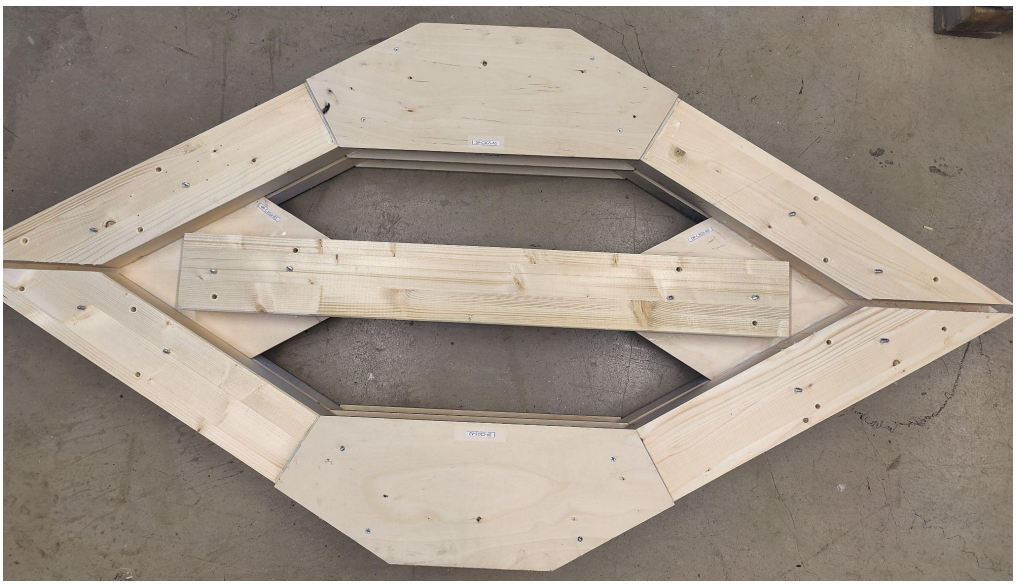

Figure A1.9.2 Specimen before testing

Figure A1.9.3 Tensile failure in plywood

Figure A1.9.4 Plywood failure, area is painted to measure strain using camera technology

Figure A1.9.5 Plywood failure broken off after testing

8.1.1.10	*Specimen 10*
Test type	Tensile
Connection type	Screw-Glued
Angle-to-grain	15
Failure	Various failures

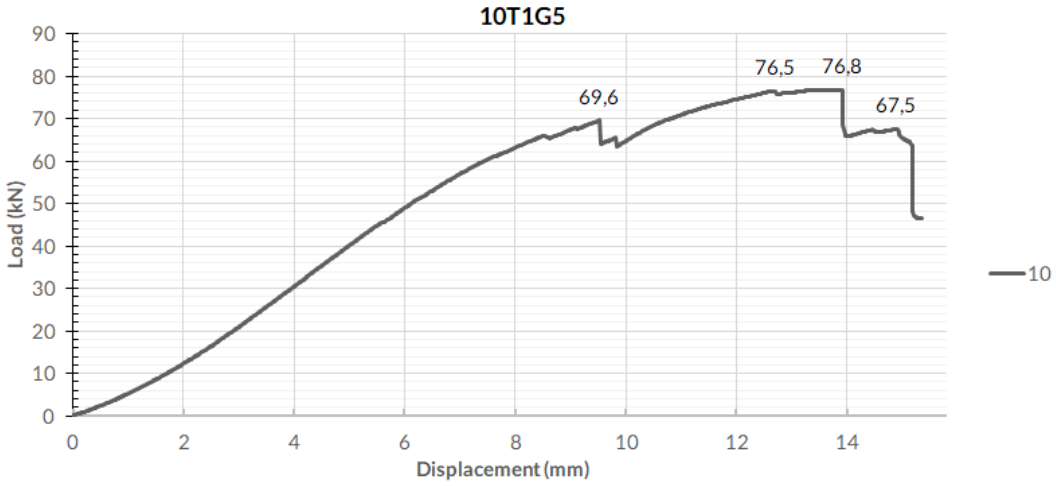

Figure A1.10.1 Testing diagram of specimen 10

Figure A1.10.2 Specimen before testing

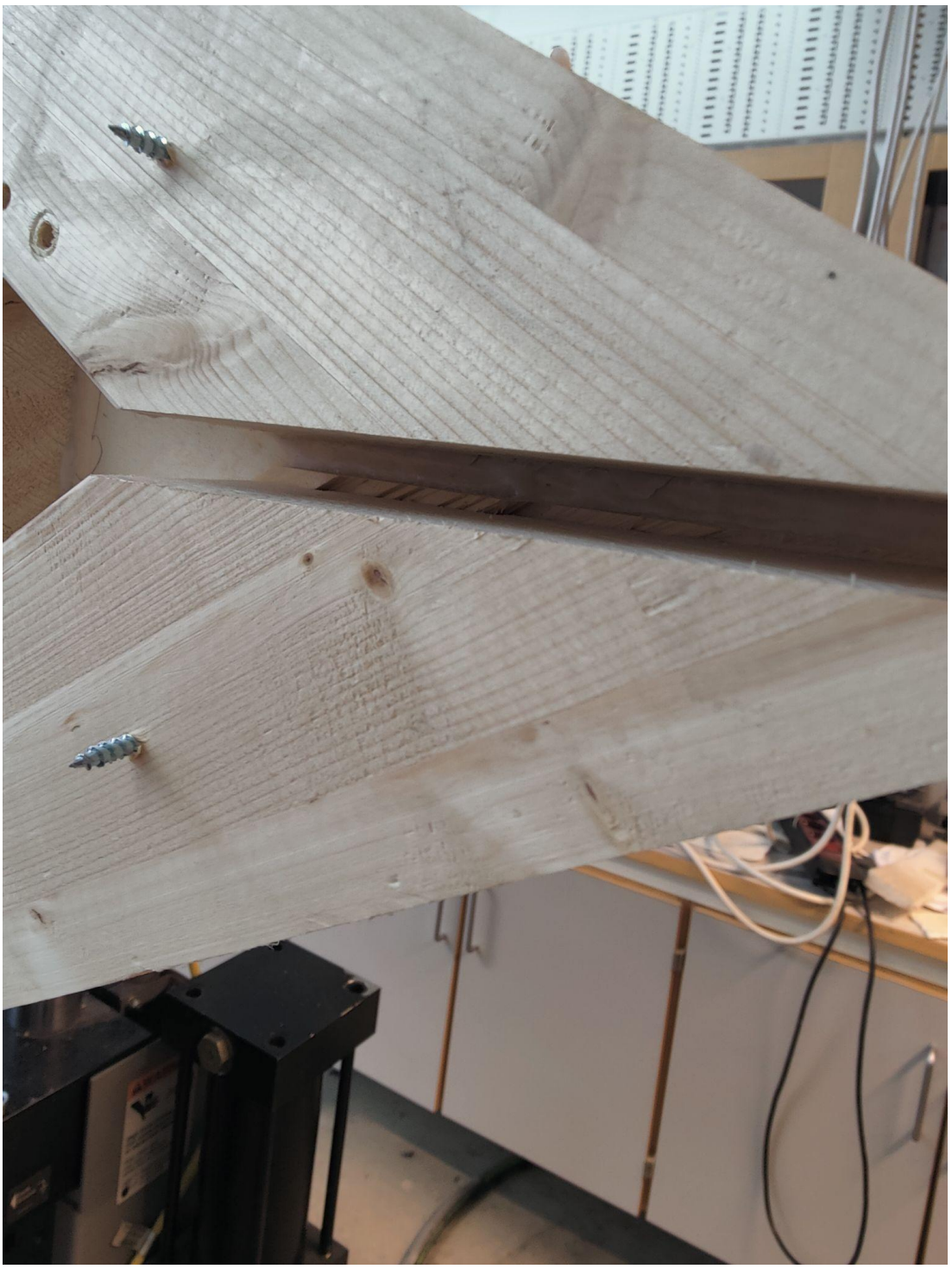

Figure A1.10.3 Delamination in glulam

Figure A1.10.4 Small crack in plywood

Figure A1.10.5 Failure in plywood

Figure A1.10.6 Glue-line failure, delamination

8.1.1.11 Specimen 11

Test type	Compressive
Connection type	Screw-Glued
Angle-to-grain	5
Failure	Horizontal glue-line failure at 70,2 kN
	Then failure at 77,2 kN

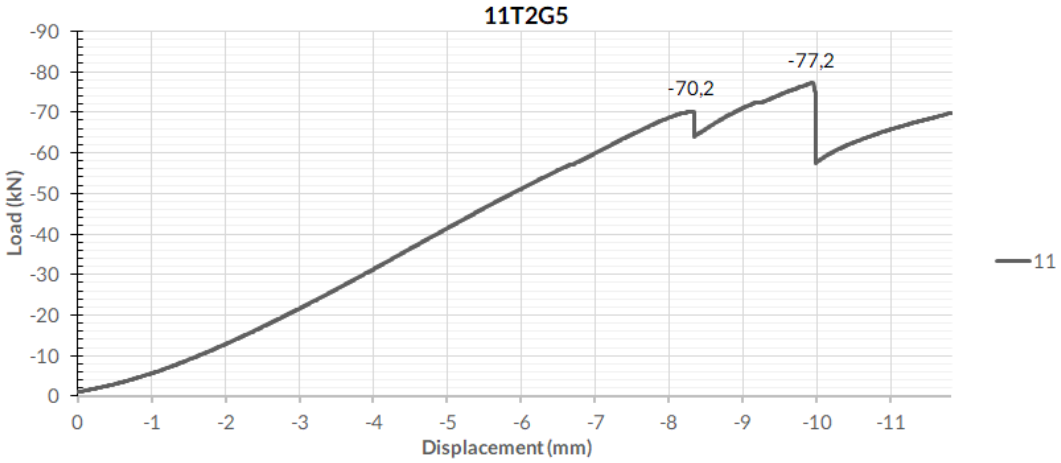

Figure A1.11.1 Testing diagram of specimen 11

Figure A1.11.2 Specimen before testing

Figure A1.11.3 Glue-line failure, slip

Figure A1.11.4 Glue-line failure, slip

8.1.1.12 Specimen 12

Test type	Tensile
Connection type	Screw-Glued
Angle-to-grain	5
Failure	Various failures

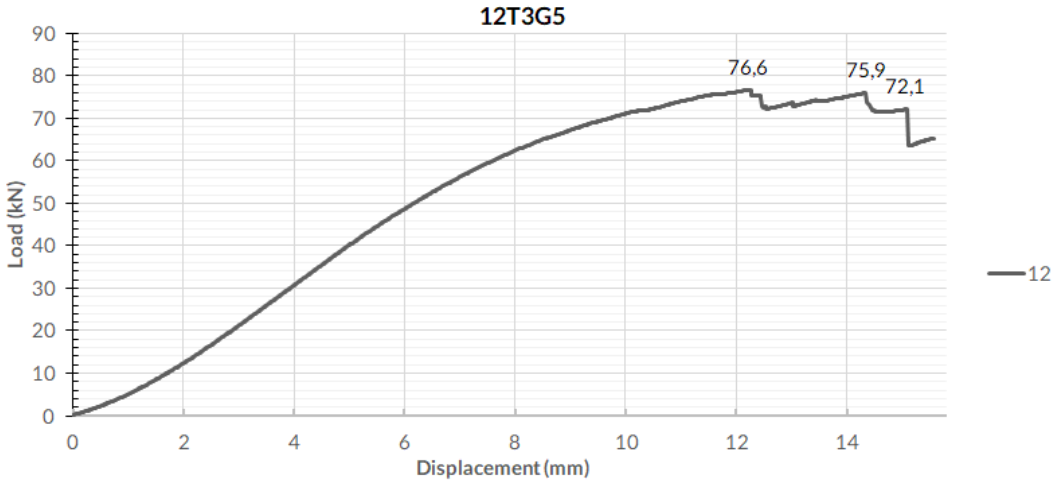

Figure A1.12.1 Testing diagram of specimen 12

Figure A1.12.2 Specimen before testing

Figure A1.12.3 Shear failure in glulam

Figure A1.12.4 Shear failure in timber and glue-line failure at top gusset plate

8.1.1.13 Specimen 13

Test type	Compressive
Connection type	Screw-Glued
Angle-to-grain	15
Failure	Various failures

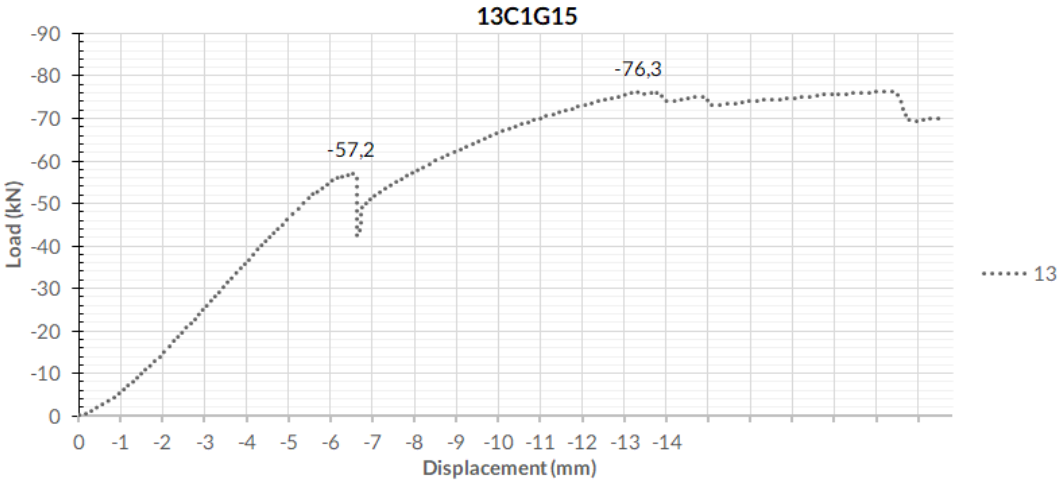

Figure A1.13.1 Testing diagram of specimen 13

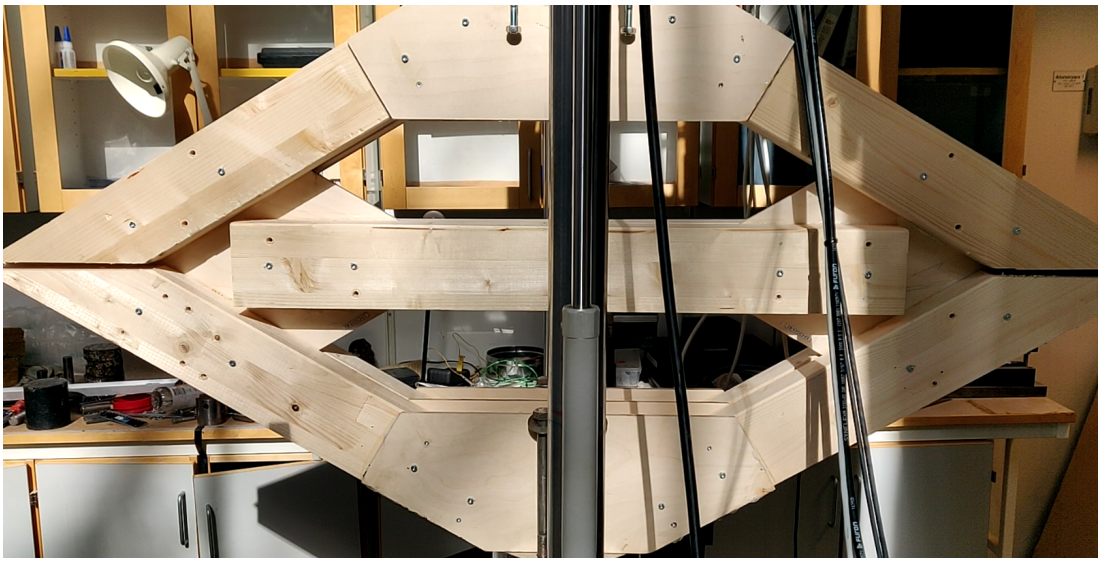

Figure A1.13.2 Specimen mounted in test rig

Figure A1.13.3 Glue-line failure at horiontal member, slip and small crack

Figure A1.13.4 Glue-line failure

Figure A1.13.5 Deformation of screws

8.1.1.14 Specimen 14

Test type	Compressive
Connection type	Screw-Glued
Angle-to-grain	15
Failure	Horizontal glue-line failure at 56,2 kN
	Then plywood failure at 68,2 kN

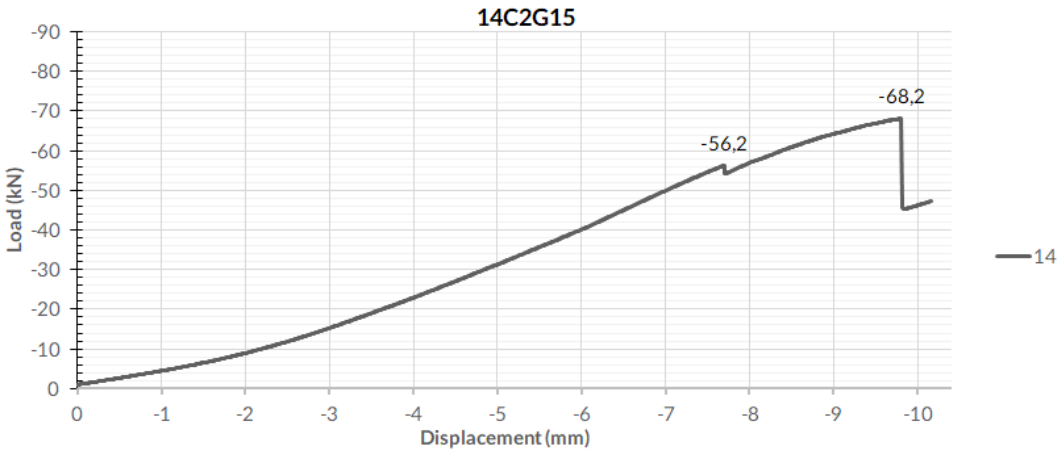

Figure A1.14.1 Testing diagram of specimen 14

Figure A1.14.2 Specimen before testing

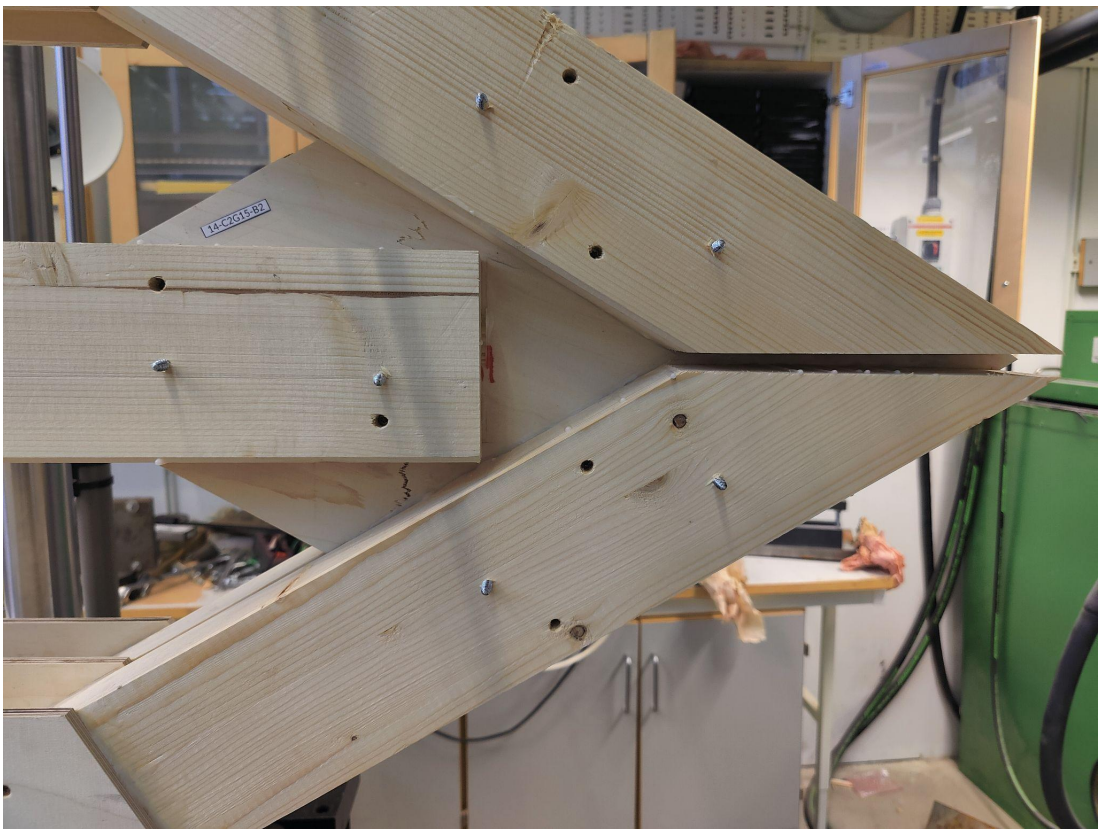

Figure A1.14.3 Tensile failure in plywood

Figure A1.14.4 Tensile failure in plywood

8.1.1.15 Specimen 15

Test type	Compressive
Connection type	Screw-Glued
Angle-to-grain	15
Failure	Plywood failure at 76,2 kN

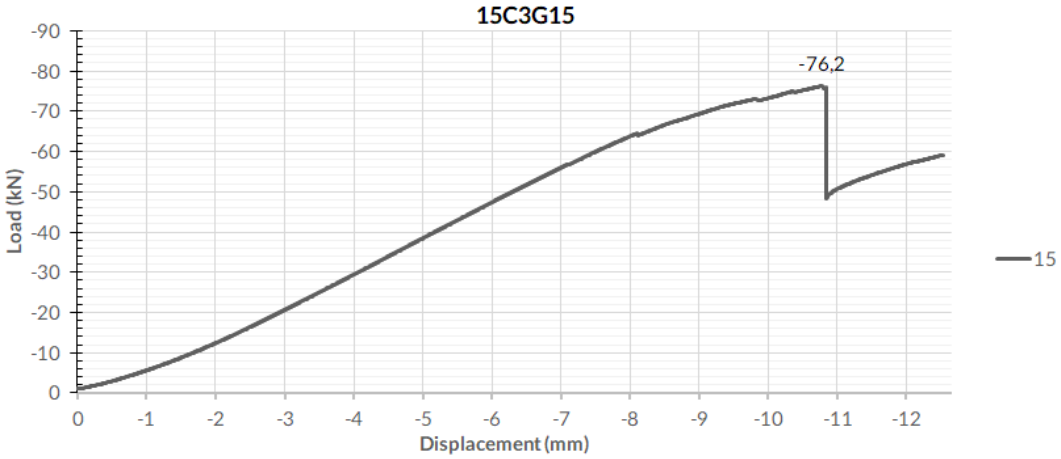

Figure A1.15.1. Testing diagram of specimen 15

Figure A1.15.1 Specimen before testing

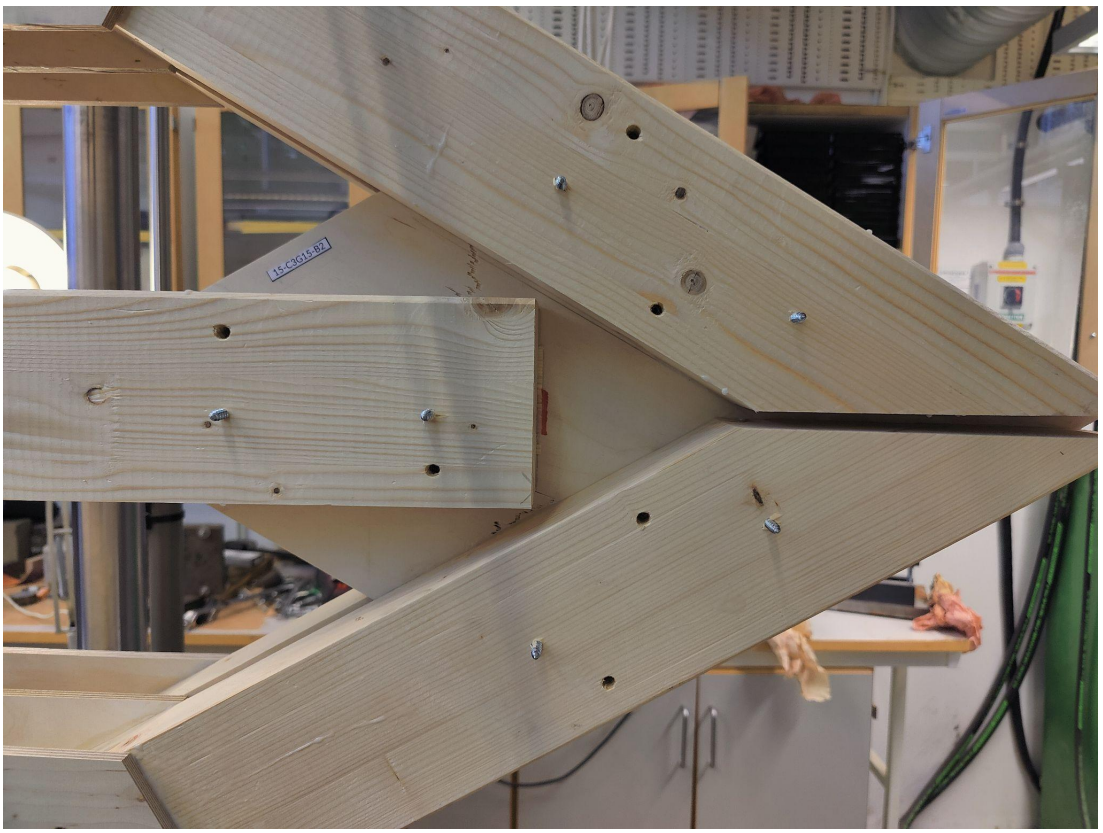

Figure A1.15.3 Tensile failure in plywood

Figure A1.15.4 Tensile failure in plywood

8.1.1.16 Specimen 16

Test type	Compressive
Connection type	Screw-Glued
Angle-to-grain	15
Failure	Horizontal glue-line failure at 72,7 kN
	Then failure at 79,5 kN

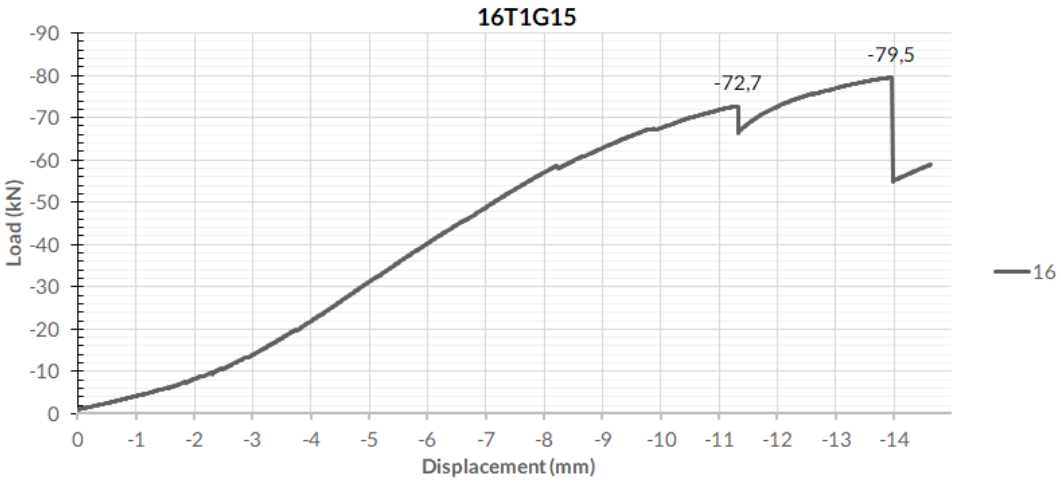

Figure A1.16.1 Testing diagram of specimen 16

Figure A1.16.2 Specimen before testing

Figure A1.16.3 Tension/shear failure in plywood

Figure A1.16.4 Tension/shear failure in plywood

8.1.1.17 Specimen 17

Test type	Compressive
Connection type	Screw-Glued
Angle-to-grain	15
Failure	Horizontal glue-line failure at 77,0 kN
	Then failure at 75,3 kN

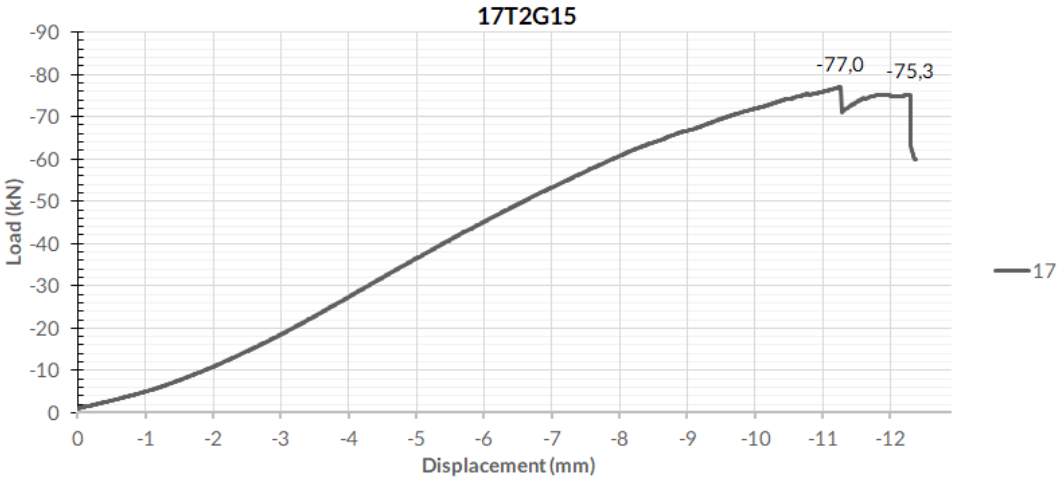

Figure A1.17.1. Testing diagram of specimen 17

Figure A1.17.2 Specimen before testing

Figure A1.17.3 Tension/shear failure in plywood

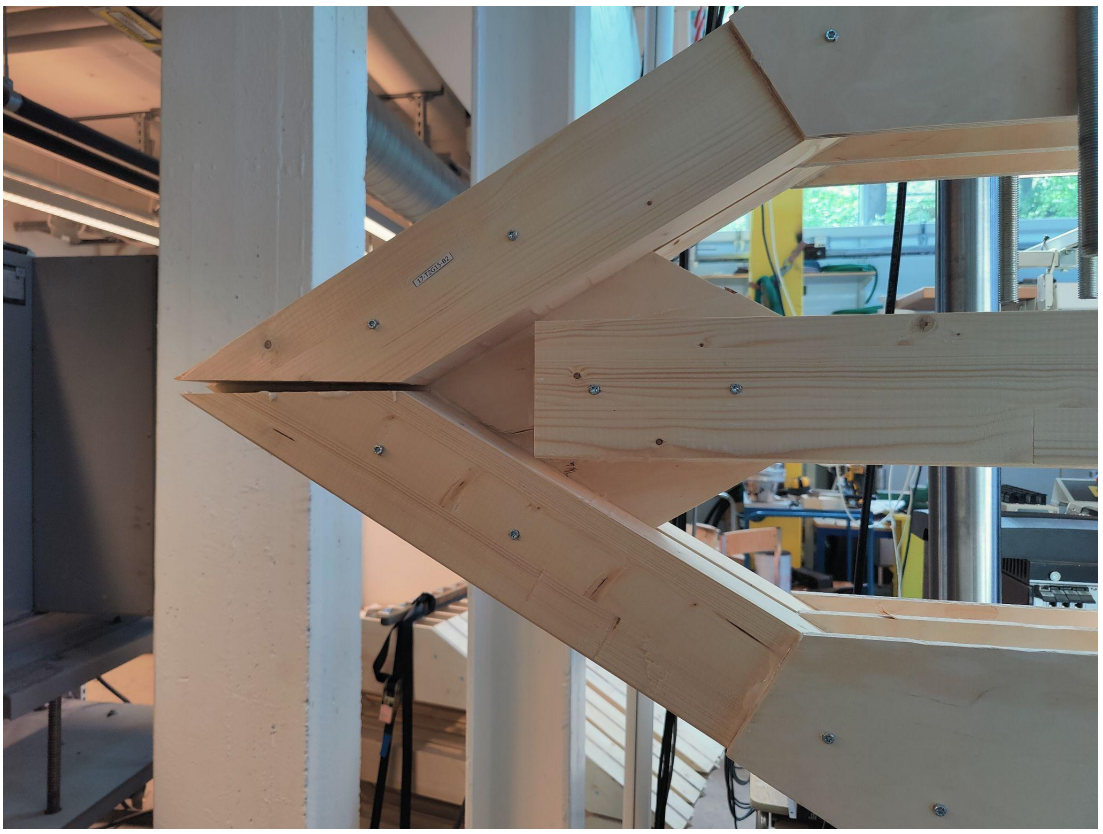

Figure A1.17.4 Tension/shear failure in plywood

Figure A1.17.5 Delamination at gusset plates, 1st failure

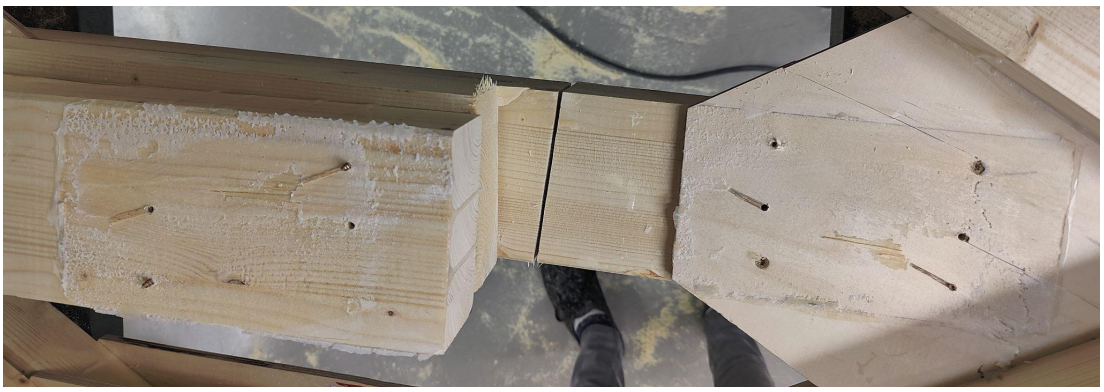

Figure A1.17.6 Glue-line failure at horizontal member

Figure A1.17.7 Glue-line failure at horizontal member

8.1.1.18	*Specimen 18*
Test type	Tensile
Connection type	Screw-Glued
Angle-to-grain	15
Failure	Various failures
	Non complete plywood failure beneath diagonal at middle plate

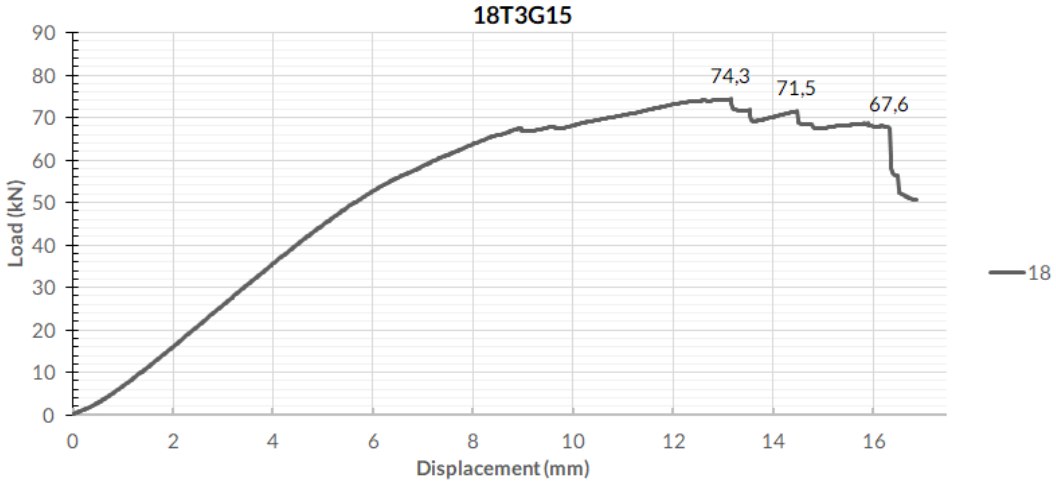

Figure A1.18.1 Testing diagram of specimen 18

Figure A1.18.2 Specimen before testing

Figure A1.18.3 Shear failure in glulam

Figure A1.18.4 Glue-line failure at horizontal member

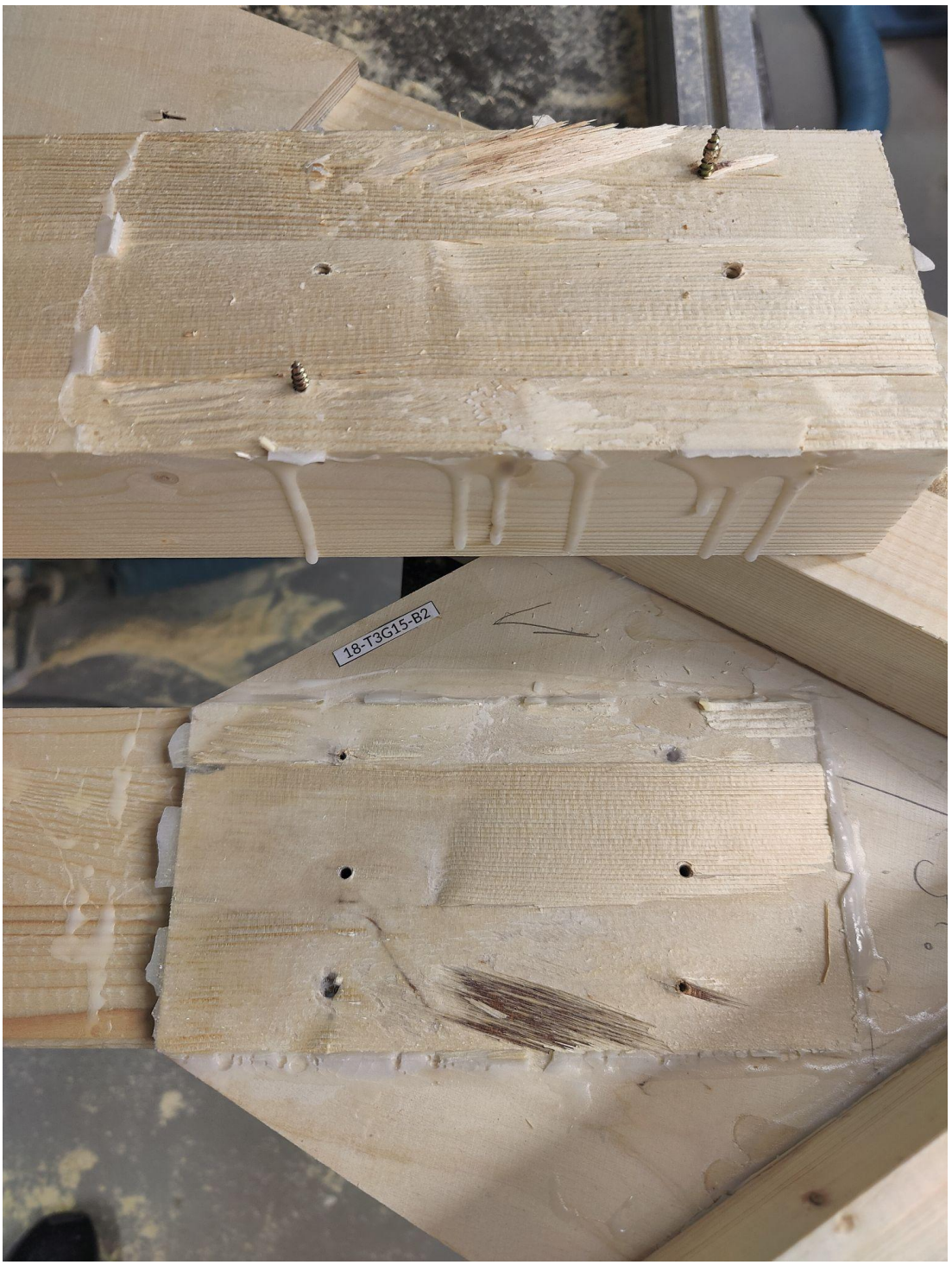

Figure A1.18.5 Glue-line failure at horizontal member

Figure A1.18.6 Glue-line failure at horizontal member

Figure A1.18.7 Glue-line failure at horizontal member

Figure A1.18.8.

Figure A1.18.9.

Figure A1.18.10.

8.1.1.19 Specimen 19

Test type	Compressive
Connection type	Doweled
Angle-to-grain	0
Failure	Plywood plate
	Tensile failure at 46 kN

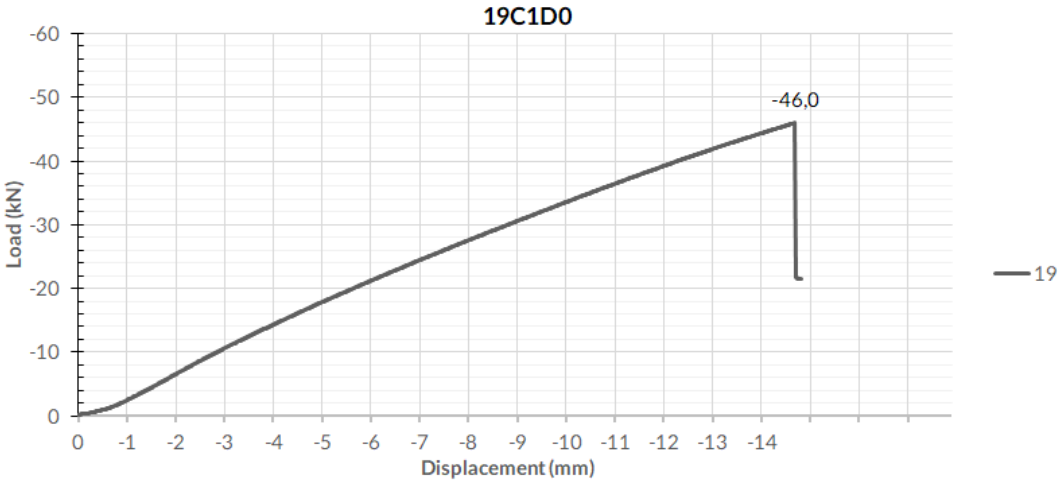

Figure A1.19.1 Testing diagram of specimen 19

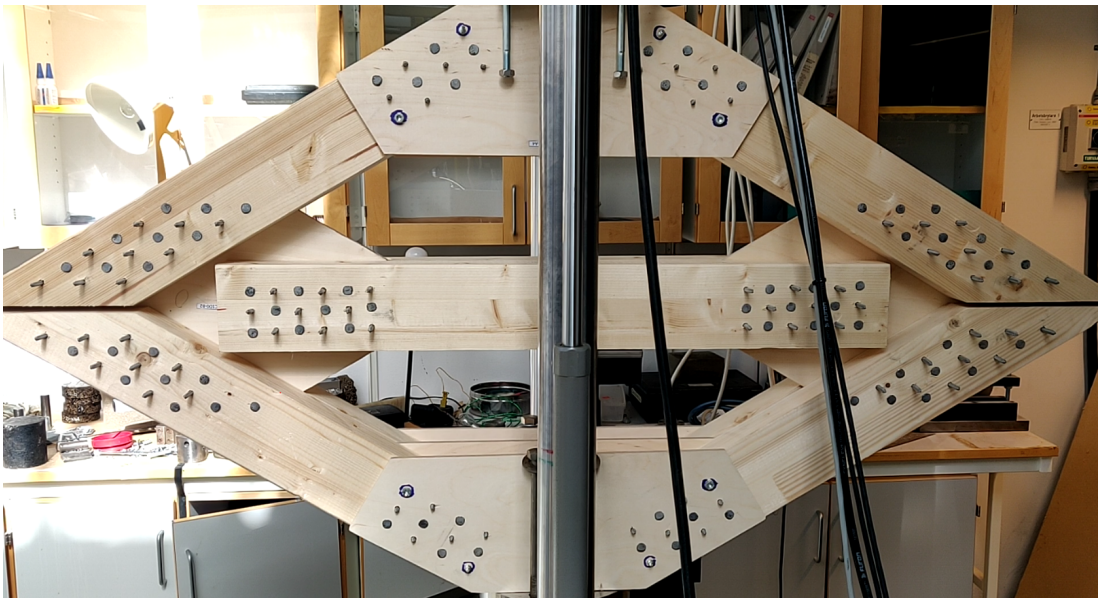

Figure A1.19.2 Specimen mounted in test rig

Figure A1.19.3 Plywood failure in tension around horizontal timber member

8.1.1.20	*Specimen 20*
Test type	Tension
Connection type	Doweled
Angle-to-grain	0
Failure	No failure in plywood plate B
	Various failures from 58 to 64 kN

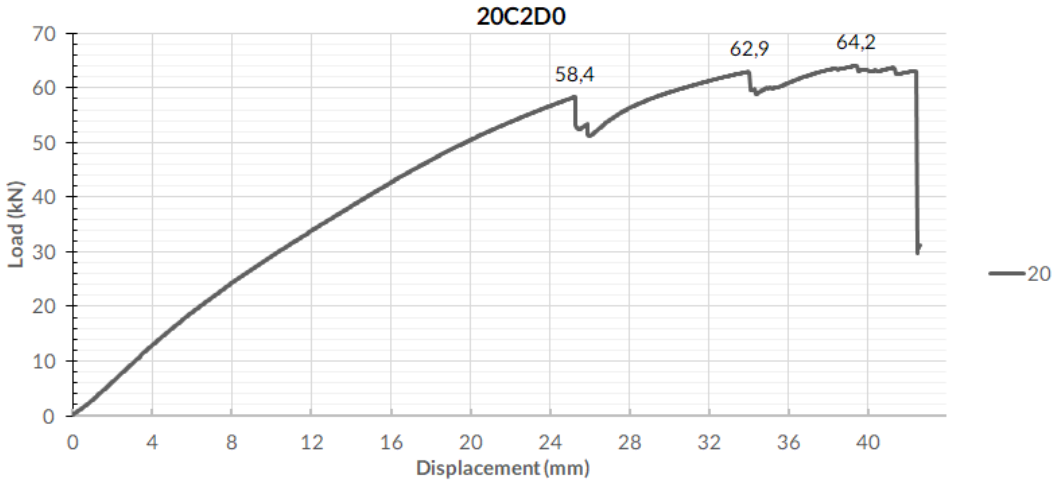

Figure A1.20.1 Testing diagram of specimen 20

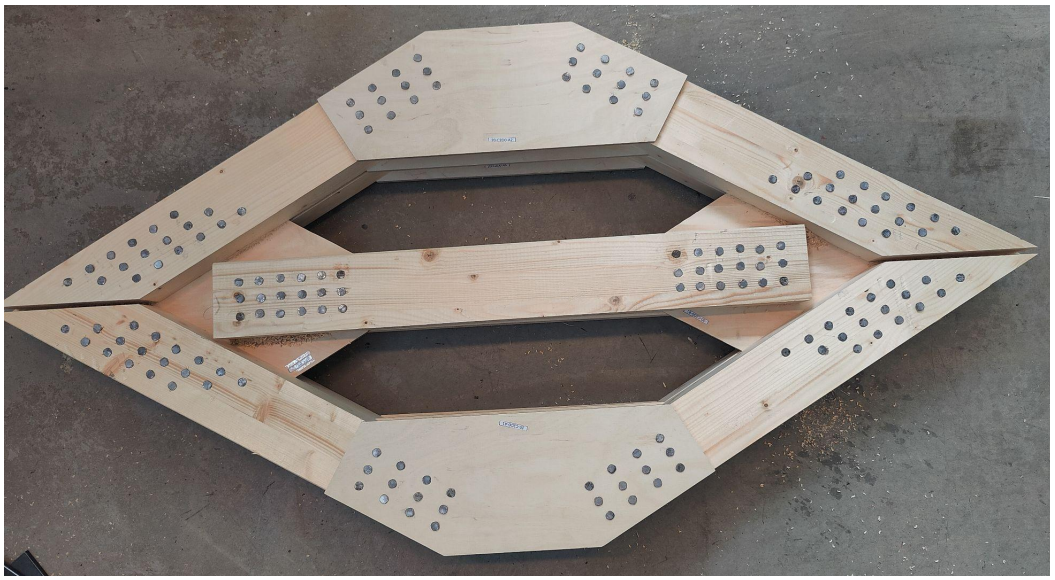

Figure A1.20.2 Specimen before testing

Figure A1.20.3 Plywood failure at upper gusset plates

A1.20.4. Horizontal connections

Figure A1.20.5 Failure along dowel group

8.1.1.21 Specimen 21

Test type	Compressive
Connection type	Doweled
Angle-to-grain	0
Failure	Plywood plate
	Tensile failure at 50,5 kN

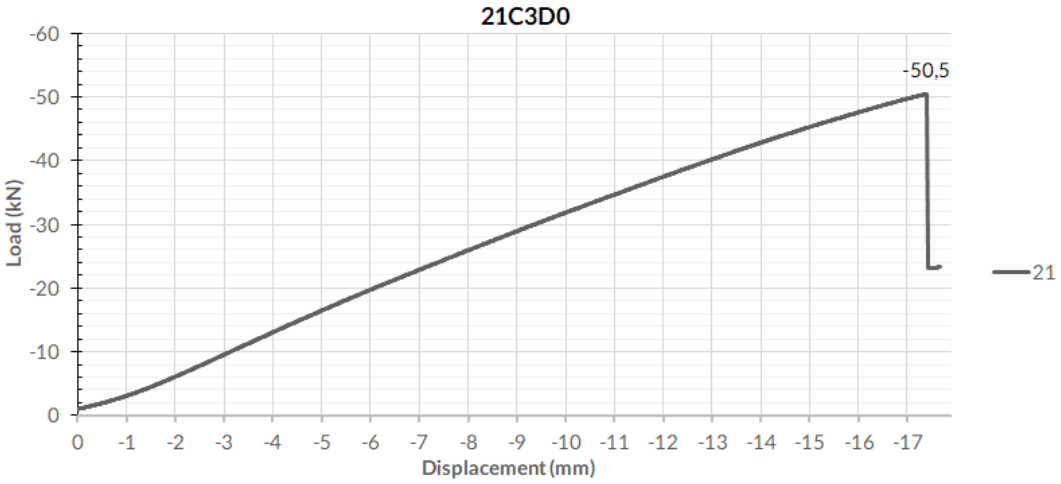

Figure A1.21.1 Testing diagram of specimen 21

Figure A1.21.2 Specimen before testing

Figure A1.21.3 Plywood failure in tension at horizontal member

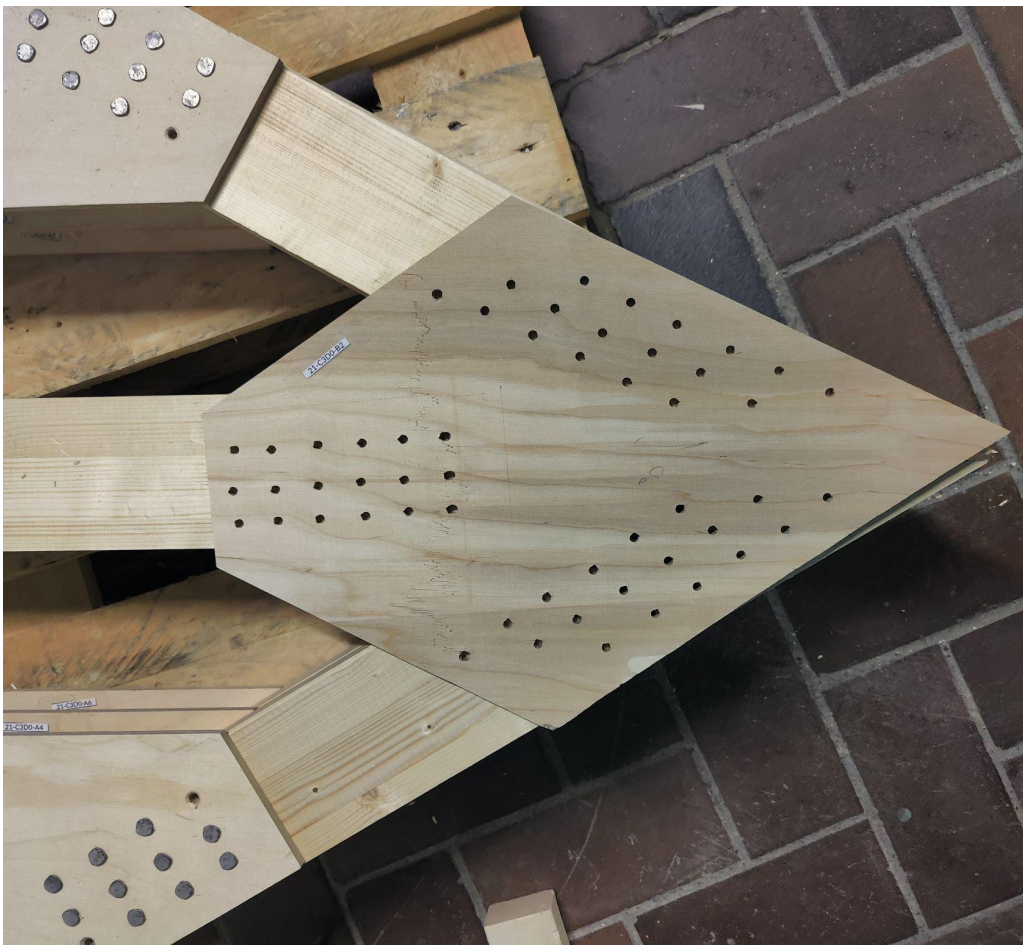

Figure A1.21.4 Plywood with failure and removed nails

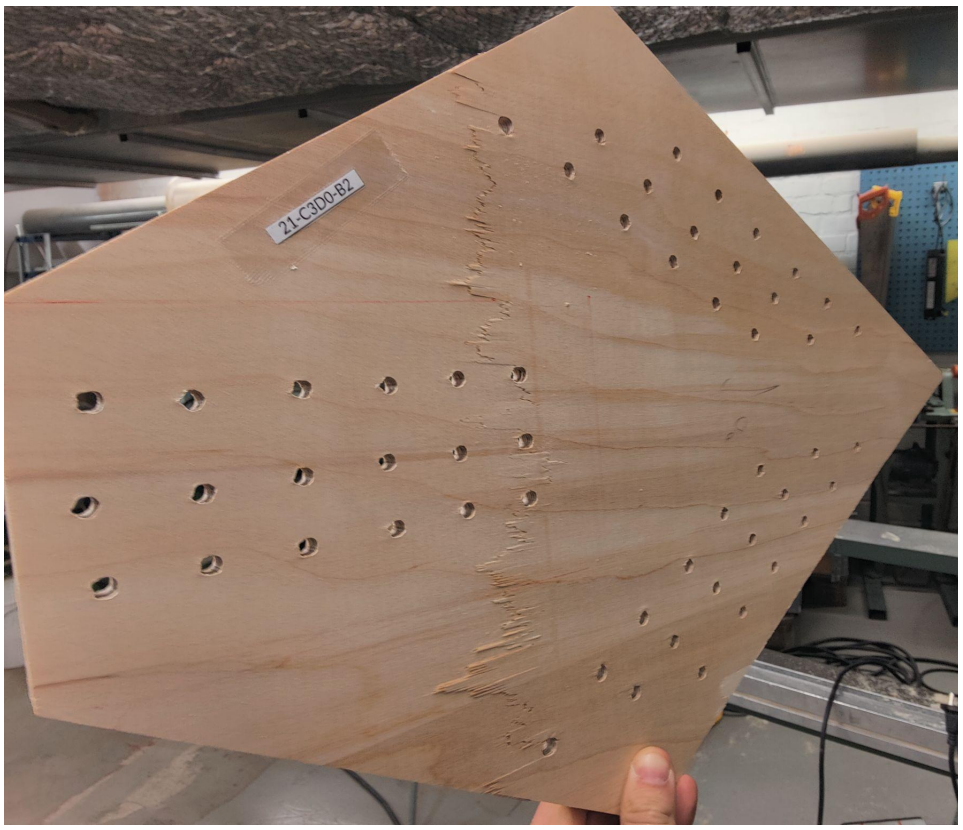

Figure A1.21.5 Plywood with tensile failure removed from specimen

8.1.1.22	*Specimen 22*
Test type	Tension
Connection type	Doweled
Angle-to-grain	0
Failure	Plywood plate B
	Tensile failure at 57,1 kN

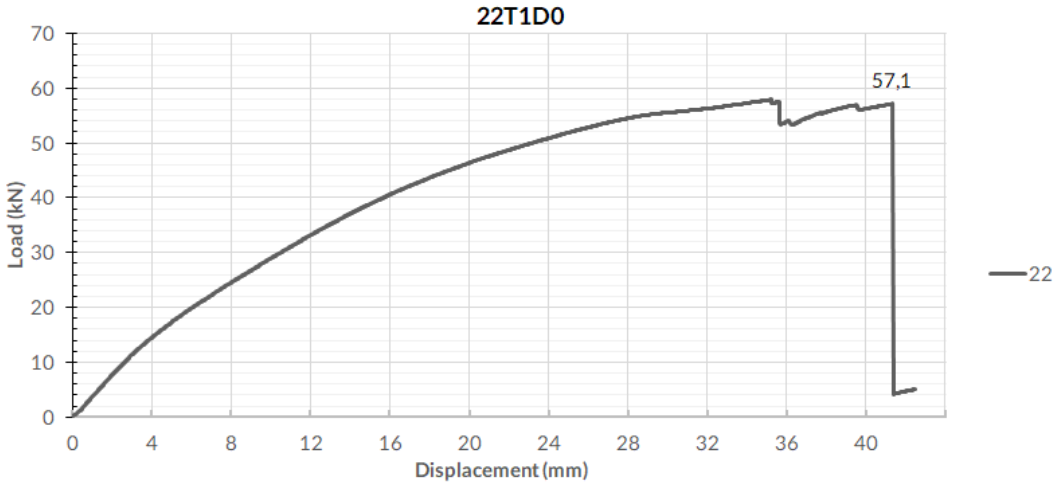

Figure A1.22.1 Testing diagram of specimen 22

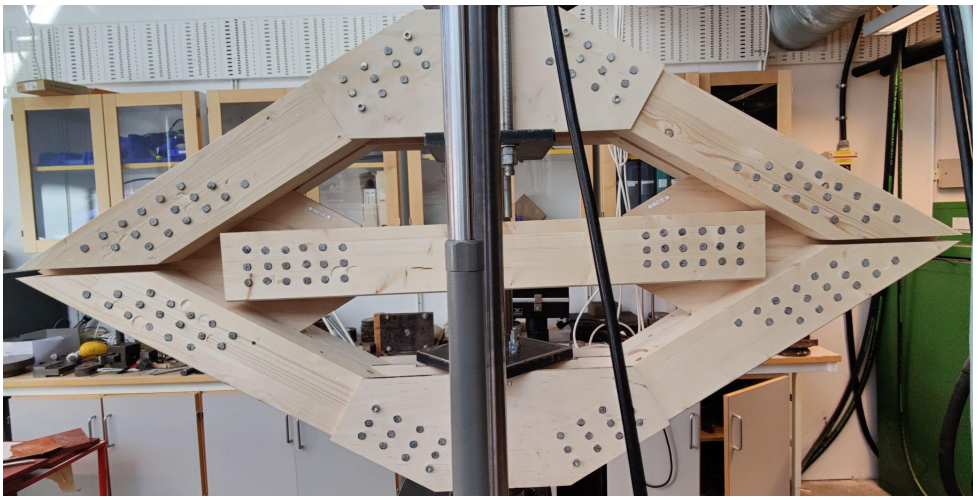

Figure A1.22.2 Specimen mounted in test rig

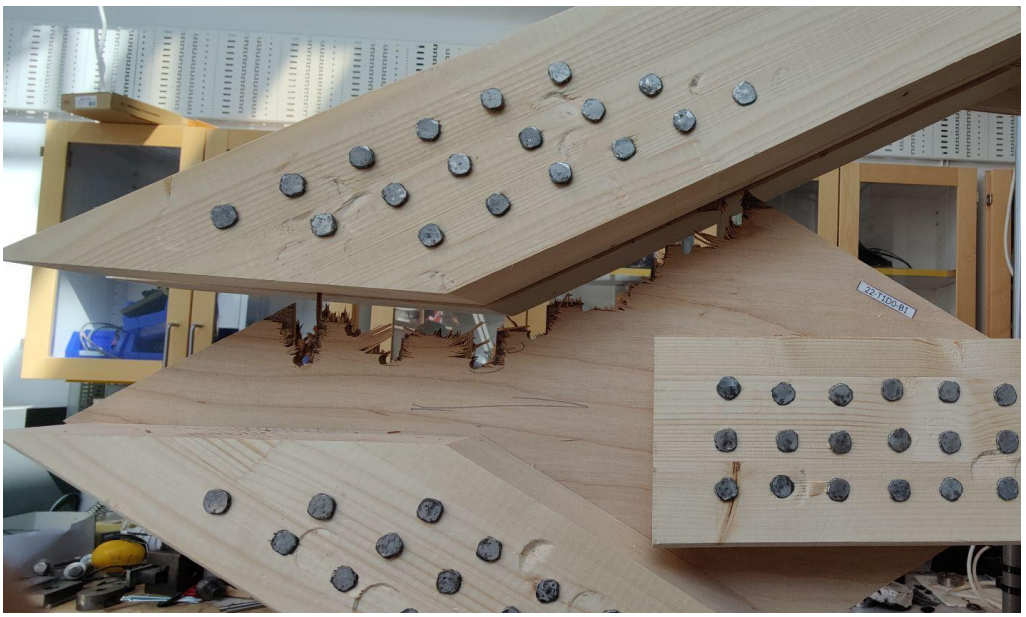

Figure A1.23.3 Plywood failure after test, tension

Figure A1.22.4 Plywood failure with nails removed

Figure A1.22.5 Plywood failure along horizontal member, local buckling

r

Figure A1.22.6 Plywood failure along horizontal member, compression/shear

Figure A1.22.7 Diagonal plywood failure removed

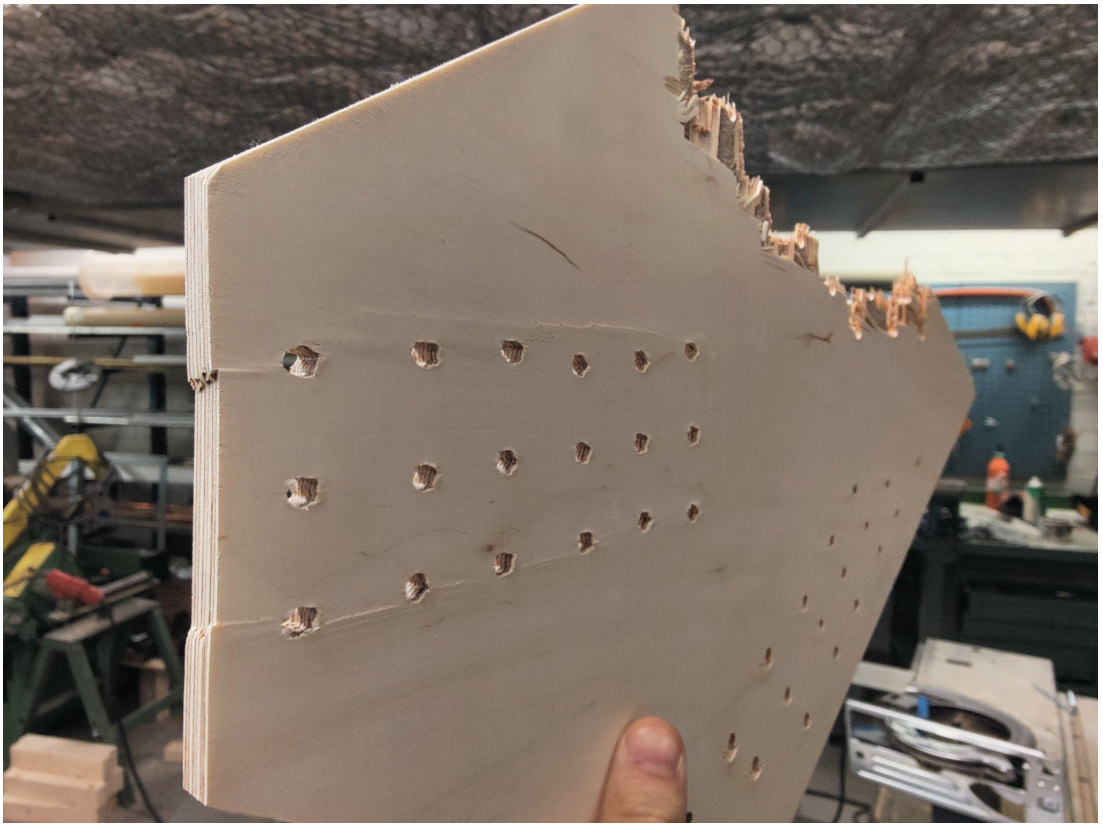

Figure A1.22.8 Diagonal plywood failure removed

8.1.1.23	*Specimen*	*23*
Test type	Tension	
Connection type	Doweled	
Angle-to-grain	0	
Failure	Plywood plate B	
	Tensile failure at 59,6 kN	

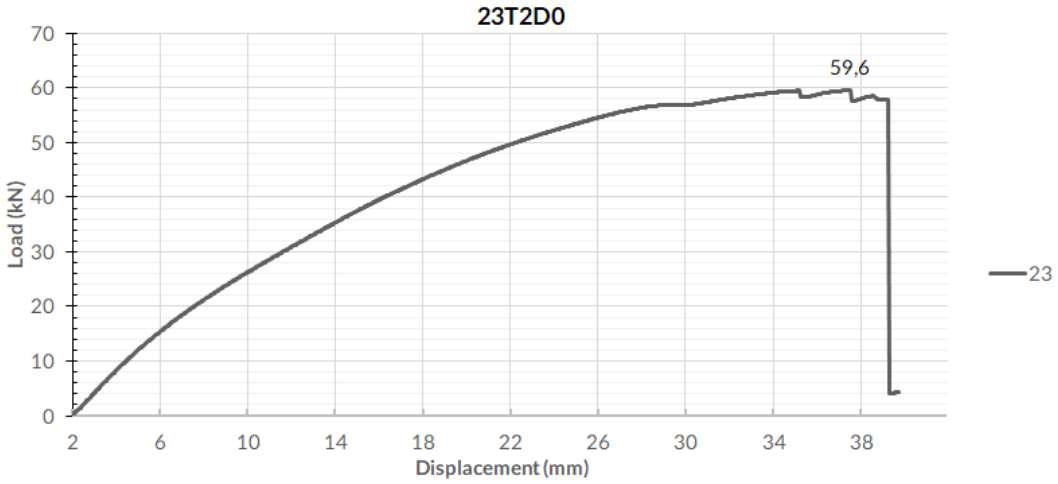

Figure A1.23.1 Testing diagram of specimen 23

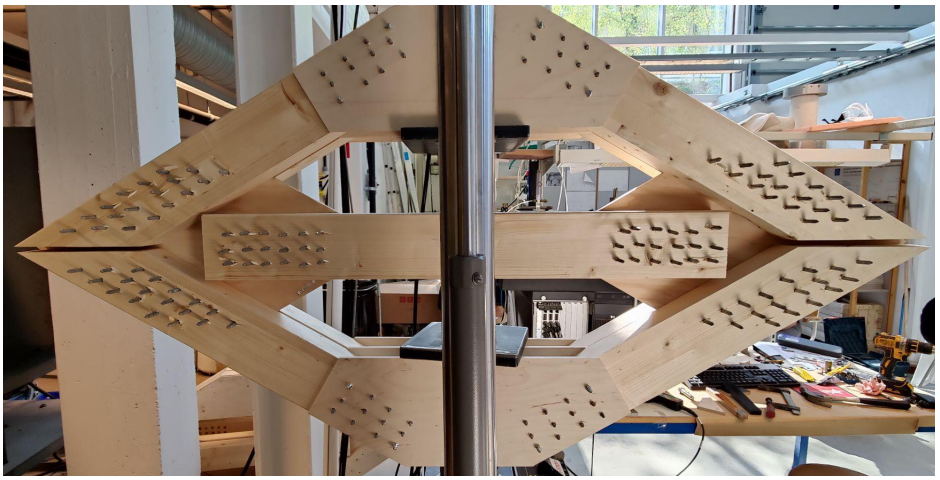

Figure A1.23.2 Specimen mounted in test rig

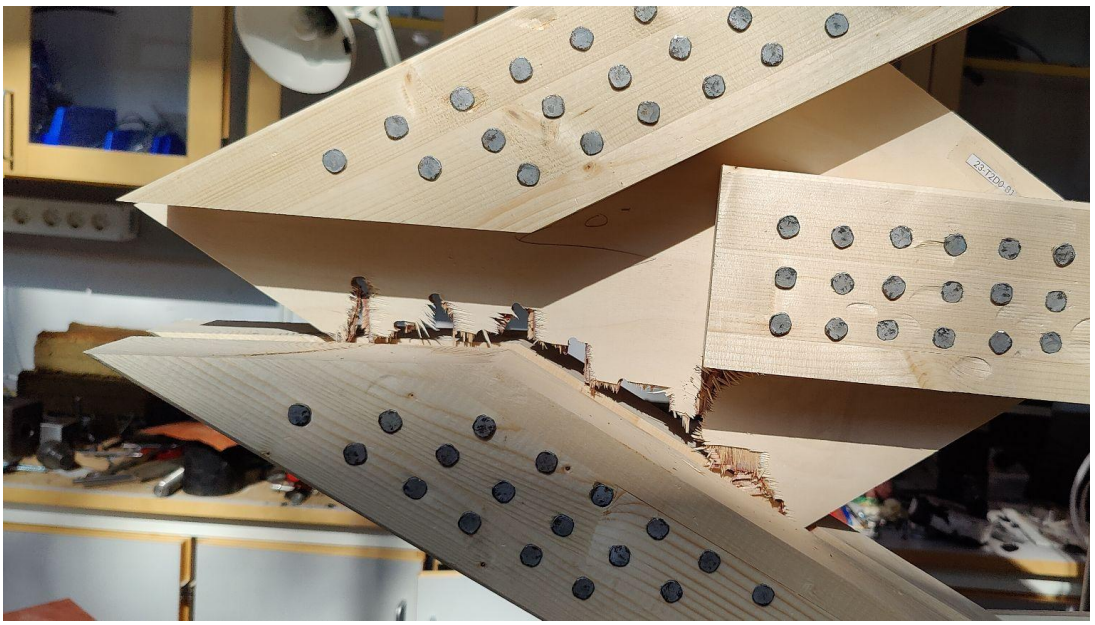

Figure A1.23.3 Plywood Failure after testing

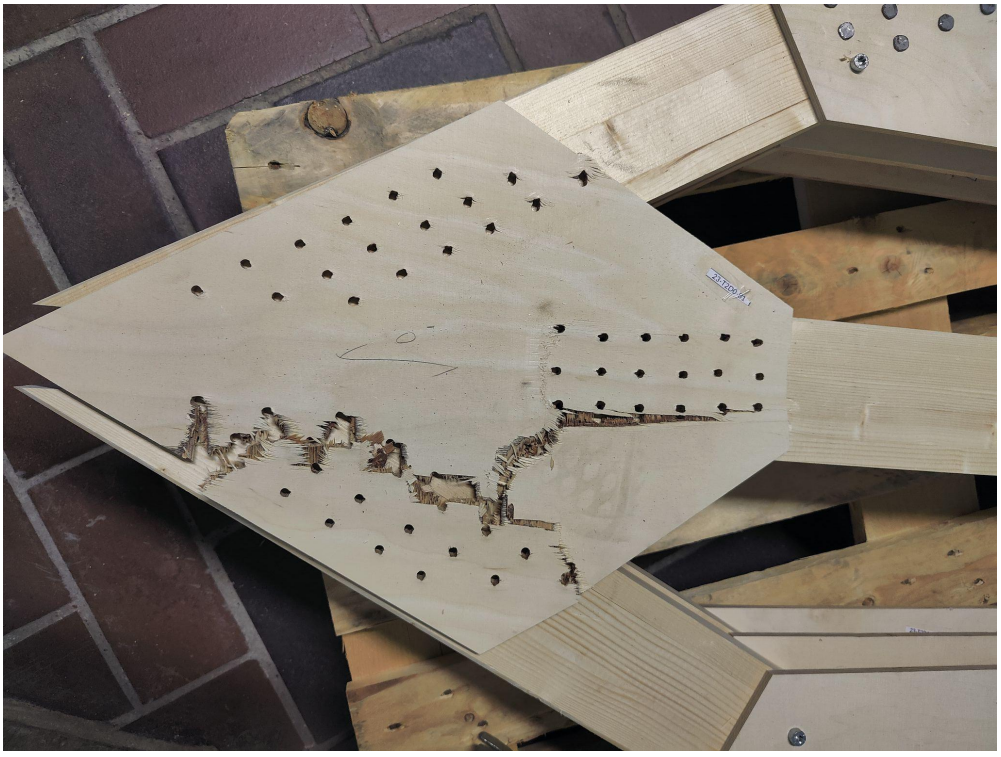

Figure A1.23.4 Plywood Failure with nails removed

Figure A1.23.5 Plywood failure of shear crack along horizontal member

Figure A1.23.6 Failure according to Johansens' theory with nail pulled through the plywood

Figure A1.23.7 Failure along dowel group

Figure A1.23.8 Compressive local buckling at dowel group

8.1.1.24	*Specimen 24*
Test type	Compressive
Connection type	Doweled
Angle-to-grain	0
Failure	Plywood plate
	Tensile failure at 51,2 kN

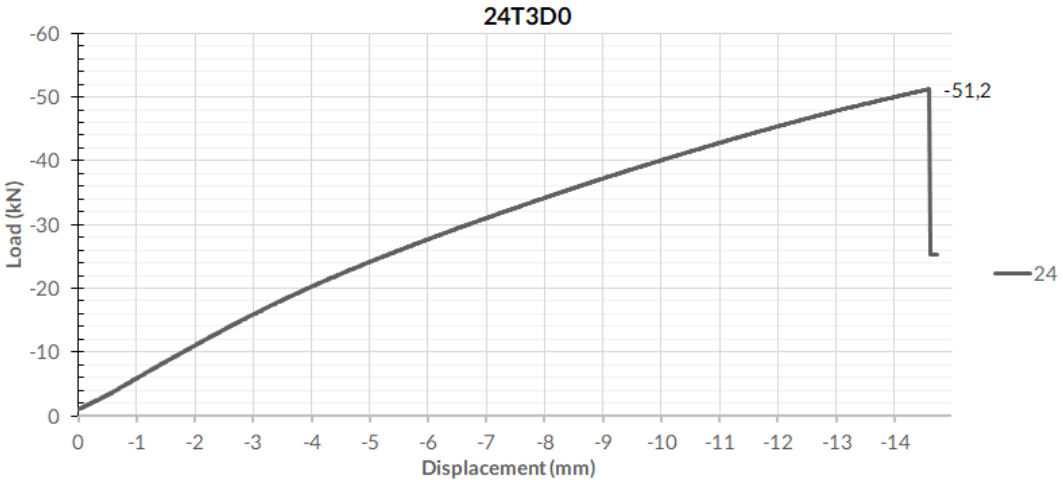

Figure A1.24.1 Testing diagram of specimen 24

Figure A1.24.2 Specimen before testing

Figure A1.24.3 Plywood failure from horizontal member

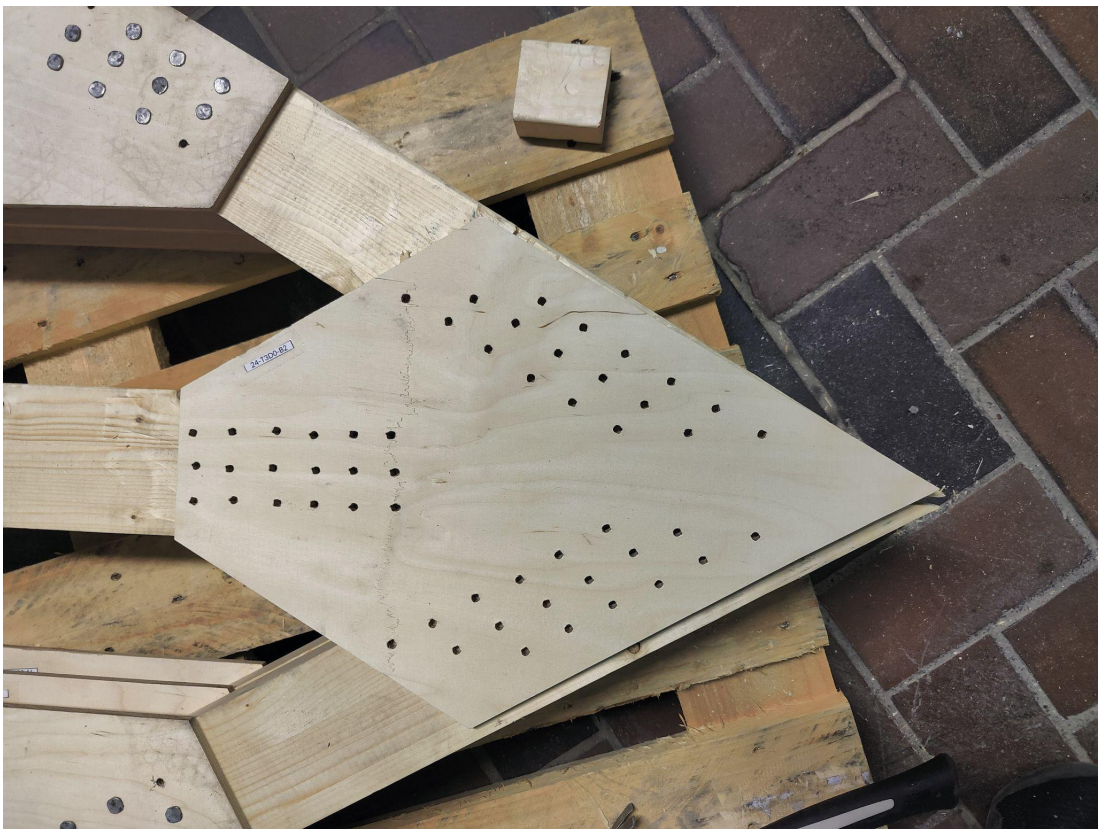

Figure A1.24.4 Plywood failure with removed nails

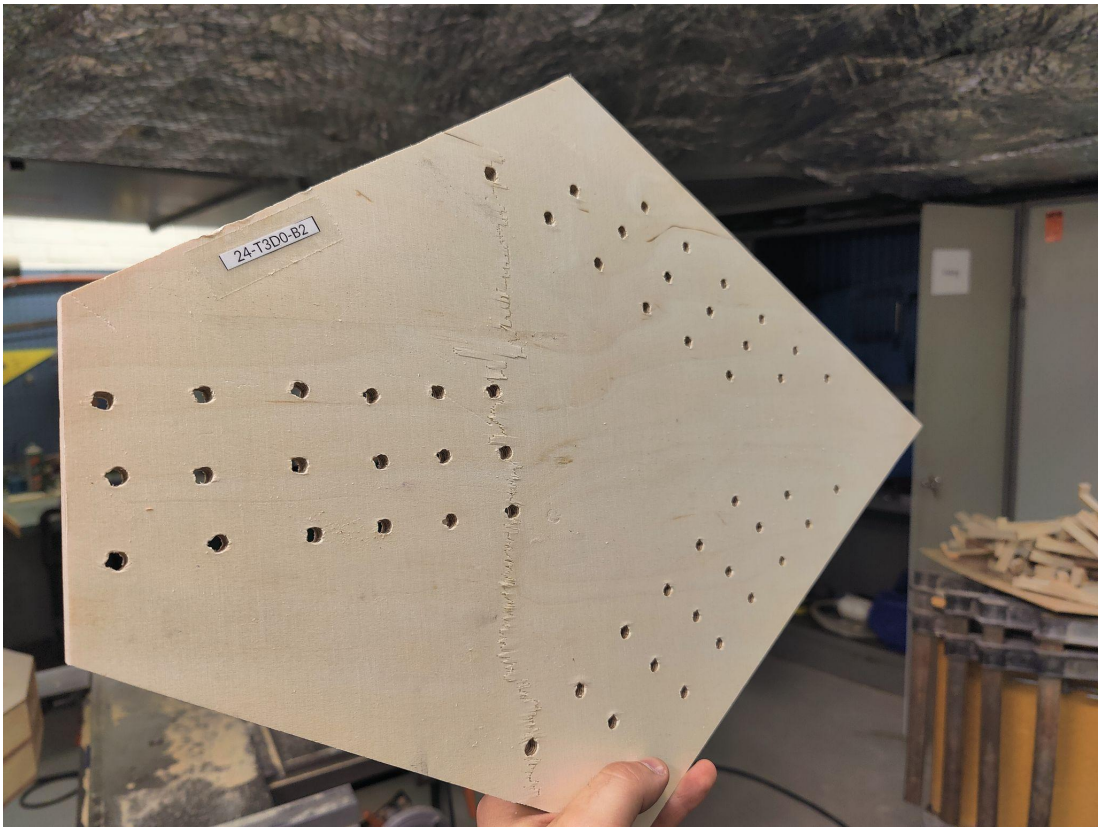

Figure A1.24.5 Plywood failure with removed nails

8.1.2 Group results

8.1.2.1 Test group A

Test type	Connection type	Angle to-grain
Compressive	Glued	0°

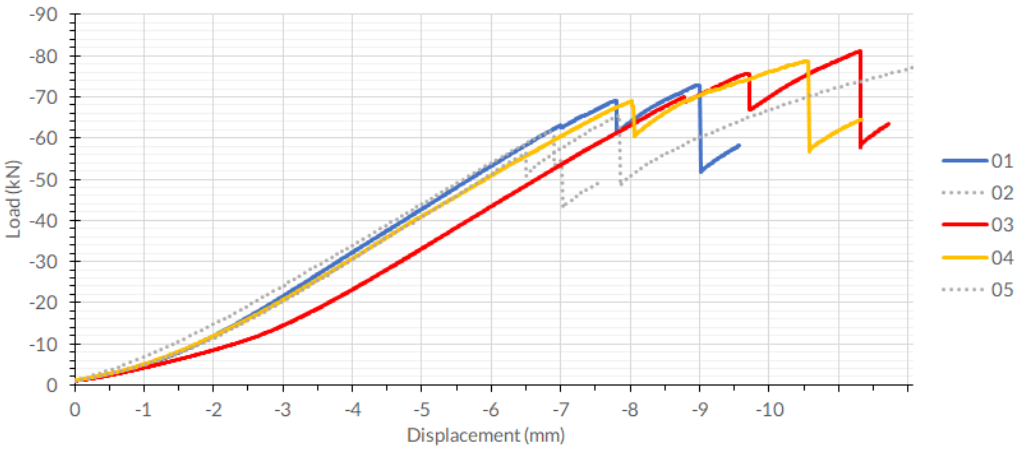

Figure A2.4.1. Testing diagram of test group A

Table A.1.1. Test results of specimens in group A

Specimen #	Failure 1 kN	Failure mode 1	Failure 2 kN	Failure mode 2
01-C1G0	-68,9	H. Glueline	-72,6	H. Glueline
02-C2G0*	-61,7	H. Glueline	-54,5	H. Glueline
03-C3G0	-75,4	H. Glueline	-81,1	H. Glueline
04-T1G0	-68,9	H. Glueline	-78,8	H. Glueline
05-T2G0*	-56,3	H. Glueline	-65,5	H. Glueline

*Not included in results

Minimum failure load	Mean 1st failure load	Mean 2nd failure load
-68,9 kN	-71,07 kN	-77,50 kN

8.1.2.2 Test group B

Test type	Connection type	Angle to-grain
Compressive	Glued	5°

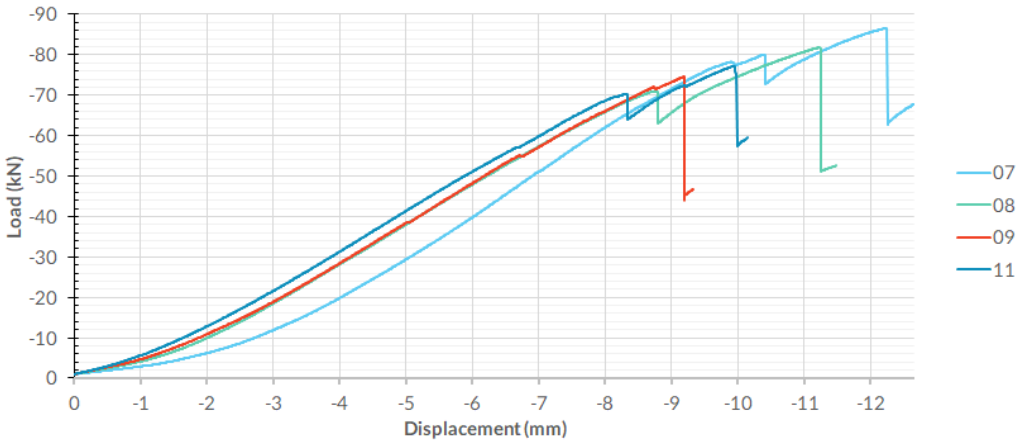

Figure A2.4.2. Testing diagram of test group B

Table A.1.2. Test results of specimens in group B

Specimen #	Failure 1 kN	Failure mode 1	Failure 2 kN	Failure mode 2
07-C1G5	-80,1	H. Glueline	-86,6	H. Glueline
08-C2G5	-70,7	H. Glueline	-81,8	H. Plywood
09-C3G5	-74,5	H. Plywood	-	-
011-T2G5	-70,2	H. Glueline	-77,2	H. Glueline

Minimum failure load	Mean 1st failure load	Mean 2nd failure load	Mean plywood failure load
-70,20 kN	-73,88 kN	-81,87 kN	-78,15 kN

8.1.2.3 Test group C

Test type	Connection type	Angle to-grain
Compressive	Glued	15°

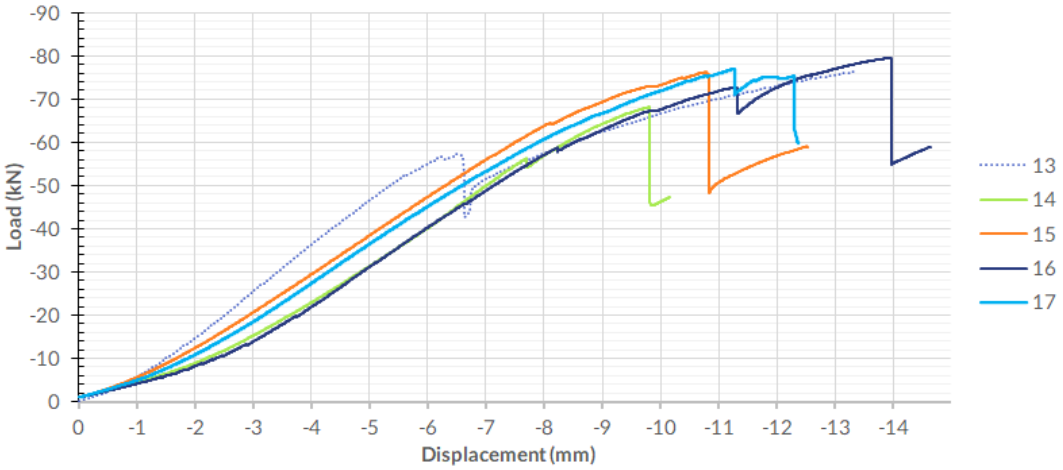

Figure A2.4.5. Testing diagram of test group C

Table A.1.3. Test results of specimens in group C

Specimen #	Failure 1 kN	Failure mode 1	Failure 2 kN	Failure mode 2
13-C1G15*	-57,2	H. Glueline	-76,3	Glueline
14-C2G15	-56,2	H. Glueline	-68,2	H. Plywood
15-C3G15	-76,2	H. Plywood	-	-
16-T1G15	-72,7	H. Glueline	-79,5	H. Plywood
17-T2G15	-77,0	H. Glueline	-75,3	H. Plywood

*Not included in results

Minimum failure load	Mean 1st failure load	Mean 2nd failure load	Mean plywood failure load
-56,2 kN	-70,53 kN	-74,30 kN	-74,80 kN

8.1.2.4 Test group D

Test type	Connection type	Angle to-grain
Tensile	Glued	0°

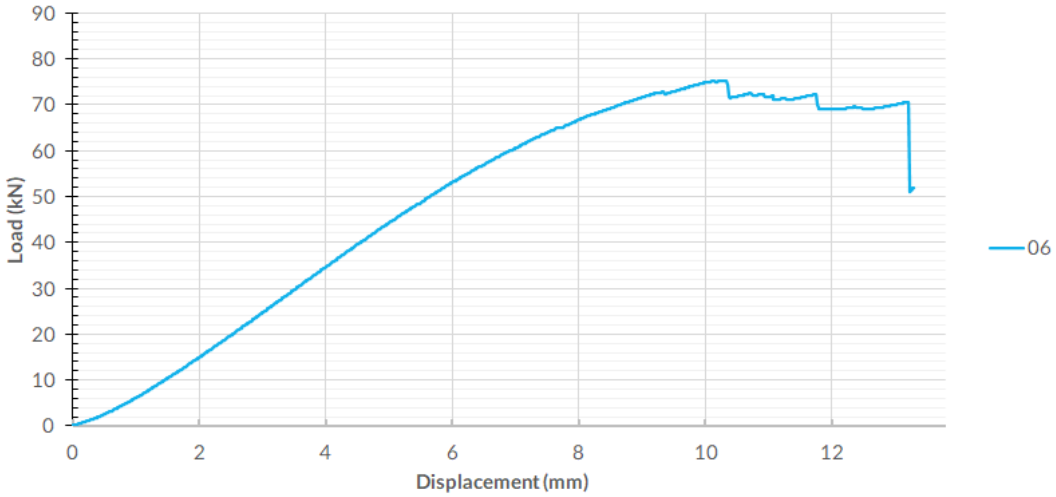

Figure A2.4.10. Testing diagram of test group D

Table A.1.4. Test results of specimens in group D

Specimen #	Failure 1 kN	Failure mode 1	Failure 2 kN	Failure mode 2
06-T3G0	75,2	D. Timber	72,2	H. Timber

Minimum failure load	Mean 1st failure load	Mean 2nd failure load
72,20 kN	75,20 kN	72,20 kN

8.1.2.5 Test group E

Test type	Connection type	Angle to-grain
Tensile	Glued	5°

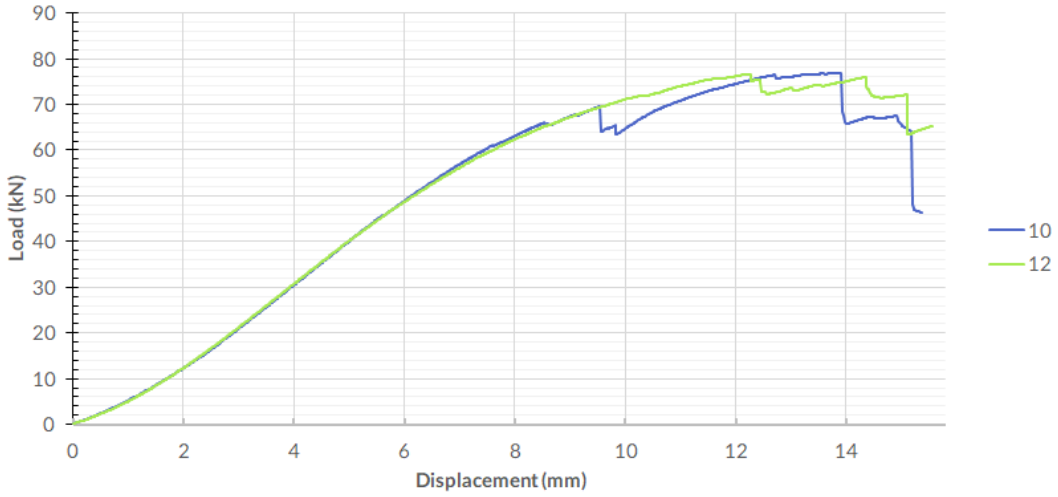

Figure A2.4.11. Testing diagram of test group E

Table A.1.5. Test results of specimens in group E

Specimen #	Failure 1 kN	Failure mode 1	Failure 2 kN	Failure mode 2
10-T1G5	69,6	D. Timber	76,5	D. Timber
12-T3G5	76,6	D. Timber	75,9	D. Timber

Minimum failure load	Mean 1st failure load	Mean 2nd failure load
69,60 kN	73,10 kN	76,20 kN

8.1.2.6 Test group F

Test type	Connection type	Angle to-grain
Tensile	Glued	15°

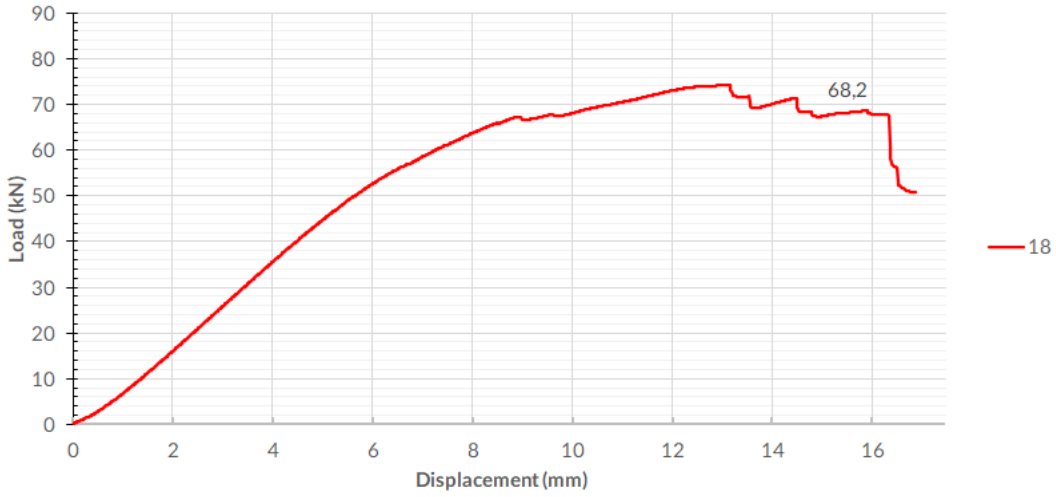

Figure A2.4.12. Testing diagram of test group F

Table A.1.6. Test results of specimens in group F

Specimen #	Failure 1 kN	Failure mode 1	Failure 2 kN	Failure mode 2
18T3G15	74,3	D. Timber	71,5	D. Timber

Minimum failure load	Mean 1st failure load	Mean 2nd failure load
71,50 kN	74,30 kN	71,50 kN

8.1.2.7 Test group G

Test type	Connection type	Angle to-grain
Compressive	Doweled	0°

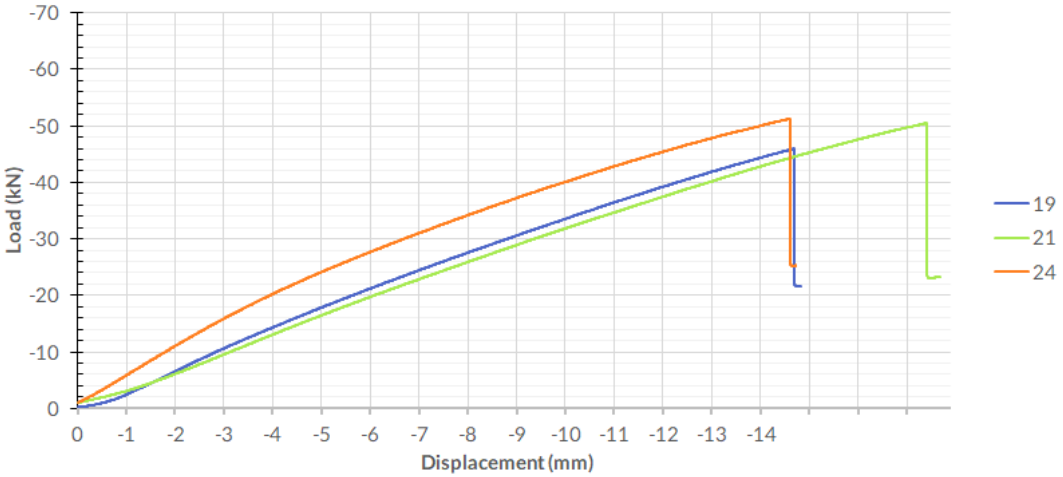

Figure A2.4.13. Testing diagram of test group G

Table A.1.7. Test results of specimens in group G

Specimen #	Failure 1 kN	Failure mode 1
19-C1D0	-46,0	Plywood
21-C3D0	-50,5	Plywood
24-T3D0	-51,2	Plywood

Minimum failure load	Mean 1st failure load	Mean 2nd failure load
-46,00 kN	-49,23 kN	-49,23 kN

8.1.2.8 Test group H

Test type	Connection type	Angle to-grain
Tensile	Doweled	0°

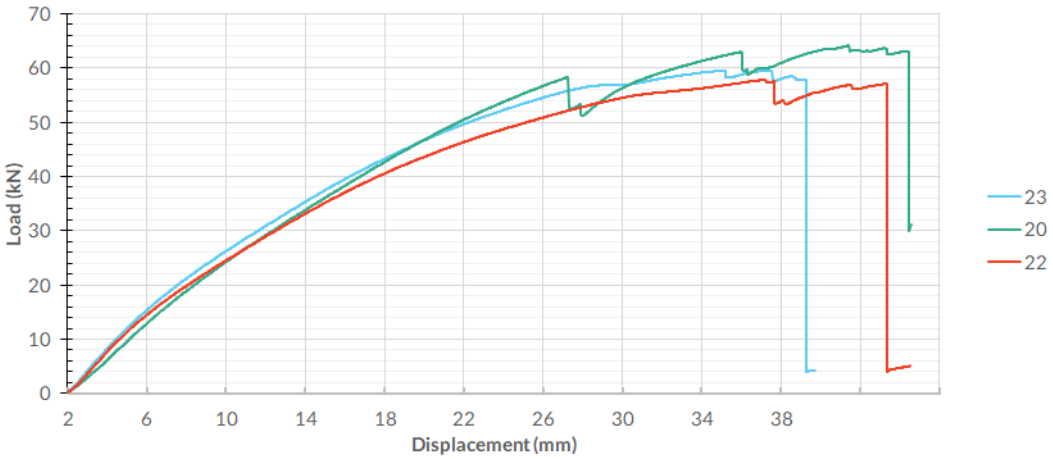

Figure A2.4.17. Testing diagram of test group H

Table A.1.8. Test results of specimens in group H

Specimen #	Failure 1 kN	Failure mode 1	Failure 2 kN	Failure mode 2
20-C2D0	58,2	H. Plywood	64,2	T. Plywood
22-T1D0	57,1	H. Plywood	-	-
23-T2D0	59,6	H. Plywood	-	-

Minimum failure load	Mean 1st failure load	Mean 2nd failure load	Mean plywood failure load
-57,10 kN	-58,30 kN	-64,20 kN	-58,35 kN

8.1.3 Simulation results

8.1.3.1 Simulation A

Group	Type	Config.	Load
A	Comp.	Glued 0°	-80 kN

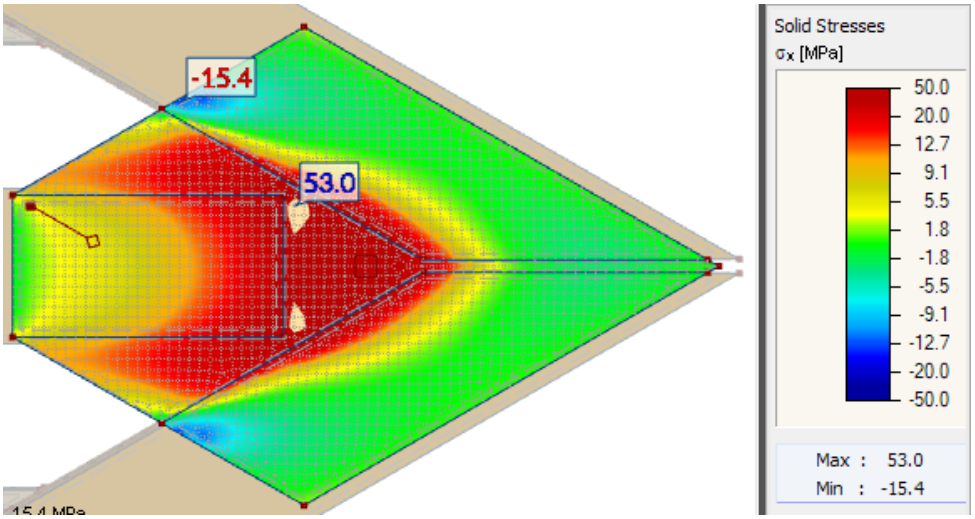

Figure A3.4.30. Normal stress local x-direction simulation A

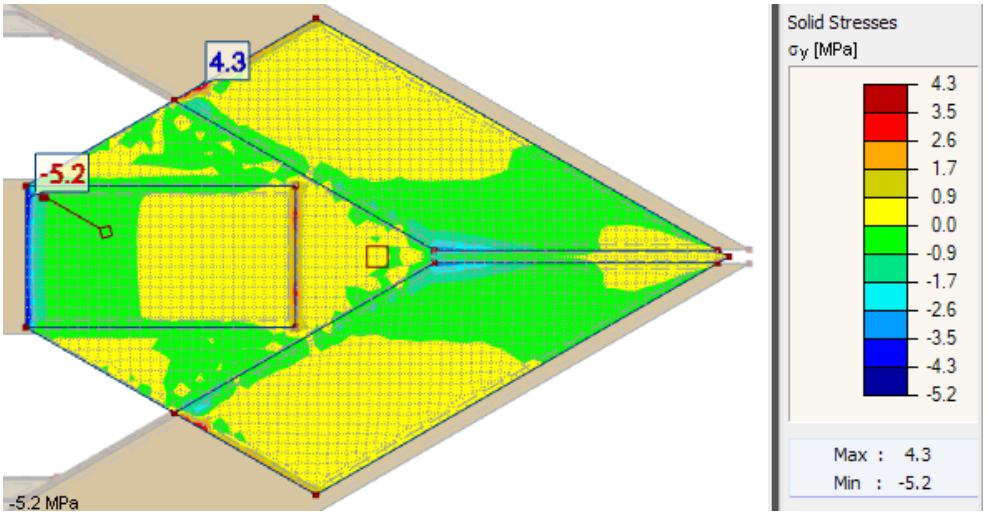

Figure A3.4.31. Normal stress local y-direction simulation A

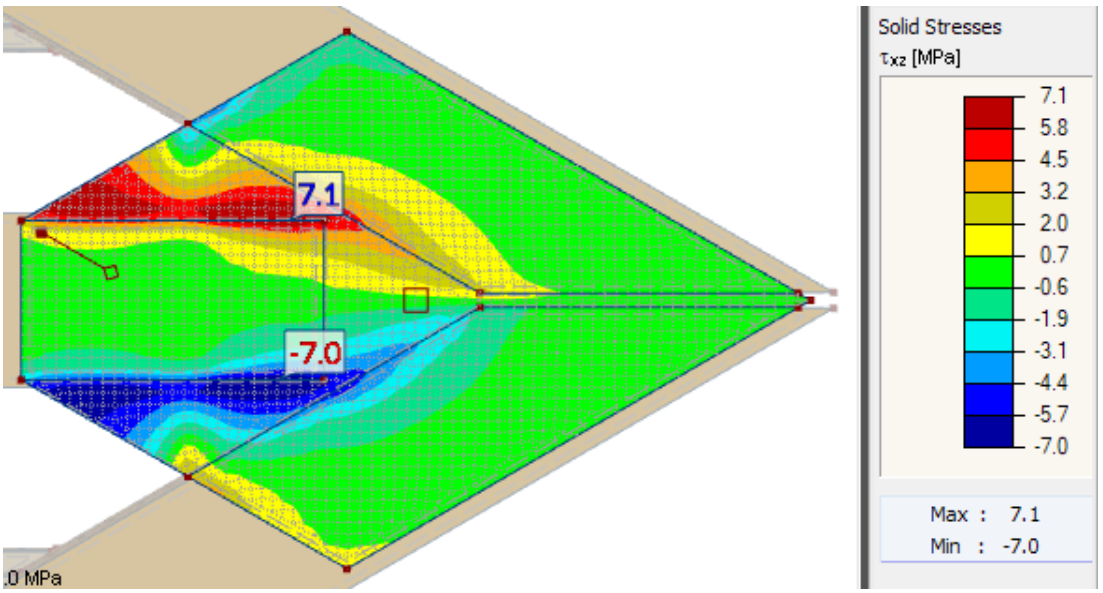

Figure A3.4.32. Shear stress xz-plane simulation A

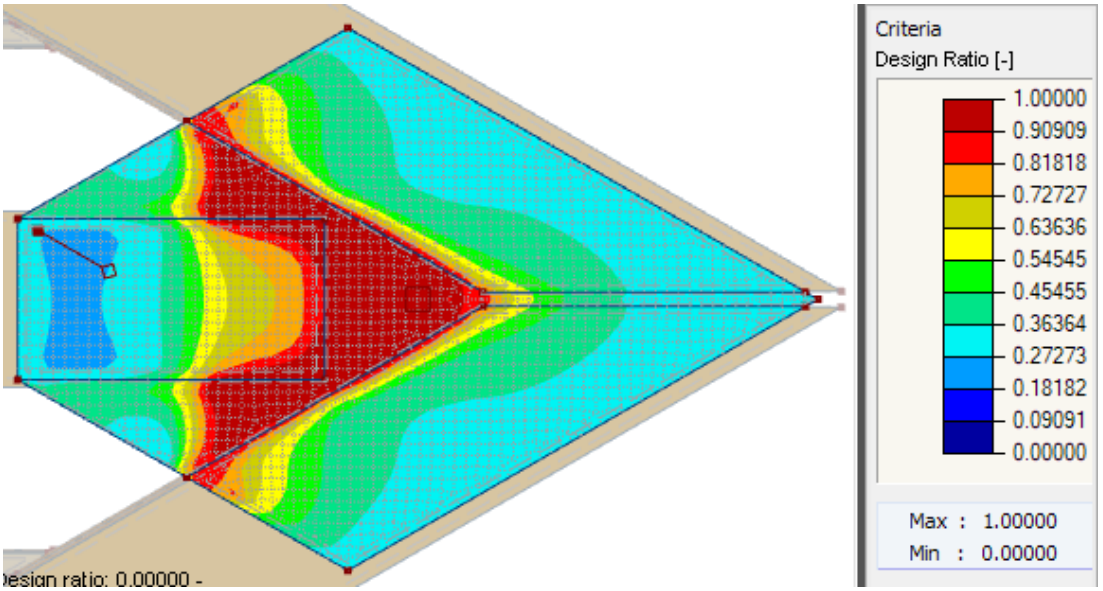

Figure A3.4.33. Tsai-Wu Critereon simulation A

8.1.3.2 Simulation C

Group	Type	Config.	Load
C	Comp.	Glued 15°	-80 kN

Note that the local coordinate x-axis is set along with the 15-degree inclination of the grain, and therefore also the resulting stresses direction.

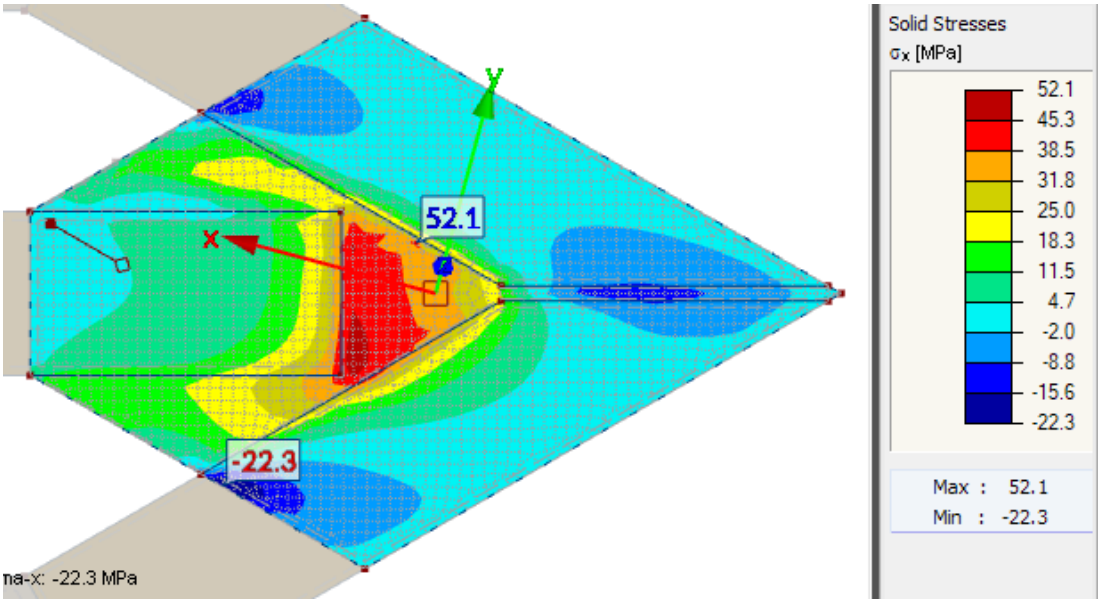

Figure A3.4.34. Normal stress local x-direction simulation C

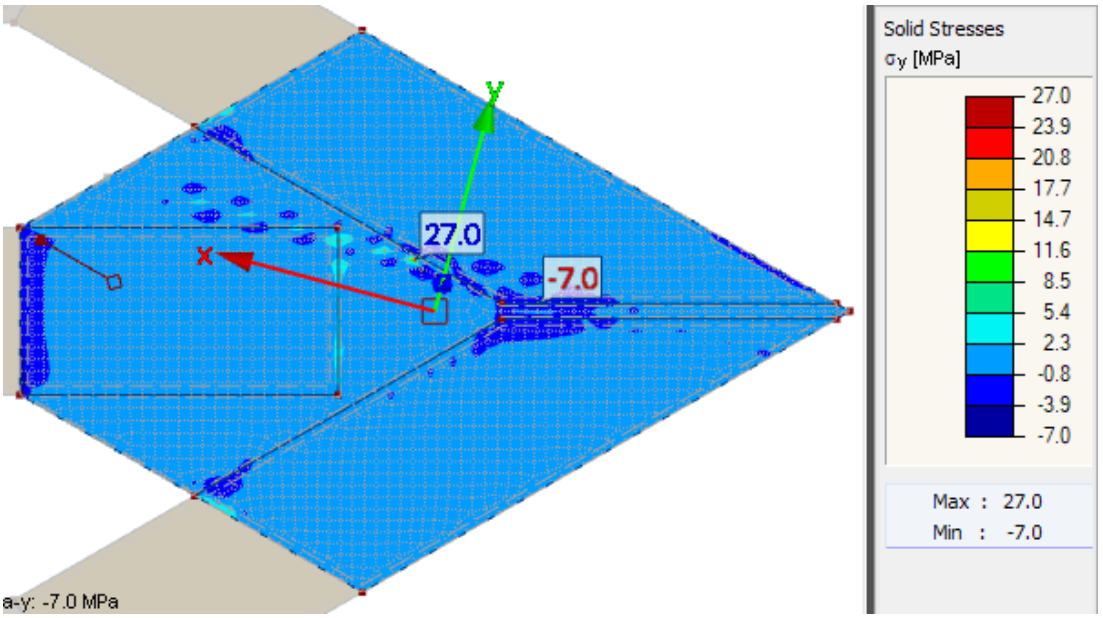

Figure A3.4.35. Normal stress local y-direction simulation C

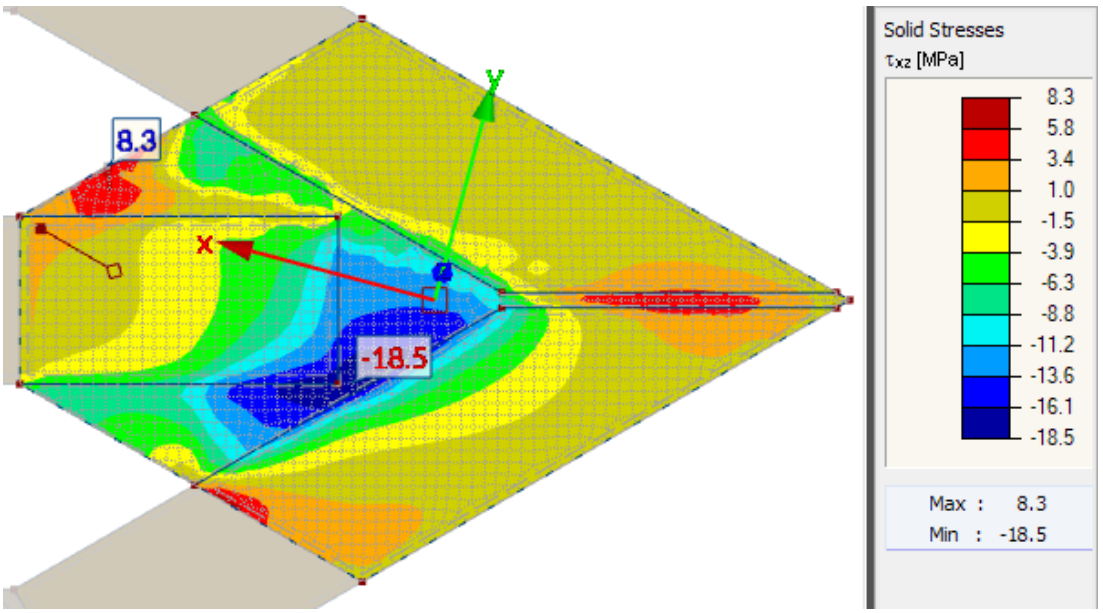

Figure A3.4.36. Shear stress in xz-plane simulation C

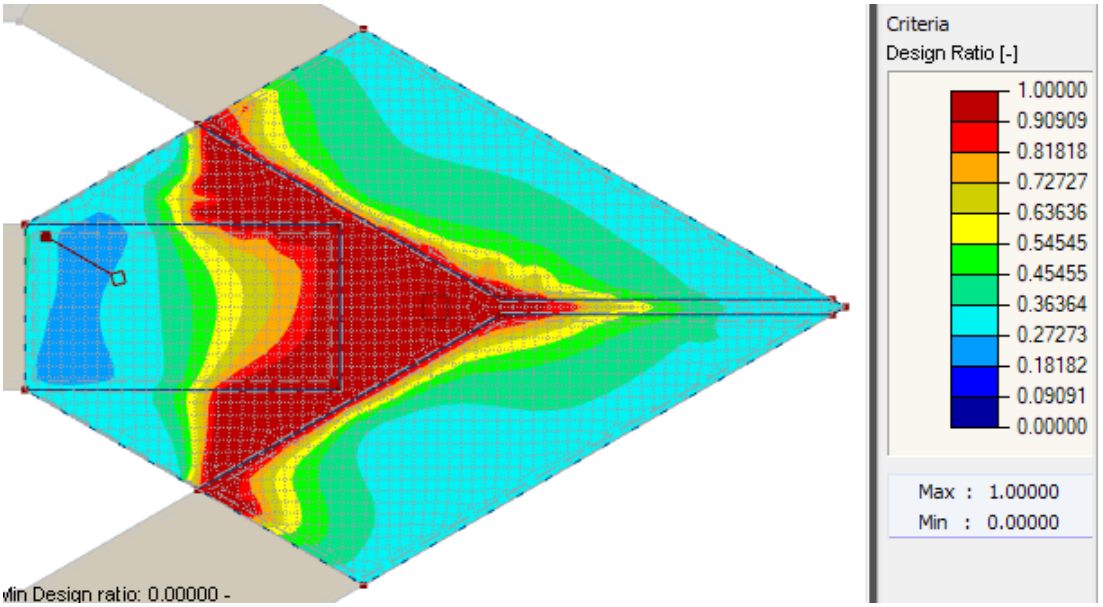

Figure 4.37. Tsai-Wu criterion simulation C

8.1.3.3 Simulation D

Group	Type	Config.	Load
D	Tens.	Glued 0°	80 kN

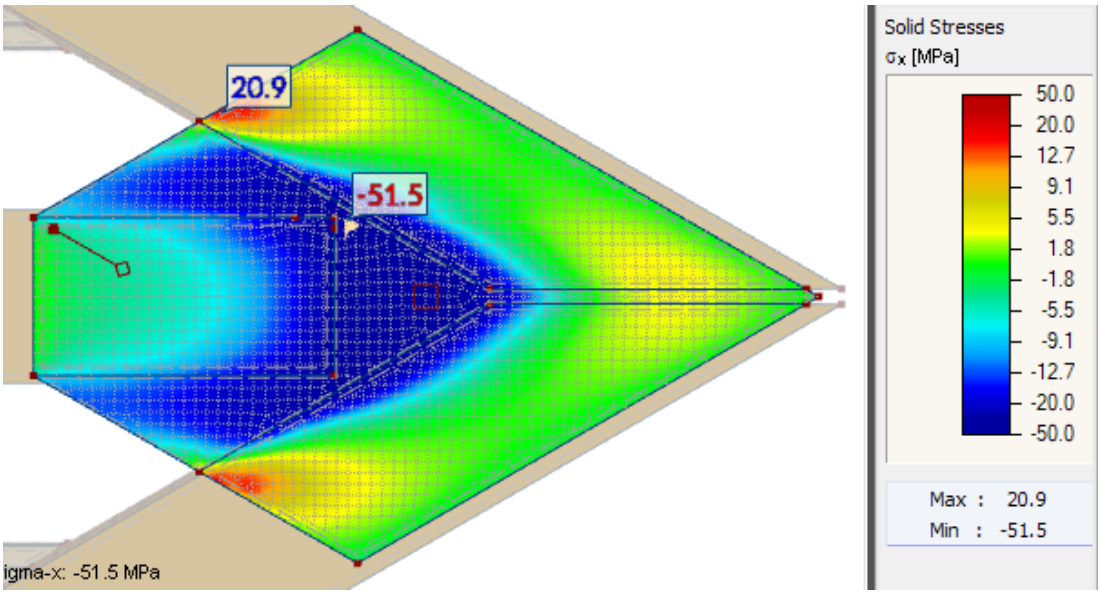

Figure A3.4.38. Normal stress local x-direction simulation D

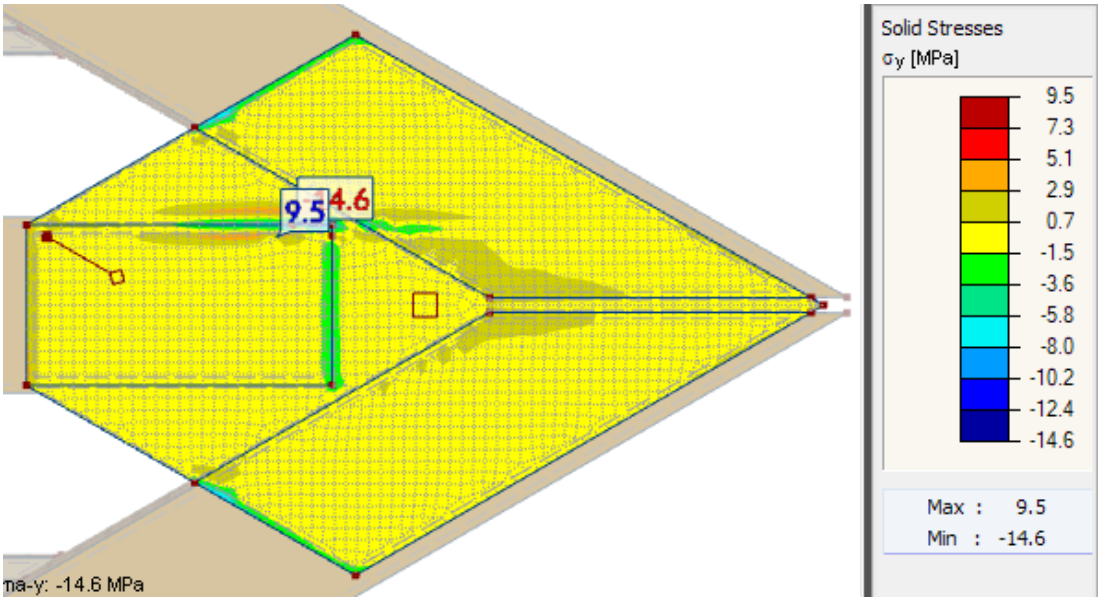

Figure A3.4.39. Normal stress local y-direction simulation D

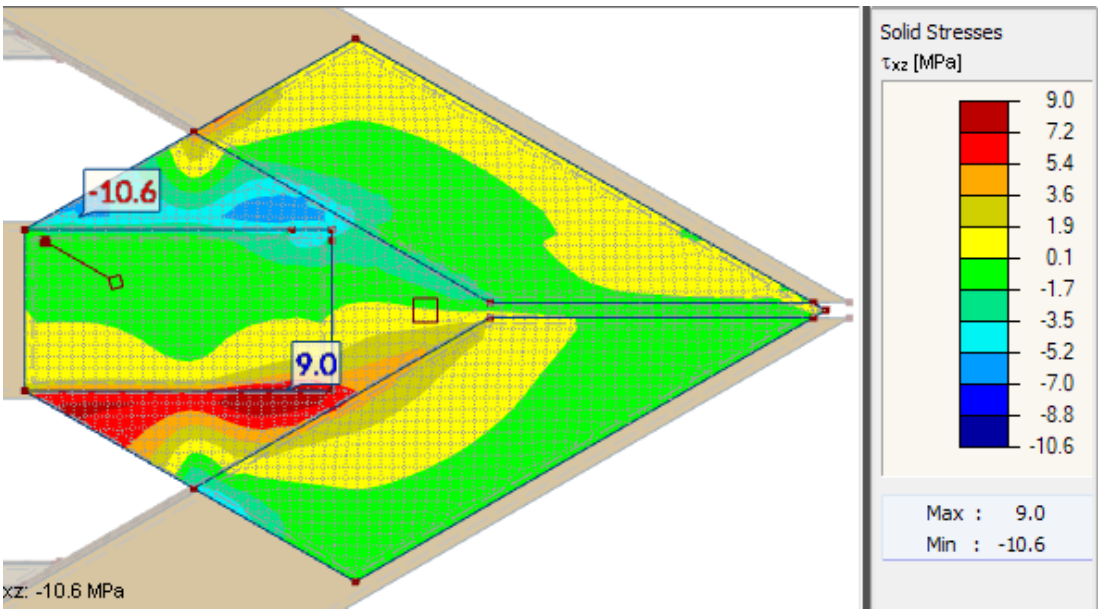

Figure A3.4.40. Shear stress in xz-plane simulation D

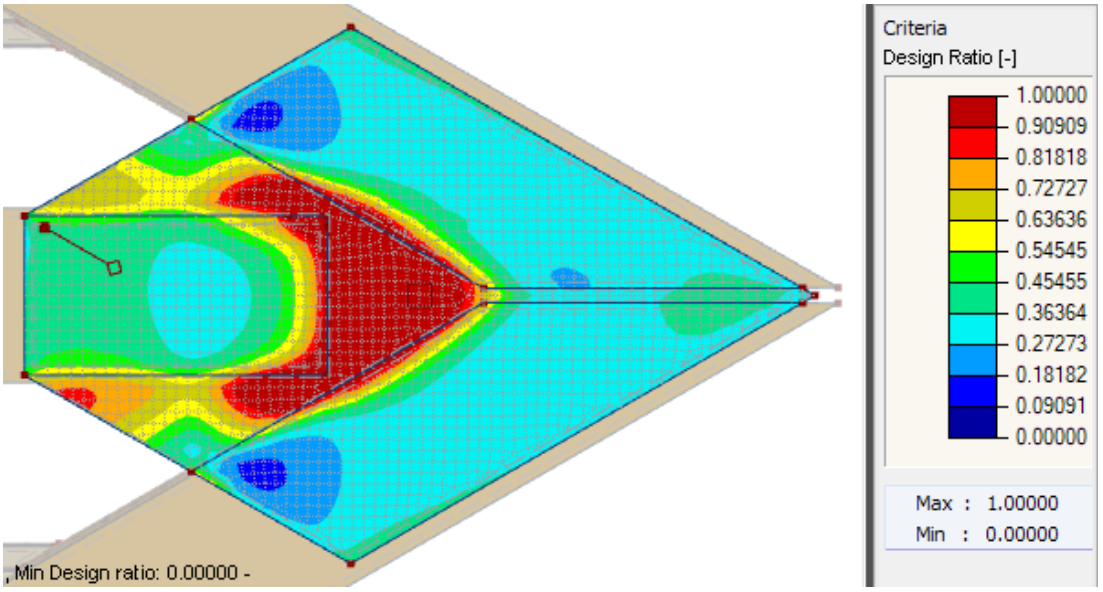

Figure A3.4.41. Tsai-wu Criterion simulation D

8.1.3.4 *Simulation F*

Group	Type	Config.	Load
F	Tens.	Glued 15°	80 kN

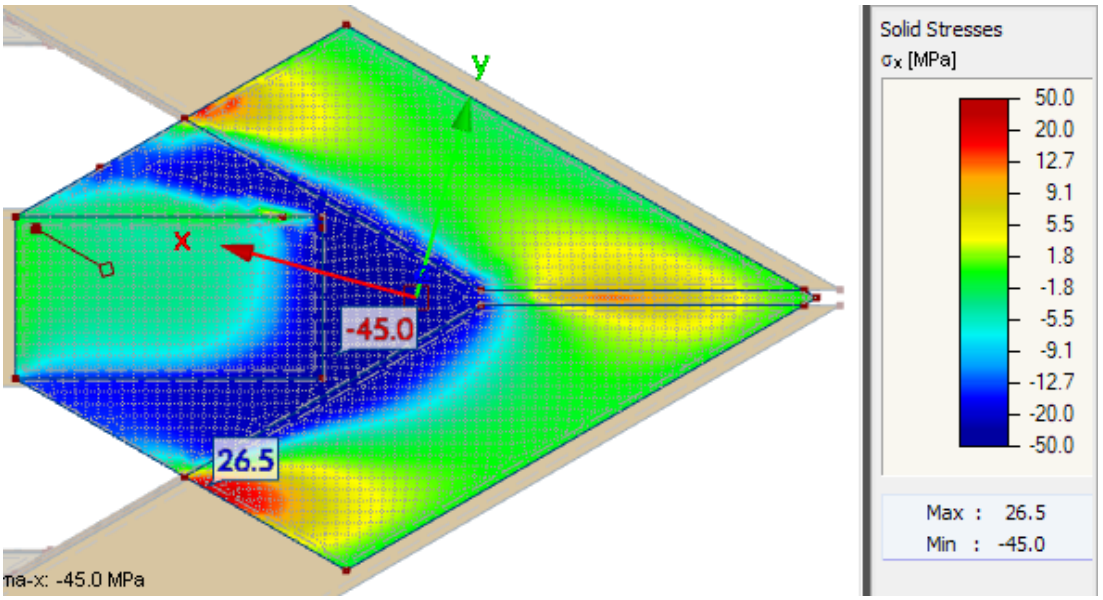

Figure A3.4.42. Normal stress local x-direction simulation F

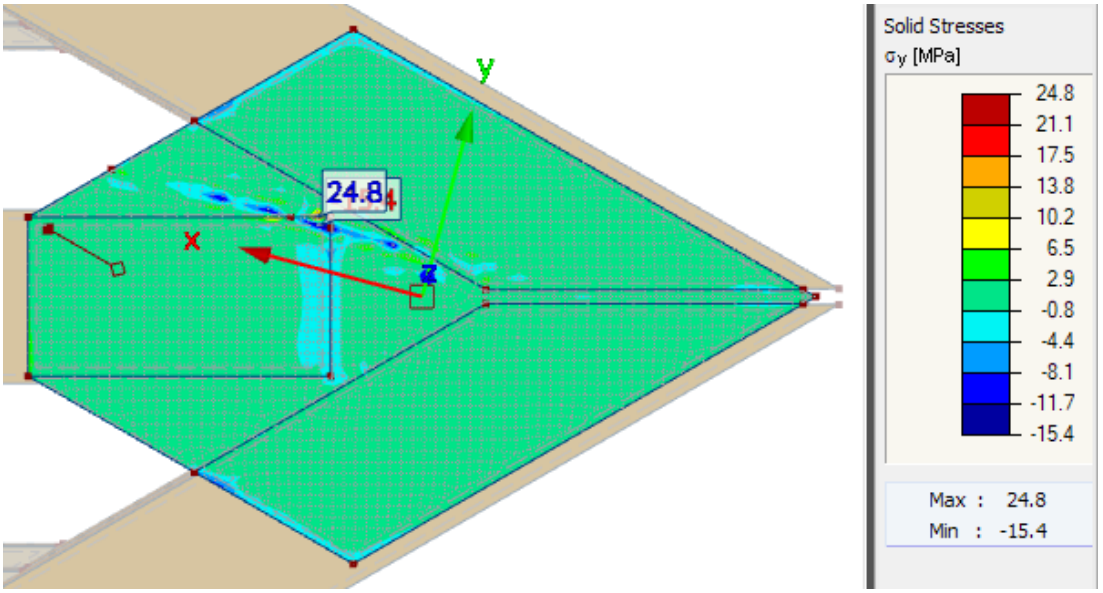

Figure A3.4.43. Normal stress local y-direction simulation F

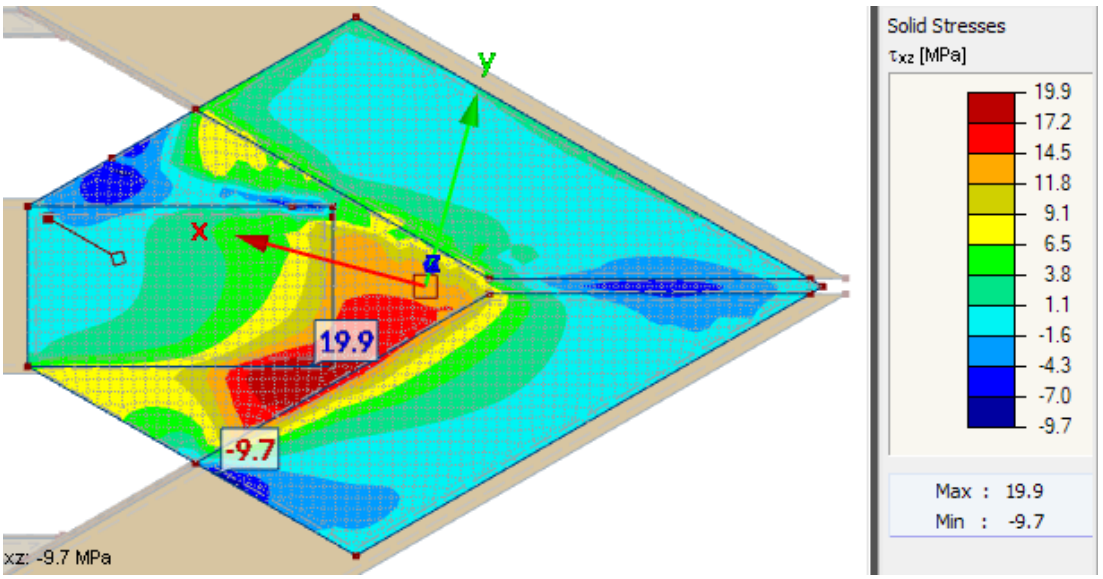

Figure A3.4.44. Shear stress in xz-plane simulation F

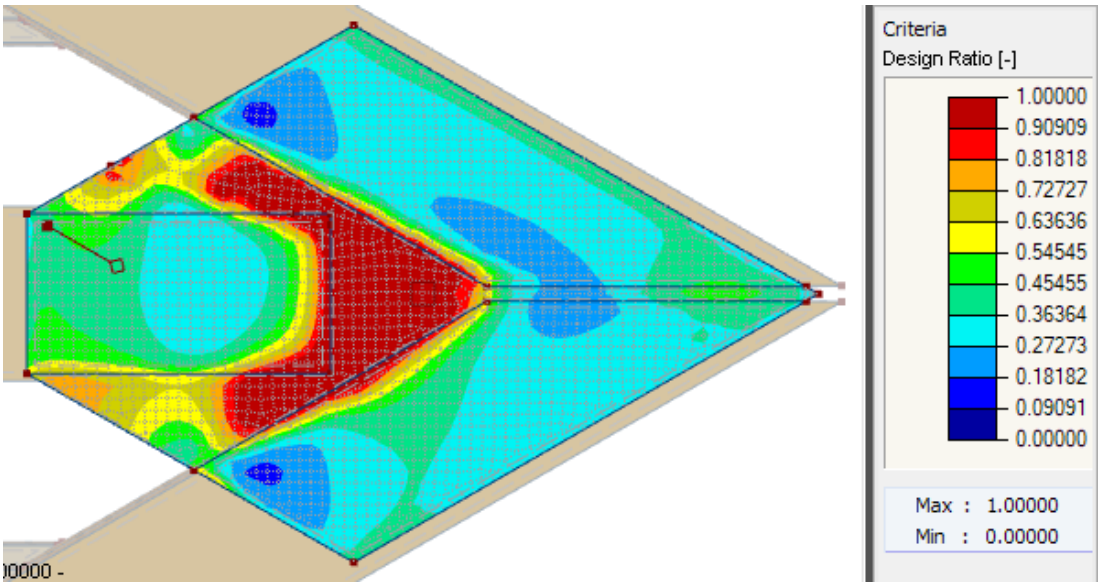

Figure A3.4.45. Tsai-wu critereon simulation F

8.2 Appendix B - Density and Moisture content

Results from density and moisture measurements

8.2.1 Calculations

Mean and standard deviation

Table B.1.1. Moisture content

		Glulam beams	Birch plywood
Mean MC	%	12,6	8,92
Standard deviation	%	1,12	0,42
Min MC	%	9,9	8,05
Max MC	%	15,3	9,38

Table B.1.2. Density

		Glulam beams	Birch plywood
Mean density	kg/m^3	462,5	714,4
Standard deviation	kg/m^3	17,31	29,32
Min density	kg/m^3	401,4	645,2
Max density	kg/m^3	501,0	788,1

8.2.2 Measurements

Table B.1.3. Moisture content, Oven test birch plywood

Sample number	m_{wet}	m_{dry}	$m_w = m_{wet} - m_{dry}$	$u = m_w/m_{dry}$
01	35,30	32,30	3,00	9,29
02	28,20	26,10	2,10	8,05
03	25,80	23,60	2,20	9,32
04	30,40	27,90	2,50	8,96
05	24,50	22,40	2,10	9,38
06	36,40	33,50	2,90	8,66
07	24,20	22,30	1,90	8,52
08	24,70	22,70	2,00	8,81
09	30,70	28,10	2,60	9,25
10	25,60	23,50	2,10	8,94

Part names were numbered according to figure below

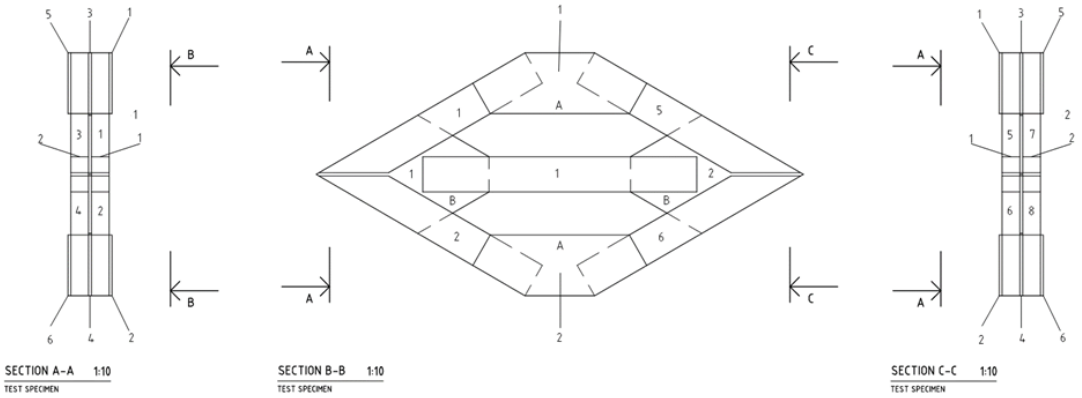

D- Diagonal timber member, H- Horizontal timber member, A- Plywood plate A, B- Plywood plate B

8.2.2.1 Specimen 01

Part name	Littera	Part #	Volume [dm3]	Mass [g]	Density [g/dm3]
D	01-C1G0-D1	1	4,038	1891	468,30
D	01-C1G0-D2	2	4,038	1920	475,48
D	01-C1G0-D3	3	4,038	1947	482,17
D	01-C1G0-D4	4	4,038	1890	468,05
D	01-C1G0-D5	5	4,038	1826	452,20
D	01-C1G0-D6	6	4,038	1902	471,03
D	01-C1G0-D7	7	4,038	1929	477,71
D	01-C1G0-D8	8	4,038	1877	464,83
H	01-C1G0-H1	1	5,322	2394	449,83
H	01-C1G0-H2	2	5,322	2477	465,43
				Mean	467,50

Part name	Littera	Part #	Volume [dm3]	Mass [g]	Density [g/dm3]
A	01-C1G0-A1	1	0,7524	527	700,43
A	01-C1G0-A2	2	0,7524	519	689,79
A	01-C1G0-A3	3	0,7524	532	707,07
A	01-C1G0-A4	4	0,7524	546	725,68
A	01-C1G0-A5	5	0,7524	538	715,05
A	01-C1G0-A6	6	0,7524	532	707,07
B	01-C1G0-B1	1	1,0198	658	645,22
B	01-C1G0-B2	2	1,0198	758	743,28
				Mean	704,20

D- Diagonal timber member, H- Horizontal timber member, A- Plywood plate A, B- Plywood plate B

8.2.2.2 Specimen 02 + MC

Part name	Littera	Part #	Volume [dm3]	Mass [g]	Density [g/dm3]	%MC [%]
D	02-C2G0-D1	1	4,038	1713	424,22	10,7
D	02-C2G0-D2	2	4,038	1861	460,87	10,8
D	02-C2G0-D3	3	4,038	1872	463,60	11,3
D	02-C2G0-D4	4	4,038	1900	470,53	12,2
D	02-C2G0-D5	5	4,038	1907	472,26	11,8
D	02-C2G0-D6	6	4,038	1732	428,93	10,9
D	02-C2G0-D7	7	4,038	1952	483,41	13,3
D	02-C2G0-D8	8	4,038	1914	474,00	12,4
H	02-C2G0-H1	1	5,322	2433	457,16	12,5
H	02-C2G0-H2	2	5,322	2414	453,59	10
				Mean	458,86	

Part name	Littera	Part #	Volume [dm3]	Mass [g]	Density [g/dm3]
A	02-C2G0-A1	1	0,7524	555	737,64
A	02-C2G0-A2	2	0,7524	558	741,63
A	02-C2G0-A3	3	0,7524	549	729,67
A	02-C2G0-A4	4	0,7524	534	709,73
A	02-C2G0-A5	5	0,7524	547	727,01
A	02-C2G0-A6	6	0,7524	536	712,39
B	02-C2G0-B1	1	1,0198	748	733,48
B	02-C2G0-B2	2	1,0198	660	647,19
				Mean	717,34

D- Diagonal timber member, H- Horizontal timber member, A- Plywood plate A, B- Plywood plate B

8.2.2.3 Specimen 03

Part name	Littera	Part #	Volume [dm3]	Mass [g]	Density [g/dm3]
D	03-C3G0-D1	1	4,038	1830	453,19
D	03-C3G0-D2	2	4,038	1892	468,55
D	03-C3G0-D3	3	4,038	1824	451,71
D	03-C3G0-D4	4	4,038	1898	470,03
D	03-C3G0-D5	5	4,038	1802	446,26
D	03-C3G0-D6	6	4,038	1829	452,95
D	03-C3G0-D7	7	4,038	1759	435,61
D	03-C3G0-D8	8	4,038	1876	464,59
H	03-C3G0-H1	1	5,322	2463	462,80
H	03-C3G0-H2	2	5,322	2590	486,66
				Mean	459,23

Part name	Littera	Part #	Volume [dm3]	Mass [g]	Density [g/dm3]
A	03-C3G0-A1	1	0,7524	541	719,03
A	03-C3G0-A2	2	0,7524	545	724,35
A	03-C3G0-A3	3	0,7524	534	709,73
A	03-C3G0-A4	4	0,7524	539	716,37
A	03-C3G0-A5	5	0,7524	527	700,43
A	03-C3G0-A6	6	0,7524	525	697,77
B	03-C3G0-B1	1	1,0198	684	670,72
B	03-C3G0-B2	2	1,0198	761	746,22
				Mean	710,58

D- Diagonal timber member, H- Horizontal timber member, A- Plywood plate A, B- Plywood plate B

8.2.2.4 Specimen 04

Part name	Littera	Part #	Volume [dm3]	Mass [g]	Density [g/dm3]
D	04-T1G0-D1	1	4,038	1875	464,34
D	04-T1G0-D2	2	4,038	1896	469,54
D	04-T1G0-D3	3	4,038	1841	455,92
D	04-T1G0-D4	4	4,038	1848	457,65
D	04-T1G0-D5	5	4,038	1861	460,87
D	04-T1G0-D6	6	4,038	1903	471,27
D	04-T1G0-D7	7	4,038	1724	426,94
D	04-T1G0-D8	8	4,038	1851	458,40
H	04-T1G0-H1	1	5,322	2326	437,05
H	04-T1G0-H2	2	5,322	2517	472,94
				Mean	457,49

Part name	Littera	Part #	Volume [dm3]	Mass [g]	Density [g/dm3]
A	04-T1G0-A1	1	0,7524	512	680,49
A	04-T1G0-A2	2	0,7524	551	732,32
A	04-T1G0-A3	3	0,7524	511	679,16
A	04-T1G0-A4	4	0,7524	510	677,83
A	04-T1G0-A5	5	0,7524	532	707,07
A	04-T1G0-A6	6	0,7524	528	701,75
B	04-T1G0-B1	1	1,0198	754	739,36
B	04-T1G0-B2	2	1,0198	766	751,13
				Mean	708,64

D- Diagonal timber member, H- Horizontal timber member, A- Plywood plate A, B- Plywood plate B

8.2.2.5 Specimen 05 + MC

Part name	Littera	Part #	Volume [dm3]	Mass [g]	Density [g/dm3]	%MC [%]
D	05-T2G0-D1	1	4,038	1935	479,20	13
D	05-T2G0-D2	2	4,038	1974	488,86	11,3
D	05-T2G0-D3	3	4,038	1875	464,34	11,8
D	05-T2G0-D4	4	4,038	1962	485,88	12,5
D	05-T2G0-D5	5	4,038	1973	488,61	13,8
D	05-T2G0-D6	6	4,038	1752	433,88	11,2
D	05-T2G0-D7	7	4,038	1873	463,84	12,8
D	05-T2G0-D8	8	4,038	1963	486,13	12,9
H	05-T2G0-H1	1	5,322	2485	466,93	14,6
H	05-T2G0-H2	2	5,322	2425	455,66	12,7
				Mean	471,33	

Part name	Littera	Part #	Volume [dm3]	Mass [g]	Density [g/dm3]
A	05-T2G0-A1	1	0,7524	589	782,83
A	05-T2G0-A2	2	0,7524	593	788,14
A	05-T2G0-A3	3	0,7524	563	748,27
A	05-T2G0-A4	4	0,7524	583	774,85
A	05-T2G0-A5	5	0,7524	524	696,44
A	05-T2G0-A6	6	0,7524	590	784,16
B	05-T2G0-B1	1	1,0198	733	718,77
B	05-T2G0-B2	2	1,0198	751	736,42
				Mean	753,74

D- Diagonal timber member, H- Horizontal timber member, A- Plywood plate A, B- Plywood plate B

8.2.2.6 Specimen 06

Part name	Littera	Part #	Volume [dm3]	Mass [g]	Density [g/dm3]
D	06-T3G0-D1	1	4,038	1733	429,17
D	06-T3G0-D2	2	4,038	1857	459,88
D	06-T3G0-D3	3	4,038	1757	435,12
D	06-T3G0-D4	4	4,038	2023	500,99
D	06-T3G0-D5	5	4,038	1979	490,09
D	06-T3G0-D6	6	4,038	1897	469,79
D	06-T3G0-D7	7	4,038	1869	462,85
D	06-T3G0-D8	8	4,038	1892	468,55
H	06-T3G0-H1	1	5,322	2550	479,14
H	06-T3G0-H2	2	5,322	2415	453,78
				Mean	464,94

Part name	Littera	Part #	Volume [dm3]	Mass [g]	Density [g/dm3]
A	06-T3G0-A1	1	0,7524	552	733,65
A	06-T3G0-A2	2	0,7524	565	750,93
A	06-T3G0-A3	3	0,7524	547	727,01
A	06-T3G0-A4	4	0,7524	546	725,68
A	06-T3G0-A5	5	0,7524	544	723,02
A	06-T3G0-A6	6	0,7524	549	729,67
B	06-T3G0-B1	1	1,0198	673	659,93
B	06-T3G0-B2	2	1,0198	745	730,54
				Mean	722,55

D- Diagonal timber member, H- Horizontal timber member, A- Plywood plate A, B- Plywood plate B

8.2.2.7 Specimen 07 + MC

Part name	Littera	Part #	Volume [dm3]	Mass [g]	Density [g/dm3]	%MC [%]
D	07-C1G5-D1	1	4,038	1909	472,76	14,2
D	07-C1G5-D2	2	4,038	1973	488,61	15,3
D	07-C1G5-D3	3	4,038	1827	452,45	12,7
D	07-C1G5-D4	4	4,038	1911	473,25	14
D	07-C1G5-D5	5	4,038	1852	458,64	13,1
D	07-C1G5-D6	6	4,038	1896	469,54	13,6
D	07-C1G5-D7	7	4,038	1945	481,67	13
D	07-C1G5-D8	8	4,038	1858	460,13	14,9
H	07-C1G5-H1	1	5,322	2478	465,61	12,2
H	07-C1G5-H2	2	5,322	2367	444,76	13,2
				Mean	466,74	

Part name	Littera	Part #	Volume [dm3]	Mass [g]	Density [g/dm3]
A	07-C1G5-A1	1	0,7524	533	708,40
A	07-C1G5-A2	2	0,7524	532	707,07
A	07-C1G5-A3	3	0,7524	534	709,73
A	07-C1G5-A4	4	0,7524	530	704,41
A	07-C1G5-A5	5	0,7524	530	704,41
A	07-C1G5-A6	6	0,7524	532	707,07
B	07-C1G5-B1	1	1,0198	696	682,49
B	07-C1G5-B2	2	1,0198	697	683,47
				Mean	700,88

D- Diagonal timber member, H- Horizontal timber member, A- Plywood plate A, B- Plywood plate B

8.2.2.8 Specimen 08 + MC

Part name	Littera	Part #	Volume [dm3]	Mass [g]	Density [g/dm3]	%MC [%]
D	08-C2G5-D1	1	4,038	1933	478,70	13,8
D	08-C2G5-D2	2	4,038	1942	480,93	13,7
D	08-C2G5-D3	3	4,038	1825	451,96	11,8
D	08-C2G5-D4	4	4,038	1816	449,73	12,8
D	08-C2G5-D5	5	4,038	1836	454,68	13
D	08-C2G5-D6	6	4,038	1769	438,09	14,2
D	08-C2G5-D7	7	4,038	1818	450,22	12,9
D	08-C2G5-D8	8	4,038	1875	464,34	14,4
H	08-C2G5-H1	1	5,322	2474	464,86	12,2
H	08-C2G5-H2	2	5,322	2442	458,85	12,8
				Mean	459,24	

Part name	Littera	Part #	Volume [dm3]	Mass [g]	Density [g/dm3]
A	08-C2G5-A1	1	0,7524	543	721,69
A	08-C2G5-A2	2	0,7524	586	778,84
A	08-C2G5-A3	3	0,7524	560	744,28
A	08-C2G5-A4	4	0,7524	579	769,54
A	08-C2G5-A5	5	0,7524	541	719,03
A	08-C2G5-A6	6	0,7524	526	699,10
B	08-C2G5-B1	1	1,0198	703	689,35
B	08-C2G5-B2	2	1,0198	703	689,35
				Mean	726,40

D- Diagonal timber member, H- Horizontal timber member, A- Plywood plate A, B- Plywood plate B

8.2.2.9 Specimen 09

Part name	Littera	Part #	Volume [dm3]	Mass [g]	Density [g/dm3]
D	09-C3G5-D1	1	4,038	1964	486,38
D	09-C3G5-D2	2	4,038	1655	409,86
D	09-C3G5-D3	3	4,038	1880	465,58
D	09-C3G5-D4	4	4,038	1783	441,56
D	09-C3G5-D5	5	4,038	1816	449,73
D	09-C3G5-D6	6	4,038	1892	468,55
D	09-C3G5-D7	7	4,038	1903	471,27
D	09-C3G5-D8	8	4,038	1846	457,16
H	09-C3G5-H1	1	5,322	2565	481,96
H	09-C3G5-H2	2	5,322	2534	476,14
				Mean	460,82

Part name	Littera	Part #	Volume [dm3]	Mass [g]	Density [g/dm3]
A	09-C3G5-A1	1	0,7524	521	692,45
A	09-C3G5-A2	2	0,7524	544	723,02
A	09-C3G5-A3	3	0,7524	549	729,67
A	09-C3G5-A4	4	0,7524	530	704,41
A	09-C3G5-A5	5	0,7524	545	724,35
A	09-C3G5-A6	6	0,7524	537	713,72
B	09-C3G5-B1	1	1,0198	701	687,39
B	09-C3G5-B2	2	1,0198	689	675,62
				Mean	706,33

D- Diagonal timber member, H- Horizontal timber member, A- Plywood plate A, B- Plywood plate B

8.2.2.10 Specimen 10

Part name	Littera	Part #	Volume [dm3]	Mass [g]	Density [g/dm3]
D	10-T1G5-D1	1	4,038	1857	459,88
D	10-T1G5-D2	2	4,038	1942	480,93
D	10-T1G5-D3	3	4,038	1975	489,10
D	10-T1G5-D4	4	4,038	1961	485,64
D	10-T1G5-D5	5	4,038	1819	450,47
D	10-T1G5-D6	6	4,038	1880	465,58
D	10-T1G5-D7	7	4,038	1870	463,10
D	10-T1G5-D8	8	4,038	1998	494,80
H	10-T1G5-H1	1	5,322	2447	459,79
H	10-T1G5-H2	2	5,322	2482	466,37
				Mean	471,57

Part name	Littera	Part #	Volume [dm3]	Mass [g]	Density [g/dm3]
A	10-T1G5-A1	1	0,7524	524	696,44
A	10-T1G5-A2	2	0,7524	508	675,17
A	10-T1G5-A3	3	0,7524	560	744,28
A	10-T1G5-A4	4	0,7524	541	719,03
A	10-T1G5-A5	5	0,7524	532	707,07
A	10-T1G5-A6	6	0,7524	529	703,08
B	10-T1G5-B1	1	1,0198	703	689,35
B	10-T1G5-B2	2	1,0198	680	666,80
				Mean	700,15

D- Diagonal timber member, H- Horizontal timber member, A- Plywood plate A, B- Plywood plate B

8.2.2.11 Specimen 11

Part name	Littera	Part #	Volume [dm3]	Mass [g]	Density [g/dm3]
D	11-T2G5-D1	1	4,038	1870	463,10
D	11-T2G5-D2	2	4,038	1950	482,91
D	11-T2G5-D3	3	4,038	1906	472,02
D	11-T2G5-D4	4	4,038	1621	401,44
D	11-T2G5-D5	5	4,038	1948	482,42
D	11-T2G5-D6	6	4,038	1937	479,69
D	11-T2G5-D7	7	4,038	1797	445,02
D	11-T2G5-D8	8	4,038	1957	484,65
H	11-T2G5-H1	1	5,322	2558	480,65
H	11-T2G5-H2	2	5,322	2313	434,61
				Mean	462,65

Part name	Littera	Part #	Volume [dm3]	Mass [g]	Density [g/dm3]
A	11-T2G5-A1	1	0,7524	544	723,02
A	11-T2G5-A2	2	0,7524	545	724,35
A	11-T2G5-A3	3	0,7524	540	717,70
A	11-T2G5-A4	4	0,7524	551	732,32
A	11-T2G5-A5	5	0,7524	547	727,01
A	11-T2G5-A6	6	0,7524	546	725,68
B	11-T2G5-B1	1	1,0198	706	692,29
B	11-T2G5-B2	2	1,0198	683	669,74
				Mean	714,01

D- Diagonal timber member, H- Horizontal timber member, A- Plywood plate A, B- Plywood plate B

8.2.2.12 Specimen 12

Part name	Littera	Part #	Volume [dm3]	Mass [g]	Density [g/dm3]
D	12-T3G5-D1	1	4,038	1802	446,26
D	12-T3G5-D2	2	4,038	1769	438,09
D	12-T3G5-D3	3	4,038	1903	471,27
D	12-T3G5-D4	4	4,038	1872	463,60
D	12-T3G5-D5	5	4,038	1928	477,46
D	12-T3G5-D6	6	4,038	1881	465,82
D	12-T3G5-D7	7	4,038	1897	469,79
D	12-T3G5-D8	8	4,038	1842	456,17
H	12-T3G5-H1	1	5,322	2471	464,30
H	12-T3G5-H2	2	5,322	2269	426,34
				Mean	457,91

Part name	Littera	Part #	Volume [dm3]	Mass [g]	Density [g/dm3]
A	12-T3G5-A1	1	0,7524	533	708,40
A	12-T3G5-A2	2	0,7524	535	711,06
A	12-T3G5-A3	3	0,7524	533	708,40
A	12-T3G5-A4	4	0,7524	537	713,72
A	12-T3G5-A5	5	0,7524	519	689,79
A	12-T3G5-A6	6	0,7524	515	684,48
B	12-T3G5-B1	1	1,0198	690	676,60
B	12-T3G5-B2	2	1,0198	691	677,58
				Mean	696,25

D- Diagonal timber member, H- Horizontal timber member, A- Plywood plate A, B- Plywood plate B

8.2.2.13 Specimen 13 + MC

Part name	Littera	Part #	Volume [dm3]	Mass [g]	Density [g/dm3]	%MC [%]
D	13-C1G15-D1	1	4,038	1792	443,78	11,6
D	13-C1G15-D2	2	4,038	1920	475,48	12,1
D	13-C1G15-D3	3	4,038	1800	445,77	12,4
D	13-C1G15-D4	4	4,038	1814	449,23	12,7
D	13-C1G15-D5	5	4,038	1844	456,66	13,4
D	13-C1G15-D6	6	4,038	1833	453,94	9,9
D	13-C1G15-D7	7	4,038	1744	431,90	12,8
D	13-C1G15-D8	8	4,038	1876	464,59	13,3
H	13-C1G15-H1	1	5,322	2268	426,16	11,3
H	13-C1G15-H2	2	5,322	2428	456,22	11,8
				Mean	450,37	

Part name	Littera	Part #	Volume [dm3]	Mass [g]	Density [g/dm3]
A	13-C1G15-A1	1	0,7524	546	725,68
A	13-C1G15-A2	2	0,7524	538	715,05
A	13-C1G15-A3	3	0,7524	531	705,74
A	13-C1G15-A4	4	0,7524	538	715,05
A	13-C1G15-A5	5	0,7524	538	715,05
A	13-C1G15-A6	6	0,7524	541	719,03
B	13-C1G15-B1	1	1,0198	690	676,60
B	13-C1G15-B2	2	1,0198	735	720,73
				Mean	711,62

D- Diagonal timber member, H- Horizontal timber member, A- Plywood plate A, B- Plywood plate B

8.2.2.14 Specimen 14

Part name	Littera	Part #	Volume [dm3]	Mass [g]	Density [g/dm3]
D	14-C2G15-D1	1	4,038	1852	458,64
D	14-C2G15-D2	2	4,038	1851	458,40
D	14-C2G15-D3	3	4,038	1906	472,02
D	14-C2G15-D4	4	4,038	1899	470,28
D	14-C2G15-D5	5	4,038	1726	427,44
D	14-C2G15-D6	6	4,038	1894	469,04
D	14-C2G15-D7	7	4,038	1846	457,16
D	14-C2G15-D8	8	4,038	1814	449,23
H	14-C2G15-H1	1	5,322	2324	436,68
H	14-C2G15-H2	2	5,322	2628	493,80
				Mean	459,27

Part name	Littera	Part #	Volume [dm3]	Mass [g]	Density [g/dm3]
A	14-C2G15-A1	1	0,7524	549	729,67
A	14-C2G15-A2	2	0,7524	534	709,73
A	14-C2G15-A3	3	0,7524	538	715,05
A	14-C2G15-A4	4	0,7524	586	778,84
A	14-C2G15-A5	5	0,7524	552	733,65
A	14-C2G15-A6	6	0,7524	533	708,40
B	14-C2G15-B1	1	1,0198	733	718,77
B	14-C2G15-B2	2	1,0198	713	699,16
				Mean	724,16

D- Diagonal timber member, H- Horizontal timber member, A- Plywood plate A, B- Plywood plate B

8.2.2.15 Specimen 15

Part name	Littera	Part #	Volume [dm3]	Mass [g]	Density [g/dm3]
D	15-C3G15-D1	1	4,038	1949	482,66
D	15-C3G15-D2	2	4,038	1955	484,15
D	15-C3G15-D3	3	4,038	1950	482,91
D	15-C3G15-D4	4	4,038	1808	447,75
D	15-C3G15-D5	5	4,038	1903	471,27
D	15-C3G15-D6	6	4,038	1924	476,47
D	15-C3G15-D7	7	4,038	1877	464,83
D	15-C3G15-D8	8	4,038	1903	471,27
H	15-C3G15-H1	1	5,322	2533	475,95
H	15-C3G15-H2	2	5,322	2332	438,18
				Mean	469,55

Part name	Littera	Part #	Volume [dm3]	Mass [g]	Density [g/dm3]
A	15-C3G15-A1	1	0,7524	550	730,99
A	15-C3G15-A2	2	0,7524	538	715,05
A	15-C3G15-A3	3	0,7524	524	696,44
A	15-C3G15-A4	4	0,7524	510	677,83
A	15-C3G15-A5	5	0,7524	537	713,72
A	15-C3G15-A6	6	0,7524	510	677,83
B	15-C3G15-B1	1	1,0198	711	697,20
B	15-C3G15-B2	2	1,0198	708	694,25
				Mean	700,41

D- Diagonal timber member, H- Horizontal timber member, A- Plywood plate A, B- Plywood plate B

8.2.2.16 Specimen 16 + MC

Part name	Littera	Part #	Volume [dm3]	Mass [g]	Density [g/dm3]	%MC [%]
D	16-T1G15-D1	1	4,038	1841	455,92	13
D	16-T1G15-D2	2	4,038	1882	466,07	12,8
D	16-T1G15-D3	3	4,038	1770	438,34	11,6
D	16-T1G15-D4	4	4,038	1842	456,17	12,3
D	16-T1G15-D5	5	4,038	1942	480,93	12,2
D	16-T1G15-D6	6	4,038	1938	479,94	12,9
D	16-T1G15-D7	7	4,038	1819	450,47	11,6
D	16-T1G15-D8	8	4,038	1879	465,33	13,4
H	16-T1G15-H1	1	5,322	2585	485,72	12,9
H	16-T1G15-H2	2	5,322	2368	444,95	12,8
				Mean	462,38	

Part name	Littera	Part #	Volume [dm3]	Mass [g]	Density [g/dm3]
A	16-T1G15-A1	1	0,7524	589	782,83
A	16-T1G15-A2	2	0,7524	550	730,99
A	16-T1G15-A3	3	0,7524	510	677,83
A	16-T1G15-A4	4	0,7524	520	691,12
A	16-T1G15-A5	5	0,7524	592	786,82
A	16-T1G15-A6	6	0,7524	537	713,72
B	16-T1G15-B1	1	1,0198	701	687,39
B	16-T1G15-B2	2	1,0198	705	691,31
				Mean	720,25

D- Diagonal timber member, H- Horizontal timber member, A- Plywood plate A, B- Plywood plate B

8.2.2.17 Specimen 17

Part name	Littera	Part #	Volume [dm3]	Mass [g]	Density [g/dm3]
D	17-T2G15-D1	1	4,038	1840	455,67
D	17-T2G15-D2	2	4,038	1881	465,82
D	17-T2G15-D3	3	4,038	1838	455,18
D	17-T2G15-D4	4	4,038	1901	470,78
D	17-T2G15-D5	5	4,038	1845	456,91
D	17-T2G15-D6	6	4,038	1855	459,39
D	17-T2G15-D7	7	4,038	1768	437,84
D	17-T2G15-D8	8	4,038	1956	484,40
H	17-T2G15-H1	1	5,322	2554	479,89
H	17-T2G15-H2	2	5,322	2516	472,75
				Mean	463,86

Part name	Littera	Part #	Volume [dm3]	Mass [g]	Density [g/dm3]
A	17-T2G15-A1	1	0,7524	541	719,03
A	17-T2G15-A2	2	0,7524	515	684,48
A	17-T2G15-A3	3	0,7524	523	695,11
A	17-T2G15-A4	4	0,7524	588	781,50
A	17-T2G15-A5	5	0,7524	526	699,10
A	17-T2G15-A6	6	0,7524	519	689,79
B	17-T2G15-B1	1	1,0198	726	711,90
B	17-T2G15-B2	2	1,0198	699	685,43
				Mean	708,29

D- Diagonal timber member, H- Horizontal timber member, A- Plywood plate A, B- Plywood plate B

8.2.2.18 Specimen 18

Part name	Littera	Part #	Volume [dm3]	Mass [g]	Density [g/dm3]
D	18-T3G15-D1	1	4,038	1873	463,84
D	18-T3G15-D2	2	4,038	1977	489,60
D	18-T3G15-D3	3	4,038	1909	472,76
D	18-T3G15-D4	4	4,038	1912	473,50
D	18-T3G15-D5	5	4,038	1947	482,17
D	18-T3G15-D6	6	4,038	1856	459,63
D	18-T3G15-D7	7	4,038	1896	469,54
D	18-T3G15-D8	8	4,038	1800	445,77
H	18-T3G15-H1	1	5,322	2544	478,02
H	18-T3G15-H2	2	5,322	2505	470,69
				Mean	470,55

Part name	Littera	Part #	Volume [dm3]	Mass [g]	Density [g/dm3]
A	18-T3G15-A1	1	0,7524	570	757,58
A	18-T3G15-A2	2	0,7524	563	748,27
A	18-T3G15-A3	3	0,7524	534	709,73
A	18-T3G15-A4	4	0,7524	584	776,18
A	18-T3G15-A5	5	0,7524	553	734,98
A	18-T3G15-A6	6	0,7524	536	712,39
B	18-T3G15-B1	1	1,0198	705	691,31
B	18-T3G15-B2	2	1,0198	710	696,21
				Mean	728,33

D- Diagonal timber member, H- Horizontal timber member, A- Plywood plate A, B- Plywood plate B

8.2.2.19 Specimen 19

Part name	Littera	Part #	Volume [dm3]	Mass [g]	Density [g/dm3]
D	19-C1D0-D1	1	4,038	1929	477,71
D	19-C1D0-D2	2	4,038	1780	440,81
D	19-C1D0-D3	3	4,038	1759	435,61
D	19-C1D0-D4	4	4,038	1817	449,98
D	19-C1D0-D5	5	4,038	1820	450,72
D	19-C1D0-D6	6	4,038	1916	474,49
D	19-C1D0-D7	7	4,038	1878	465,08
D	19-C1D0-D8	8	4,038	1806	447,25
H	19-C1D0-H1	1	5,322	2334	438,56
H	19-C1D0-H2	2	5,322	2488	467,49
				Mean	454,77

Part name	Littera	Part #	Volume [dm3]	Mass [g]	Density [g/dm3]
A	19-C1D0-A1	1	0,7524	549	729,67
A	19-C1D0-A2	2	0,7524	564	749,60
A	19-C1D0-A3	3	0,7524	556	738,97
A	19-C1D0-A4	4	0,7524	550	730,99
A	19-C1D0-A5	5	0,7524	547	727,01
A	19-C1D0-A6	6	0,7524	538	715,05
B	19-C1D0-B1	1	1,0198	744	729,55
B	19-C1D0-B2	2	1,0198	679	665,82
				Mean	723,33

D- Diagonal timber member, H- Horizontal timber member, A- Plywood plate A, B- Plywood plate B

8.2.2.20 Specimen 20

Part name	Littera	Part #	Volume [dm3]	Mass [g]	Density [g/dm3]
D	20-C2D0-D1	1	4,038	1807	447,50
D	20-C2D0-D2	2	4,038	1888	467,56
D	20-C2D0-D3	3	4,038	1788	442,79
D	20-C2D0-D4	4	4,038	1777	440,07
D	20-C2D0-D5	5	4,038	1928	477,46
D	20-C2D0-D6	6	4,038	1838	455,18
D	20-C2D0-D7	7	4,038	1802	446,26
D	20-C2D0-D8	8	4,038	1874	464,09
H	20-C2D0-H1	1	5,322	2570	482,90
H	20-C2D0-H2	2	5,322	2446	459,60
				Mean	458,34

Part name	Littera	Part #	Volume [dm3]	Mass [g]	Density [g/dm3]
A	20-C2D0-A1	1	0,7524	524	696,44
A	20-C2D0-A2	2	0,7524	560	744,28
A	20-C2D0-A3	3	0,7524	540	717,70
A	20-C2D0-A4	4	0,7524	510	677,83
A	20-C2D0-A5	5	0,7524	529	703,08
A	20-C2D0-A6	6	0,7524	527	700,43
B	20-C2D0-B1	1	1,0198	763	748,19
B	20-C2D0-B2	2	1,0198	762	747,21
				Mean	716,89

D- Diagonal timber member, H- Horizontal timber member, A- Plywood plate A, B- Plywood plate B

8.2.2.21 Specimen 21

Part name	Littera	Part #	Volume [dm3]	Mass [g]	Density [g/dm3]
D	21-C3D0-D1	1	4,038	1932	478,45
D	21-C3D0-D2	2	4,038	1756	434,87
D	21-C3D0-D3	3	4,038	1921	475,73
D	21-C3D0-D4	4	4,038	1796	444,77
D	21-C3D0-D5	5	4,038	1956	484,40
D	21-C3D0-D6	6	4,038	1982	490,84
D	21-C3D0-D7	7	4,038	1869	462,85
D	21-C3D0-D8	8	4,038	1938	479,94
H	21-C3D0-H1	1	5,322	2286	429,54
H	21-C3D0-H2	2	5,322	2309	433,86
				Mean	461,53

Part name	Littera	Part #	Volume [dm3]	Mass [g]	Density [g/dm3]
A	21-C3D0-A1	1	0,7524	534	709,73
A	21-C3D0-A2	2	0,7524	507	673,84
A	21-C3D0-A3	3	0,7524	543	721,69
A	21-C3D0-A4	4	0,7524	521	692,45
A	21-C3D0-A5	5	0,7524	535	711,06
A	21-C3D0-A6	6	0,7524	534	709,73
B	21-C3D0-B1	1	1,0198	740	725,63
B	21-C3D0-B2	2	1,0198	672	658,95
				Mean	700,39

D- Diagonal timber member, H- Horizontal timber member, A- Plywood plate A, B- Plywood plate B

8.2.2.22 Specimen 22

Part name	Littera	Part #	Volume [dm3]	Mass [g]	Density [g/dm3]
D	22-T1D0-D1	1	4,038	1902	471,03
D	22-T1D0-D2	2	4,038	1792	443,78
D	22-T1D0-D3	3	4,038	1772	438,83
D	22-T1D0-D4	4	4,038	1760	435,86
D	22-T1D0-D5	5	4,038	1964	486,38
D	22-T1D0-D6	6	4,038	1914	474,00
D	22-T1D0-D7	7	4,038	1873	463,84
D	22-T1D0-D8	8	4,038	1857	459,88
H	22-T1D0-H1	1	5,322	2550	479,14
H	22-T1D0-H2	2	5,322	2502	470,12
				Mean	462,29

Part name	Littera	Part #	Volume [dm3]	Mass [g]	Density [g/dm3]
A	22-T1D0-A1	1	0,7524	541	719,03
A	22-T1D0-A2	2	0,7524	543	721,69
A	22-T1D0-A3	3	0,7524	559	742,96
A	22-T1D0-A4	4	0,7524	550	730,99
A	22-T1D0-A5	5	0,7524	558	741,63
A	22-T1D0-A6	6	0,7524	517	687,13
B	22-T1D0-B1	1	1,0198	682	668,76
B	22-T1D0-B2	2	1,0198	663	650,13
				Mean	707,79

D- Diagonal timber member, H- Horizontal timber member, A- Plywood plate A, B- Plywood plate B

8.2.2.23 Specimen 23

Part name	Littera	Part #	Volume [dm3]	Mass [g]	Density [g/dm3]
D	23-T2D0-D1	1	4,038	1831	453,44
D	23-T2D0-D2	2	4,038	1904	471,52
D	23-T2D0-D3	3	4,038	1863	461,37
D	23-T2D0-D4	4	4,038	1819	450,47
D	23-T2D0-D5	5	4,038	1967	487,12
D	23-T2D0-D6	6	4,038	1933	478,70
D	23-T2D0-D7	7	4,038	2001	495,54
D	23-T2D0-D8	8	4,038	1736	429,92
H	23-T2D0-H1	1	5,322	2282	428,79
H	23-T2D0-H2	2	5,322	2392	449,46
				Mean	460,63

Part name	Littera	Part #	Volume [dm3]	Mass [g]	Density [g/dm3]
A	23-T2D0-A1	1	0,7524	529	703,08
A	23-T2D0-A2	2	0,7524	525	697,77
A	23-T2D0-A3	3	0,7524	527	700,43
A	23-T2D0-A4	4	0,7524	528	701,75
A	23-T2D0-A5	5	0,7524	546	725,68
A	23-T2D0-A6	6	0,7524	554	736,31
B	23-T2D0-B1	1	1,0198	667	654,05
B	23-T2D0-B2	2	1,0198	764	749,17
				Mean	708,53

D- Diagonal timber member, H- Horizontal timber member, A- Plywood plate A, B- Plywood plate B

8.2.2.24 Specimen 24

Part name	Littera	Part #	Volume [dm3]	Mass [g]	Density [g/dm3]
D	24-T3D0-D1	1	4,038	1942	480,93
D	24-T3D0-D2	2	4,038	1880	465,58
D	24-T3D0-D3	3	4,038	1858	460,13
D	24-T3D0-D4	4	4,038	1860	460,62
D	24-T3D0-D5	5	4,038	1923	476,23
D	24-T3D0-D6	6	4,038	1859	460,38
D	24-T3D0-D7	7	4,038	1849	457,90
D	24-T3D0-D8	8	4,038	1897	469,79
H	24-T3D0-H1	1	5,322	2452	460,73
H	24-T3D0-H2	2	5,322	2633	494,74
				Mean	468,70

Part name	Littera	Part #	Volume [dm3]	Mass [g]	Density [g/dm3]
A	24-T3D0-A1	1	0,7524	552	733,65
A	24-T3D0-A2	2	0,7524	566	752,26
A	24-T3D0-A3	3	0,7524	579	769,54
A	24-T3D0-A4	4	0,7524	567	753,59
A	24-T3D0-A5	5	0,7524	585	777,51
A	24-T3D0-A6	6	0,7524	565	750,93
B	24-T3D0-B1	1	1,0198	687	673,66
B	24-T3D0-B2	2	1,0198	677	663,86
				Mean	734,37

D- Diagonal timber member, H- Horizontal timber member, A- Plywood plate A, B- Plywood plate B

8.3 Appendix C - Calculations

Calculations Plywood Gusset Plates

Frame model, load and stress distribution

Normal force:

$Load := 70\ kN$

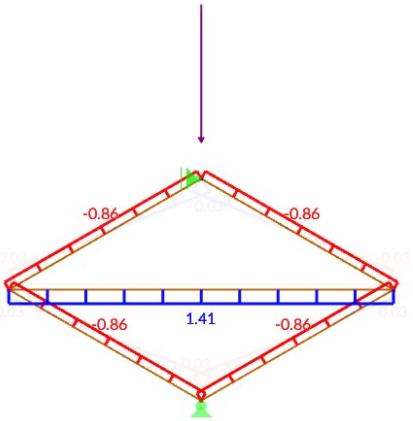

Diagonal:

$M := 0.02 \cdot Load \cdot m = 1.4\ kN \cdot m$

$V := 0.08 \cdot Load = 5.6\ kN$

$N_1 := 0.86 \cdot Load = 60.2\ kN$

Horizontal:

$N_H := 1.43 \cdot Load = 100.1\ kN$

Shear force:

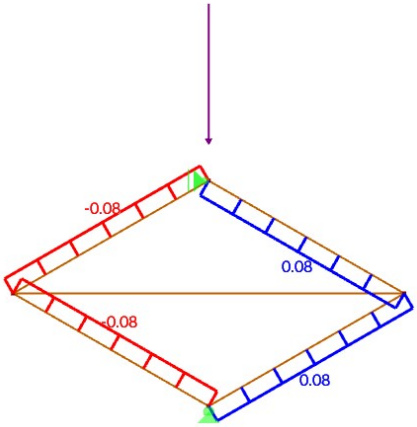

Moment:

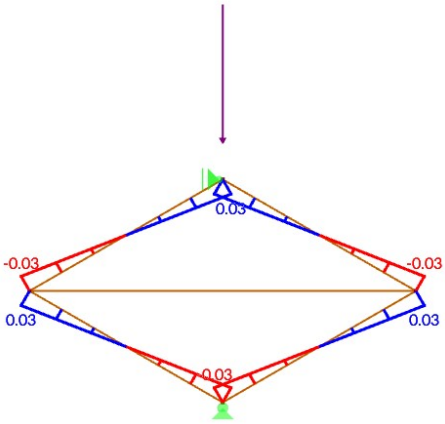

Bending moment is chosen as 0.02 to get an average over the plywood plate,

Stresses in Glueline

Cross-sectional properties

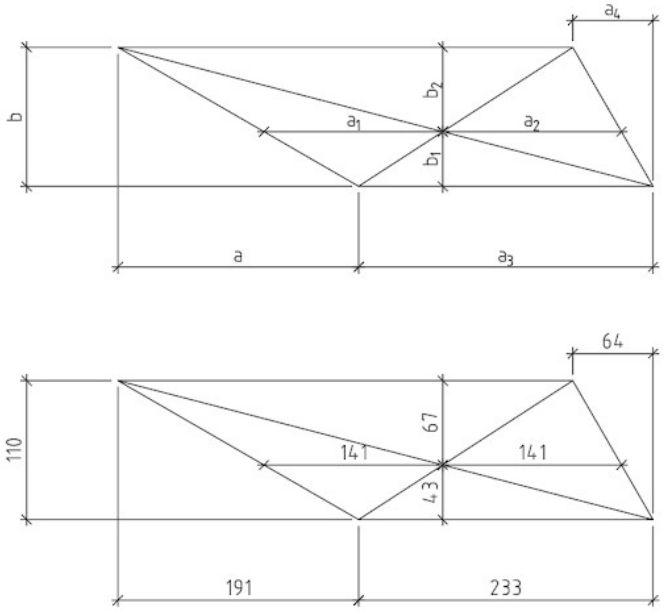

$a := 201\ mm$
$a_1 := 153\ mm$
$a_2 := 141\ mm$
$a_3 := 233\ mm$
$a_4 := 63\ mm$

$b := 110\ mm$
$b_1 := 43\ mm$
$b_2 := 67\ mm$

$$A_D := \int_{-b_1}^{b_2} \int_{\frac{-a}{b}\cdot y - a_1}^{\frac{-a_4}{b}\cdot y + a_4} 1 \, dx \, dy = \left(2.542 \cdot 10^4\right)\ mm^2$$

Glue-line area between diagonal member and gusset plate

$$A_H := 209\ mm \cdot 110\ mm = \left(2.299 \cdot 10^4\right)\ mm^2$$

Glue-line area between horizontal member and gusset plate

$$I_p = \int\int r^2 \, dx \, dy = \int\int x^2 + y^2 \, dx \, dy = I_{xx} + I_{yy}$$

Polar moment of inertia

$$I_{xx} := \int_{-b_1}^{b_2} \int_{\frac{-a}{b}\cdot y - a_1}^{\frac{-a_4}{b}\cdot y + a_4} y^2 \, dx \, dy = \left(3.263 \cdot 10^7\right)\ mm^4$$

$$I_{yy} := \int_{-b_1}^{b_2} \int_{\frac{-a}{b}\cdot y - a_1}^{\frac{-a_4}{b}\cdot y + a_4} x^2 \, dx \, dy = \left(2.696 \cdot 10^8\right)\ mm^4$$

$$I_p := I_{xx} + I_{yy} = \left(3.022 \cdot 10^8\right)\ mm^4$$

Diagonal member:

Shear stresses:

$$\tau_V := \frac{V}{2\ A_D} = 0.11\ \textit{MPa}$$

$$\tau_N := \frac{N_1}{2 \cdot A_D} = 1.184\ \textit{MPa}$$

$$\tau_M = \frac{M}{I_p} \cdot r_i$$

Top left corner:

$$r_1 := \sqrt{\left(\frac{-a}{b} \cdot b_2 - a_1\right)^2 + (b_2)^2} = 283.459\ \textit{mm}$$

Longest distance from geometrical center of glueline.

$$\tau_M := \frac{M}{2\ I_p} \cdot r_1 = 656.588\ \textit{kPa}$$

$$\tau_N = 1.184\ \textit{MPa}$$

$$\tau_V = 110.167\ \textit{kPa}$$

$$\tau := \sqrt{{\tau_N}^2 + \left(\tau_V + \tau_M\right)^2} = 1.411\ \textit{MPa}$$

Shear stresses in glueline

Horizontal member:

$$\tau_{H.Glue} := \frac{N_H}{2 \cdot A_H} = 2.177\ \textit{MPa}$$

Johansens' yield theory

Capacity of fasteners

Glulam GL30c

$d_1 := 5.1\ mm$ $t_1 := 56\ mm$

$\rho_1 := 430\ \frac{kg}{m^3}$

$f_{h.1} := 0.082 \cdot \left(1 - 0.01 \cdot \frac{d_1}{mm}\right) \cdot \frac{\rho_1}{\frac{kg}{m^3}} = 33.462$

Birch plywood

$d_2 := 5.1\ mm$ $t_2 := 9\ mm$

$\rho_2 := 690\ \frac{kg}{m^3}$

$f_{h.2} := 0.11 \cdot \left(1 - 0.01 \cdot \frac{d_2}{mm}\right) \cdot \frac{\rho_2}{\frac{kg}{m^3}} = 72.029$ *Bolted plywood to timber*

$f_{h.2.1} := 0.11 \cdot \frac{\rho_2}{\frac{kg}{m^3}} \cdot \left(\frac{d_2}{mm}\right)^{-0.3} = 46.555$ *Nailed plywood to timber*

$\beta := \frac{f_{h.2}}{f_{h.1}} = 2.153$

The embedment strength for a bolted panel to timber connection is used as it gives a results that better corresponds to the test values.

Dowel/nail

$d := 5.1\ mm$

$f_{uk} := 510\ MPa$

$M_y := 1.10 \cdot 21492$ Gunnebo 5.1x150 dokumenterat flytmoment i Nmm

$$F_{v1.Rk} := f_{h.1} \cdot \frac{t_1}{mm} \cdot \frac{d}{mm}\ N = 9.557\ kN$$

$$F_{v2.Rk} := 0.5 \cdot f_{h.2} \cdot \frac{t_2}{mm} \cdot \frac{d}{mm}\ N = 1.653\ kN$$

$$F_{v3.Rk} := 1.05 \cdot \frac{f_{h.1} \cdot \frac{t_1}{mm} \cdot \frac{d}{mm}}{2+\beta} \cdot \left(\sqrt{2 \cdot \beta \cdot (1+\beta) + \frac{4 \cdot \beta \cdot (2+\beta) \cdot M_y}{f_{h.1} \cdot \frac{d}{mm} \cdot \left(\frac{t_1}{mm}\right)^2}} - \beta \right) N = 4.205\ kN$$

$$F_{v4.Rk} := 1.15 \cdot \sqrt{\frac{2 \cdot \beta}{1+\beta}} \cdot \sqrt{2 \cdot M_y \cdot f_{h.1} \cdot \frac{d}{mm}}\ N = 3.817\ kN$$

$F_{Rk} := min\left(F_{v1.Rk}, F_{v2.Rk}, F_{v3.Rk}, F_{v4.Rk}\right) = 1.653\ kN$ *Per shear plane*

$R_{Rk} := 2 \cdot F_{Rk} = 3.306\ kN$

We see that the failure mode we can expect to see is failure mode 3, tear out failure of the fasteners in the plywood. We can also see this when performing the tensile test where the nails are pulled out of the plywood, for compression this, however does not seem to be a problem but rather we get tensile failure from the horizontal member.

Failure Modes - Nailed connection

Force on structure: $F := 38\ kN$

Forces in members

Zone A: Diagonal

$N_A := 0.86 \cdot F = 32.68\ kN$
$T_A := 0.08 \cdot F = 3.04\ kN$
$M_A := 0.02 \cdot F \cdot m = 0.76\ kN \cdot m$

$H_A := N_A \cdot \cos(30\ deg) + T_A \cdot \sin(30\ deg) = 29.822\ kN$
$V_A := N_A \cdot \sin(30\ deg) + T_A \cdot \cos(30\ deg) = 18.973\ kN$

The forces within the horizontal timber beams are transferred to components that are parallel and perpendicular the face-grain of the plywood.

Zone B: Horizontal

$H_B := 1.6 \cdot F = 60.8\ kN$
$V_B := 0.145 \cdot F = 5.51\ kN$
$M := 0\ kN \cdot m$

Cross-sectional properties

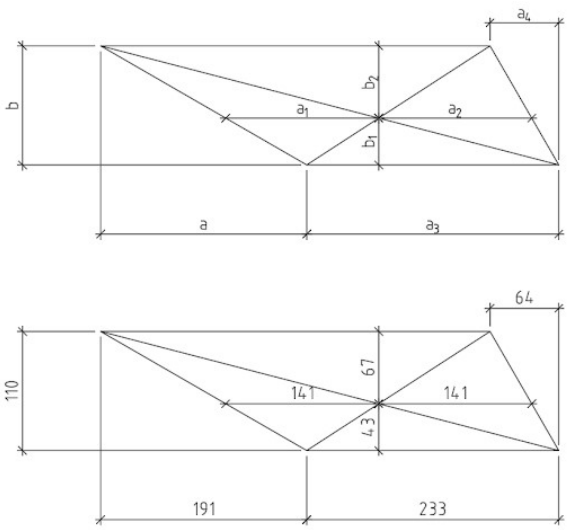

$a := 140\ mm$ $b := 80\ mm$

$a_1 := 72\ mm$ $b_1 := 25\ mm$

$a_2 := 144\ mm$ $b_2 := 60\ mm$

$a_3 := 208\ mm$

$a_4 := 63\ mm$

Corrected coordinates in relation to rotational center for nailed connection

n	x_i	y_i
$(-)$	(mm)	(mm)
1	−47	−24.5
2	−11	−24.5
3	25	−24.5
4	61	−24.5
5	97	−24.5
6	133	−24.5
7	−133	24.5
8	−97	24.5
9	−61	24.5
10	−25	24.5
11	11	24.5
12	47	24.5
13	−90	0
14	−64	0
15	−18	0
16	18	0
17	54	0
18	90	0

Coordinates for corner nails in relation to the center of the nail group

$x_1 := -59\ mm$ $y_1 := -13\ mm$ *Bottom left*

$x_2 := 121\ mm$ $y_2 := -13\ mm$ *Bottom right*

$x_3 := -145\ mm$ $y_3 := 36\ mm$ *Top left*

$x_4 := 35\ mm$ $y_4 := 36\ mm$ *Top right*

Polar bending resistance:

$$W_P = \int_{A_{ef}} r \, dA$$ Formula from Eurocode

Found articles saying what the bending resistance is equal to the polar moment of inertia divided by r. Since we already calculcated that we can use.

$$W_P = \int_{A_{ef}} r \, dA = \frac{I_p}{r} = \frac{\iint r^2 \, dx \, dy}{r} = \iint r \, dx \, dy$$

$$r^2 = x^2 + y^2$$

$$r = \sqrt{x^2 + y^2}$$

$$W_{P.A} := \int_{-b_1}^{b_2} \int_{\frac{-a}{b} \cdot y - a_1}^{\frac{-a_4}{b} \cdot y + a_4} \sqrt{(x)^2 + y^2} \, dx \, dy = \left(7.802 \cdot 10^5\right) \, mm^3$$

$$I_{P.A} := \int_{-b_1}^{b_2} \int_{\frac{-a}{b} \cdot y - a_1}^{\frac{-a_4}{b} \cdot y + a_4} x^2 + y^2 \, dx \, dy = \left(6.51 \cdot 10^7\right) \, mm^4$$

$$S_{sr} := \sum \left({x_i}^2 + {y_i}^2\right) = \left(9.861 \cdot 10^4\right) \, mm^2$$

The nailed connection will here be studied as if it was glued, meaning it has a very small slip in and force transfer throught the entire surface. The cross sectional properties are taken as the area covered by the nail group.

Geometry of rupture lines

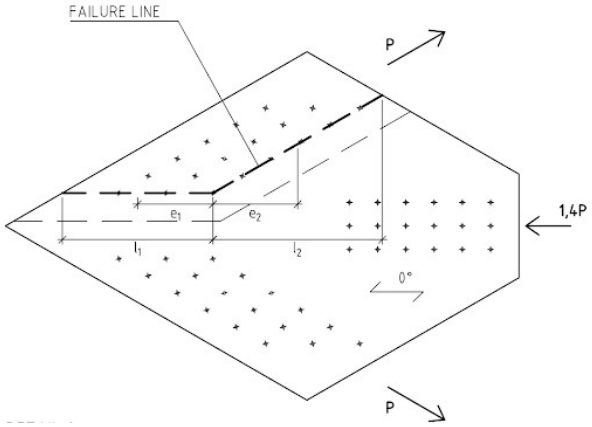

$d_{nail} := 5.1 \cdot 1.20\ mm = 6.12\ mm$

$t_{plywood} := 9\ mm$

Assume nail holes increase 20% due to deformations

$l_1 := 160\ mm - 3 \cdot d_{nail} = 141.64\ mm$

$l_2 := 180\ mm - 6 \cdot d_{nail} = 143.28\ mm$

$l := l_1 + l_2 = 284.92\ mm$

Here 3 different lengths are tested with different loads. See chapter 5.2.1.2 for results and lengths

Force transfer by quantative method:

$$\delta_A := \frac{l_1}{l} = 0.497 \qquad \delta_B := \frac{l_2}{l} = 0.503$$

Rupture line A1-A2: Along l_1

$N_{A1.A2} := \delta_A \cdot V_A = 9.432\ kN$

$T_{A1.A2} := \delta_A \cdot H_A = 14.825\ kN$

Rupture line A2-A3: Along l_2

$N_{A2.A3} := \delta_B \cdot V_A = 9.541\ kN$

$T_{A2.A3} := \delta_B \cdot H_A = 14.997\ kN$

Tsai Wu - Failure criterion

$f_{t.x} := 62.5\ MPa$ $f_{t.y} := 56.7\ MPa$ $f_{c.x} := 31.32\ MPa$

$f_{c.y} := 23.93\ MPa$ $f_{v} := 11.98\ MPa$

$\alpha_{x.y} := -0.5\ MPa$ alpha is an interaction coefficient used to obtain a close envelope for the failure criteria. Wu proposed -0.5 but 0.04 has also been used by Eberhardsteiner (2002) for clear spruce samples. Its supposed to be unitless, but that wouldnt work with the formula in mathcad. Changing the value has marginal effects on the results in this case.

Stresses along rupture lines

A1-A2

$$\sigma_x := \frac{T_{A1.A2}}{l_1 \cdot t_{plywood}} = 11.63\ MPa$$

$$\sigma_y := \frac{N_{A1.A2}}{l_1 \cdot t_{plywood}} = 7.399\ MPa$$

$x_3 := -145\ mm$ $x_1 := -59\ mm$

$r_{A1} := \sqrt{x_3^{\,2} + y_3^{\,2}} = 149.402\ mm$ $r_{A2} := \sqrt{x_1^{\,2} + y_1^{\,2}} = 60.415\ mm$

$$\tau_{M.A1} := \frac{M_A}{I_{P.A}} \cdot r_{A1} = 1.744\ MPa$$

$$\tau_{M.A2} := \frac{M_A}{I_{P.A}} \cdot r_{A2} = 0.705\ MPa$$

$$\tau := \frac{\tau_{M.A1} + \tau_{M.A2}}{2} = 1.225\ MPa$$ *Mean stress along rupture line*

$$\sigma_x \cdot \left(\frac{1}{f_{t.x}} - \frac{1}{f_{c.x}}\right) + \frac{\sigma_x^{\,2}}{f_{t.x} \cdot f_{c.x}} + \sigma_y \cdot \left(\frac{1}{f_{t.y}} + \frac{1}{f_{c.y}}\right) + \frac{\sigma_y^{\,2}}{f_{t.y} \cdot f_{c.y}} = 0.369$$
$$+ 2 \cdot \alpha_{x.y} \cdot \sqrt{\frac{1}{f_{t.x} \cdot f_{c.x} \cdot f_{t.y} \cdot f_{c.y}} \cdot \sigma_x \cdot \sigma_y + \frac{\tau^2}{f_v^{\,2}}}$$

A2-A3:

$$\sigma_x := \frac{T_{A2.A3}}{l_1 \cdot t_{plywood}} = 11.764\ \textit{MPa}$$

$$\sigma_y := \frac{N_{A2.A3}}{l_1 \cdot t_{plywood}} = 7.485\ \textit{MPa}$$

$$x_2 := 121\ \textit{mm} \qquad y_2 := -13\ \textit{mm}$$

$$r_{A3} := \sqrt{x_2^{\,2} + y_2^{\,2}} = 121.696\ \textit{mm}$$

$$\tau_{M.A3} := \frac{M_A}{I_{P.A}} \cdot r_{A3} = 1.421\ \textit{MPa}$$

$$\tau := \frac{\tau_{M.A3} + \tau_{M.A2}}{2} = 1.063\ \textit{MPa}$$

Mean stress along rupture line

$$\sigma_x \cdot \left(\frac{1}{f_{t.x}} - \frac{1}{f_{c.x}}\right) + \frac{\sigma_x^{\,2}}{f_{t.x} \cdot f_{c.x}} + \sigma_y \cdot \left(\frac{1}{f_{t.y}} + \frac{1}{f_{c.y}}\right) + \frac{\sigma_y^{\,2}}{f_{t.y} \cdot f_{c.y}} = 0.371$$
$$+ 2 \cdot \alpha_{x.y} \cdot \sqrt{\frac{1}{f_{t.x} \cdot f_{c.x} \cdot f_{t.y} \cdot f_{c.y}} \cdot \sigma_x \cdot \sigma_y + \frac{\tau^2}{f_v^{\,2}}}$$

Horizontal member tensile failure

Geometry:

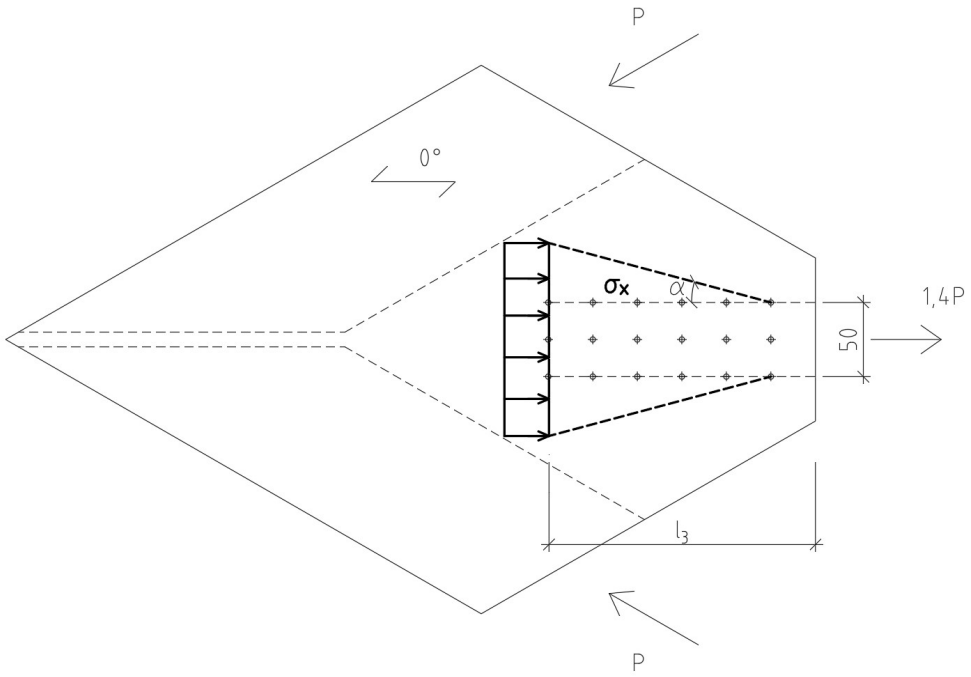

$Load1 := 55\ \boldsymbol{kN}$

$N_H := 1.41 \cdot Load1 = 77.55\ \boldsymbol{kN}$

Assume that the load spreads with an angle of 10-20 degrees from the first screw.

Effective height

$l_3 := 150\ \boldsymbol{mm}$

$h_3 := \tan(15\ \boldsymbol{deg}) \cdot l_3 = 40.192\ \boldsymbol{mm}$

$h_{eff} := 50\ \boldsymbol{mm} + h_3 \cdot 2 = 130.385\ \boldsymbol{mm}$

$f_{eff} := \frac{N_H}{h_{eff} \cdot t_{plywood}} = 66.086\ \boldsymbol{MPa}$ $\qquad \frac{f_{eff}}{f_{t.x}} = 1.057$

Removing the nail holes

$h_{netto} := h_{eff} - d_{nail} \cdot 3 = 112.025\ \boldsymbol{mm}$

$f_{netto} := \frac{N_H}{h_{netto} \cdot t_{plywood}} = 76.918\ \boldsymbol{MPa}$ $\qquad \frac{f_{netto}}{f_{t.x}} = 1.231$

Failure Modes - Glued connection

Horizontal member tensile failure, 0 degree face grain angle

$Load := 117\ kN$

$l_3 := 160\ mm$

l_3 varied between 160mm-180mm as these were the distances we saw during testing. Angle is varied between 10-20 degrees.

$N_H := 1.43 \cdot Load = 167.31\ kN$

$N_{eff} := \frac{l_3}{210\ mm} \cdot N_H = 127.474\ kN$

Multiplier for the normal forces is 1.41 for a perfect moment resisting connection and 1.73 for a joint.

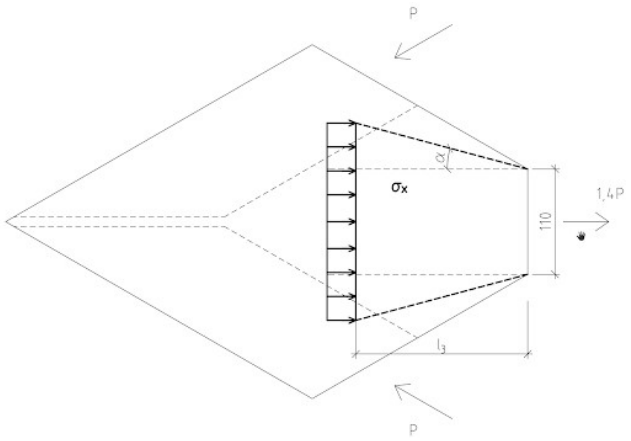

Effective height and stresses

$h_3 := \tan(20\ deg) \cdot l_3 = 58.235\ mm$

$h_{eff} := 110\ mm + h_3 \cdot 2 = 226.47\ mm$

$\sigma_x := \frac{N_{eff}}{h_{eff} \cdot t_{plywood}} = 62.542\ MPa$

$\sigma_y := \frac{0\ kN}{h_{eff} \cdot t_{plywood}} = 0\ MPa$

$\tau := 0\ MPa$

Tsai-Wu

$$\sigma_x \cdot \left(\frac{1}{f_{t.x}} - \frac{1}{f_{c.x}}\right) + \frac{{\sigma_x}^2}{f_{t.x} \cdot f_{c.x}} + \sigma_y \cdot \left(\frac{1}{f_{t.y}} + \frac{1}{f_{c.y}}\right) + \frac{{\sigma_y}^2}{f_{t.y} \cdot f_{c.y}} = 1.002$$
$$+ 2 \cdot \alpha_{x.y} \cdot \sqrt{\frac{1}{f_{t.x} \cdot f_{c.x} \cdot f_{t.y} \cdot f_{c.y}} \cdot \sigma_x \cdot \sigma_y + \frac{\tau^2}{{f_v}^2}}$$

Linear quadratic failure criterion

$$\left(\frac{\sigma_x}{f_{t.x}}\right)^2 + \left(\frac{\sigma_y}{f_{t.y}}\right)^2 + \left(\frac{\tau}{f_v}\right)^2 = 1.001$$

The linear quadratic failure criterion is not used but simply here for comparison

Horizontal member tensile failure, 5 degree face grain angle

$Load := 100\ \boldsymbol{kN}$

$l_3 := 180\ \boldsymbol{mm}$

$N_H := \frac{l_3}{210\ \boldsymbol{mm}} \cdot 1.43 \cdot Load = 122.571\ \boldsymbol{kN}$

$N_1 := N_H \cdot \cos(5\ \boldsymbol{deg}) = 122.105\ \boldsymbol{kN}$

$V_1 := N_H \cdot \sin(5\ \boldsymbol{deg}) = 10.683\ \boldsymbol{kN}$

Forces are here converted to components parallel and perpendicular to the plywood face-grain

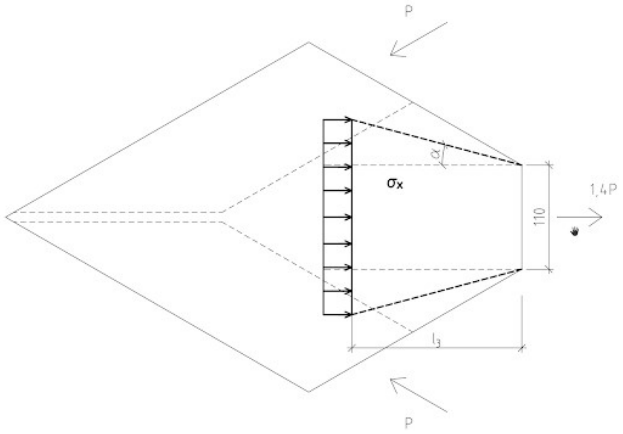

Effective height

$h_3 := \tan(20\ \boldsymbol{deg}) \cdot l_3 = 65.515\ \boldsymbol{mm}$

$h_{eff} := 110\ \boldsymbol{mm} + h_3 \cdot 2 = 241.029\ \boldsymbol{mm}$

$\sigma_x := \frac{N_1}{h_{eff} \cdot t_{plywood}} = 56.289\ \boldsymbol{MPa}$

$\sigma_y := \frac{V_1}{h_{eff} \cdot t_{plywood}} = 4.925\ \boldsymbol{MPa}$

$\tau := 0\ \boldsymbol{MPa}$

Tsai-Wu

$$\sigma_x \cdot \left(\frac{1}{f_{t.x}} - \frac{1}{f_{c.x}}\right) + \frac{{\sigma_x}^2}{f_{t.x} \cdot f_{c.x}} + \sigma_y \cdot \left(\frac{1}{f_{t.y}} + \frac{1}{f_{c.y}}\right) + \frac{{\sigma_y}^2}{f_{t.y} \cdot f_{c.y}} \hookleftarrow = 1.022$$
$$+ 2 \cdot \alpha_{x.y} \cdot \sqrt{\frac{1}{f_{t.x} \cdot f_{c.x} \cdot f_{t.y} \cdot f_{c.y}} \cdot \sigma_x \cdot \sigma_y + \frac{\tau^2}{{f_v}^2}}$$

Linear quadratic failure criterion

$$\left(\frac{\sigma_x}{f_{t.x}}\right)^2 + \left(\frac{\sigma_y}{f_{t.y}}\right)^2 + \left(\frac{\tau}{f_v}\right)^2 = 0.819$$

Horizontal member tensile failure, 5 degree face grain angle

$Load := 77\ kN$

$l_3 := 180\ mm$

$N_H := \frac{l_3}{210\ mm} \cdot 1.43 \cdot Load = 94.38\ kN$

$N_1 := N_H \cdot \cos(15\ deg) = 91.164\ kN$

$V_1 := N_H \cdot \sin(15\ deg) = 24.427\ kN$

Forces are here converted to components parallel and perpendicular to the plywood face-grain

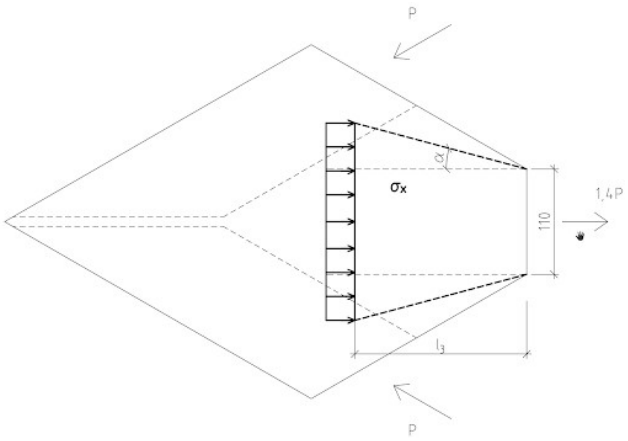

Effective height

$h_3 := \tan(20\ deg) \cdot l_3 = 65.515\ mm$

$h_{eff} := 110\ mm + h_3 \cdot 2 = 241.029\ mm$

$\sigma_x := \frac{N_1}{h_{eff} \cdot t_{plywood}} = 42.025\ MPa$

$\sigma_y := \frac{V_1}{h_{eff} \cdot t_{plywood}} = 11.261\ MPa$

$\tau := 0\ MPa$

Tsai-Wu

$$\sigma_x \cdot \left(\frac{1}{f_{t.x}} - \frac{1}{f_{c.x}}\right) + \frac{\sigma_x^{\,2}}{f_{t.x} \cdot f_{c.x}} + \sigma_y \cdot \left(\frac{1}{f_{t.y}} + \frac{1}{f_{c.y}}\right) + \frac{\sigma_y^{\,2}}{f_{t.y} \cdot f_{c.y}} \hookleftarrow = 0.982$$
$$+ 2 \cdot \alpha_{x.y} \cdot \sqrt{\frac{1}{f_{t.x} \cdot f_{c.x} \cdot f_{t.y} \cdot f_{c.y}} \cdot \sigma_x \cdot \sigma_y + \frac{\tau^2}{f_v^{\,2}}}$$

Linear quadratic failure criterion

$$\left(\frac{\sigma_x}{f_{t.x}}\right)^2 + \left(\frac{\sigma_y}{f_{t.y}}\right)^2 + \left(\frac{\tau}{f_v}\right)^2 = 0.492$$

8.4 Appendix D - Drawings

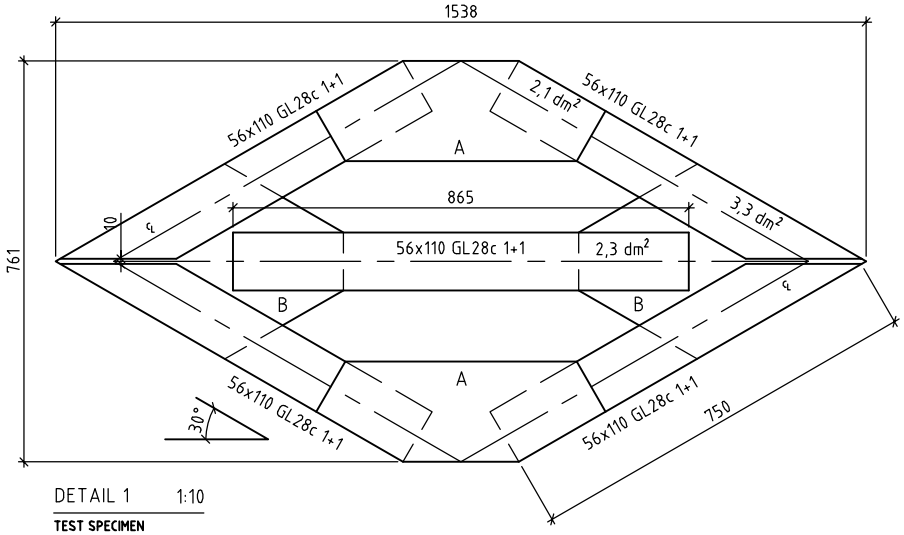

DETAIL 1 1:10

TEST SPECIMEN

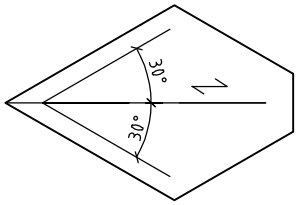

DETAIL 2 1:10

ANGLE TO GRAIN VARIANT 1
0 DEGREES - DOWEL TYPE CONNECTION
12 PCS (6 COMPRESSIVE 6 TENSILE)

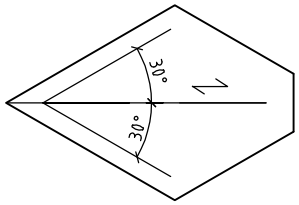

DETAIL 3 1:10

ANGLE TO GRAIN VARIANT 1
0 DEGREES
12 PCS (6 COMPRESSIVE 6 TENSILE)

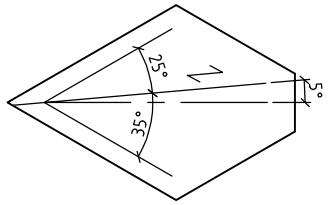

DETAIL 4 1:10

ANGLE TO GRAIN VARIANT 2
5 DEGREES
12 PCS (6 COMPRESSIVE 6 TENSILE)

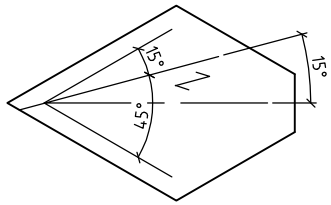

DETAIL 5 1:10

ANGLE TO GRAIN VARIANT 4
15 DEGREES
12 PCS (6 COMPRESSIVE 6 TENSILE)

There are three different types of angle to grain variants. The 0 degree variant will also be checked with dowels instead of screw-glueing. Each variant will be tested in both tension and compression, with 3 repetitions.

BOLD = TO BE MANUFACTURED

NUMBER OF SPECIMENS		1	3	6	18	24
HORISONTAL MEM.	56x110 GL28c	2	4	12	36	**48**
DIAGONAL MEM.	56x110 GL28c	8	24	48	144	**192**
PLATE A	BIRCH PLYWOOD	6	18	36	108	**144**
PLATE B	BIRCH PLYWOOD	2	6	12	36	**48**
GLUED AREA (m2)	DYNEA MUF	0,7	2,1	4,2	**12,6**	16,8
SMALL SCREWS	HBS 3,2x50	40	120	240	**720**	960
LARGE SCREWS	VGZ 5,6x140	20	40	120	**360**	480
DOWELS (NAILS)	BLANKSPIK 5,1x150	80	240	**480**		

REFERENCES

CONTROL GROUPS	K-20-2-1001
MATERIAL CUTTING PROPOSAL	K-20-2-1002
SCREWED CONNECTION	K-20-6-1001
DOWELED CONNECTION	K-20-6-1002

C		K-PM03	210406	PP
B	-	K-PM02	210308	PP
A	-	K-PM01	210224	PP
-	-	K-PM00	210217	PP
BET	ANT	ÄNDRINGEN AVSER	DATUM	SIGN

CONSTRUCTION DOC.

Master Thesis, KTH

	BH
	A
X	K ABE KTH
	V
	E
	L

UPPDRAG.NR	RITAD/KONSTR AV	HANDLÄGGARE
001	PP	PP
DATUM	ANSVARIG	
21-02-17	PH	

MSc BIRCH PLYWOOD CONNECTION
TEST SAMPLE
CONTROL GROUPS

SKALA	NUMMER	BET
1:10	K-20-2-1001	C

REF:

LAGER:

PLO:

PRODUCED BY AN AUTODESK STUDENT VERSION
PRODUCED BY AN AUTODESK STUDENT VERSION

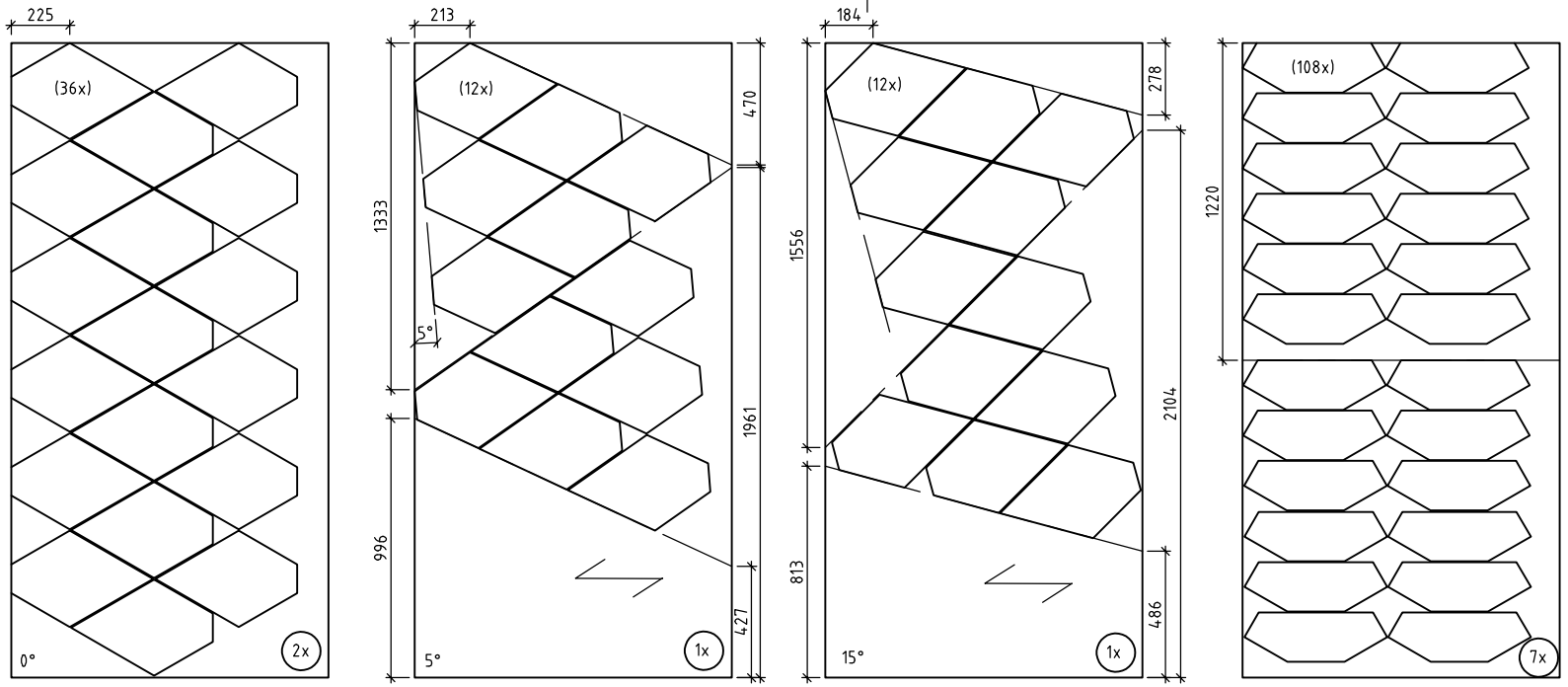

DETAIL 1 1:20

CUTTING PATTERN PROPOSAL
PLYWOOD BOARD 2440x1220
11 boards total

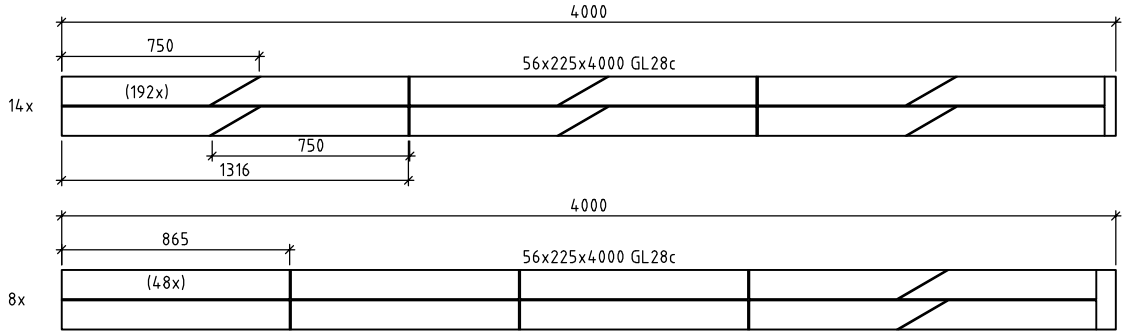

DETAIL 2 1:20

CUTTING PATTERN PROPOSAL
GLULAM BEAM 56x220 GL28c
TOTAL 22 PCS

To save material, the above cutting patterns are recommended for the glulam beams. First, cleave the beam at a width of 110mm. Then cut corresponding number of members according to attached table.

BOLD = TO BE MANUFACTURED

NUMBER OF SPECIMENS		1	3	6	18	24
HORISONTAL MEM.	56x110 GL28c	2	4	12	36	**48**
DIAGONAL MEM.	56x110 GL28c	8	24	48	144	**192**
PLATE A	BIRCH PLYWOOD	6	18	36	108	**144**
PLATE B	BIRCH PLYWOOD	2	6	12	36	**48**
GLUED AREA (m2)	DYNEA MUF	0,7	2,1	4,2	**12,6**	16,8
SMALL SCREWS	HBS 3,2x50	40	120	240	**720**	960
LARGE SCREWS	VGZ 5,6x140	20	40	120	**360**	480
DOWELS (NAILS)	BLANKSPIK 5,1x150	80	240	**480**	-	-

C		K-PM03	210406	PP
BET	ANT	ÄNDRINGEN AVSER	DATUM	SIGN

CONSTRUCTION DOC.

Master Thesis, KTH

BH
A
K
V
E
L

UPPDRAG.NR	RITAD/KONSTR AV	HANDLÄGGARE
001	PP	PP
DATUM	ANSVARIG	
21-02-17	PH	

MSc BIRCH PLYWOOD CONNECTION
TEST SAMPLE
MATERIAL CUTTING PROPOSAL

SKALA	NUMMER	BET
1:20	K-20-2-1002	C

REF:
LAGER:
PLO:

PRODUCED BY AN AUTODESK STUDENT VERSION
PRODUCED BY AN AUTODESK STUDENT VERSION
PRODUCED BY AN AUTODESK STUDENT VERSION

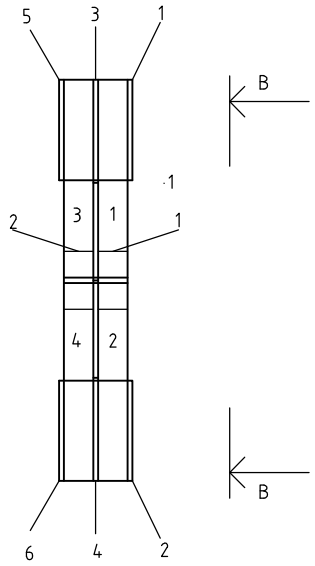

SECTION A-A 1:10

TEST SPECIMEN

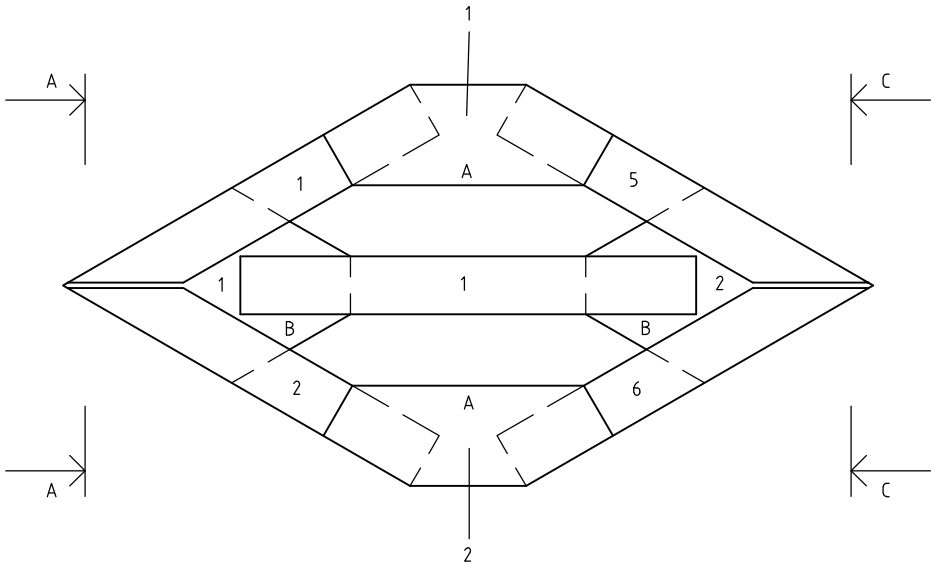

SECTION B-B 1:10

TEST SPECIMEN

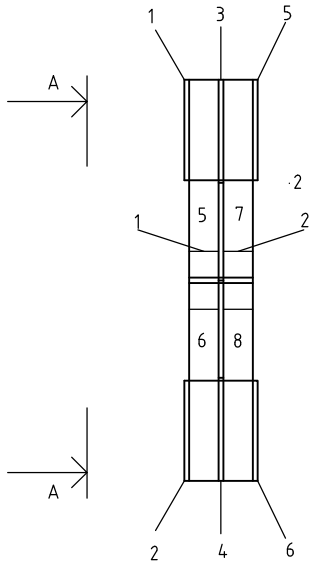

SECTION C-C 1:10

TEST SPECIMEN

BET	ANT	ÄNDRINGEN AVSER	DATUM	SIGN

CONSTRUCTION DOC.

Master Thesis, KTH

	BH
	A
X	K
	V
	E
	L

UPPDRAG.NR	RITAD/KONSTR AV	HANDLÄGGARE
001	PP	PP
DATUM	ANSVARIG	
21-04-15	PH	

MSc BIRCH PLYWOOD CONNECTION
TEST SAMPLE - SCREW GLUED
PART NUMBERING

SKALA	NUMMER	BET
1:10	K-20-2-1003	-

REF:

LAGER:

PL0:

PRODUCED BY AN AUTODESK STUDENT VERSION

PRODUCED BY AN AUTODESK STUDENT VERSION

PRODUCED BY AN AUTODESK STUDENT VERSION

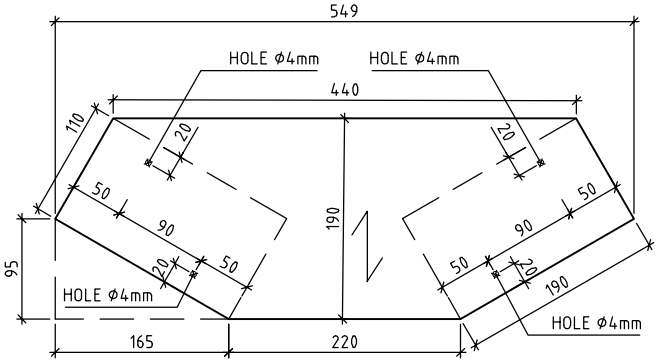

DETAIL 1 1:5

PLATE TYPE A
6 PCS PER SPECIMEN
108 total

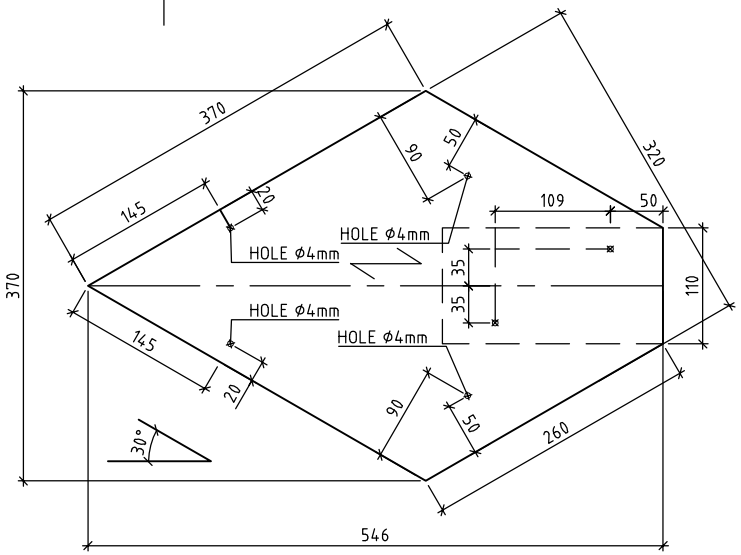

DETAIL 2 1:5

PLATE TYPE B
2 PCS PER SPECIMEN
36 total

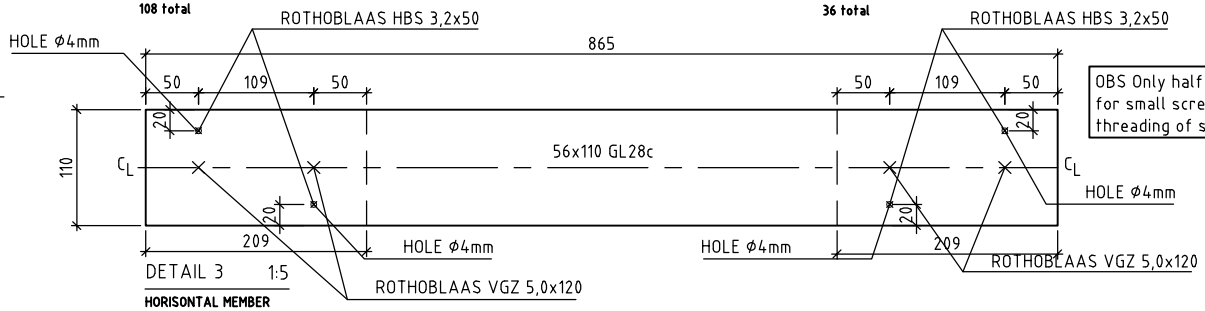

DETAIL 3 1:5

HORISONTAL MEMBER
2 PCS PER SPECIMEN
36 total

OBS Only half the amount of timber Members need predrilling for small screws, and only about 2cm into material. Otherwise threading of screw will not get traction.

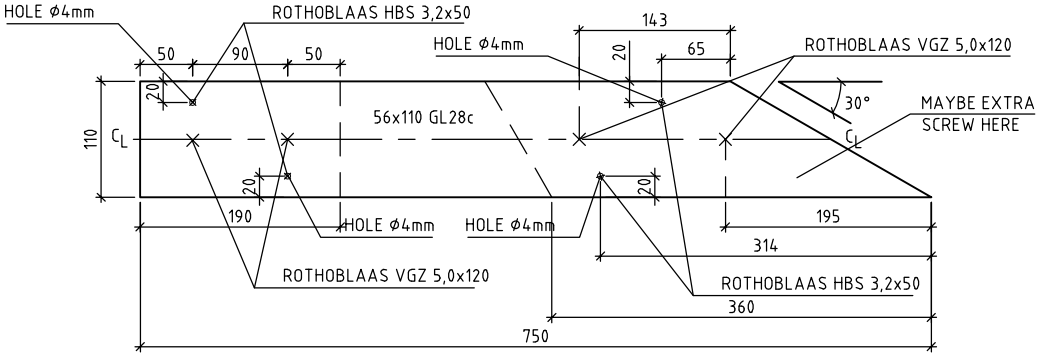

DETAIL 4 1:5

DIAGONAL MEMBER
8 PCS PER SPECIMEN
144 total

Proposed manufacturing procedure:

1. Cut corresponding parts from timber material
2. Predrill plywood and timber members according to K-20-6-1002 if doweled connection or K-20-6-1001 if screw-glued connection
   - 2.1. PS Only half the amount of timber Members need predrilling for small screws, and only about 2cm into material. Otherwise threading of screw will not get traction.
3. Roughen adjacent surfaces with sanding paper
4. Glue connecting surfaces
5. Clamp
6. Screw small screws through plywood into timber
7. Repeat steps 3-5
8. Screw small screws through timber onto plywood
9. Predrill for large screws with screwdriver
10. Screw large screws

REFERENCES

CONTROL GROUPS	K-20-2-1001
MATERIAL CUTTING PROPOSAL	K-20-2-1002
SCREWED CONNECTION	K-20-6-1001
DOWELED CONNECTION	K-20-6-1002

C		K-PM03	210406	PP
B	-	K-PM02	210308	PP
A	-	K-PM01	210224	PP
-	-	K-PM00	210217	PP
BET	ANT	ÄNDRINGEN AVSER	DATUM	SIGN

CONSTRUCTION DOC.

Master thesis, KTH

	BH
	A
X	K
	V
	E
	L

UPPDRAG.NR	RITAD/KONSTR AV	HANDLÄGGARE
001	PP	PP
DATUM	ANSVARIG	
21-02-17	PH	

MSc BIRCH PLYWOOD CONNECTION
TEST SAMPLE
SCREWED CONNECTION

SKALA	NUMMER	BET
1:5	K-20-6-1001	C

REF:
LAGER:
PLO:

PRODUCED BY AN AUTODESK STUDENT VERSION
PRODUCED BY AN AUTODESK STUDENT VERSION
PRODUCED BY AN AUTODESK STUDENT VERSION

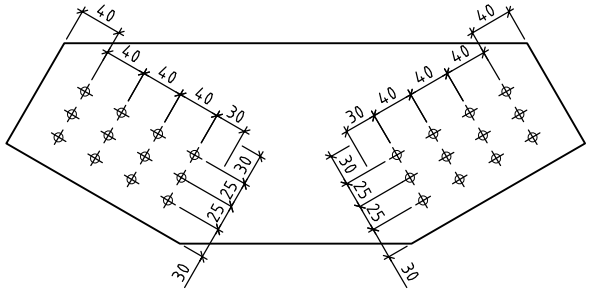

DETAIL 1 1:5

PLATE TYPE A
8 PCS PER SPECIMEN
48 total

A = 83600.12 mm2 = 8.360012 dm2
V = 8.360012 x 0.09 = 0,7524 dm3

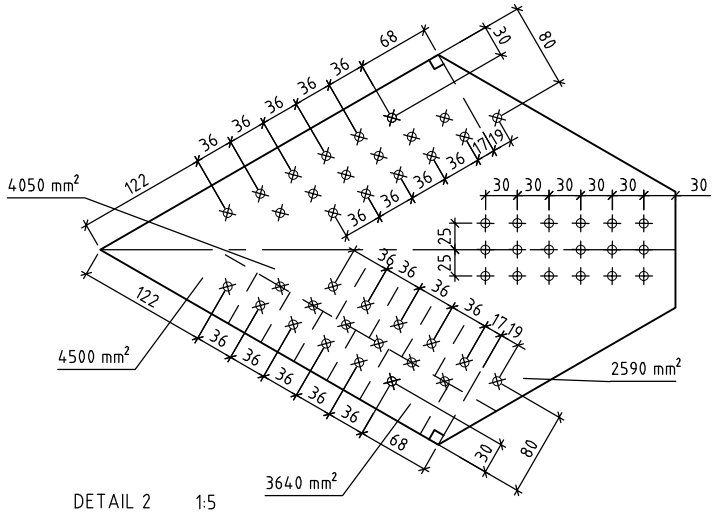

DETAIL 2 1:5

PLATE TYPE B
4 PCS PER SPECIMEN
24 total

A = 113319.42 mm2 = 11.331942 dm2
V = 11.331942 x 0.09 = 1,01987 dm3

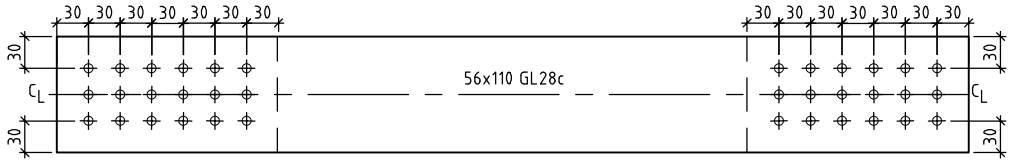

DETAIL 3 1:5

HORISONTAL MEMBER
2 PCS PER SPECIMEN
12 total

A = 95040.00 mm2 = 9.504 dm2
V = 7.210359 x 0.56 = 5,322 dm3

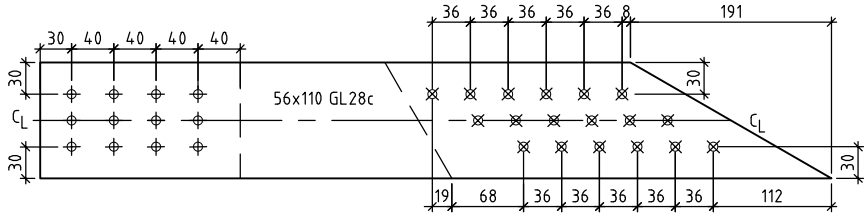

DETAIL 4 1:5

DIAGONAL MEMBER
8 PCS PER SPECIMEN
48 total

A = 72103.59 mm2 = 7.210359 dm2
V = 7.210359 x 0.56 = 4,038 dm3

All holes in this drawing are ⌀5,5mm

REFERENCES

CONTROL GROUPS	K-20-2-1001
MATERIAL CUTTING PROPOSAL	K-20-2-1002
SCREWED CONNECTION	K-20-6-1001
DOWELED CONNECTION	K-20-6-1002

C	-	K-PM03	210406	PP
B	-	K-PM02	210308	PP
A	-	K-PM01	210224	PP
-	-	K-PM00	210217	PP
BET	ANT	ÄNDRINGEN AVSER	DATUM	SIGN

CONSTRUCTION DOC.

Master thesis, KTH

	BH
	A
X	K
	V
	E
	L

UPPDRAG.NR	RITAD/KONSTR AV	HANDLÄGGARE
001	PP	PP
DATUM	ANSVARIG	
21-02-17	PH	

MSc BIRCH PLYWOOD CONNECTION
TEST SAMPLE
DOWELED CONNECTION

SKALA	NUMMER	BET
1:5	K-20-6-1002	C

REF:
LAGER:
PLO:

PRODUCED BY AN AUTODESK STUDENT VERSION
PRODUCED BY AN AUTODESK STUDENT VERSION
PRODUCED BY AN AUTODESK STUDENT VERSION

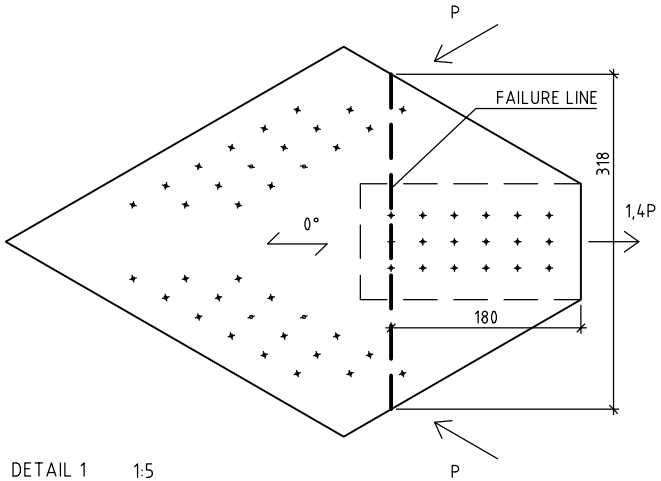

DETAIL 1 1:5

FAILURE MODE
COMPRESSIVE LOAD
DOWELED TYPE SPECIMEN
0 DEGREE ANGLE TO FACE-GRAIN

Holes were drilled with Ø6mm drill

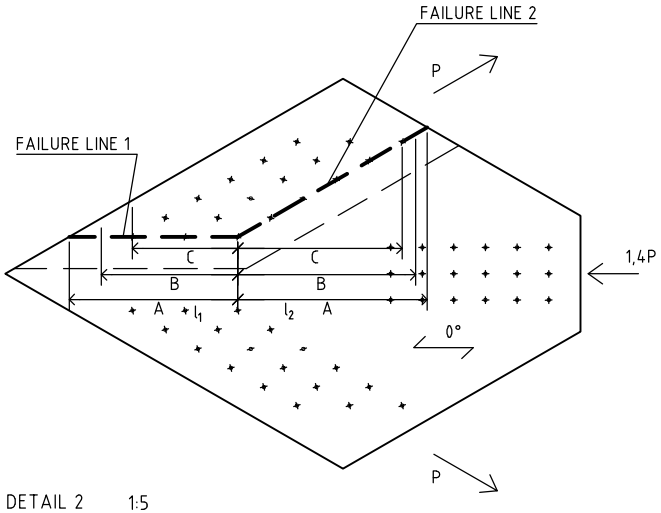

DETAIL 2 1:5

FAILURE MODE
TENSILE LOAD
DOWELED TYPE SPECIMEN
0 DEGREE ANGLE TO FACE-GRAIN

Holes were drilled with Ø6mm drill

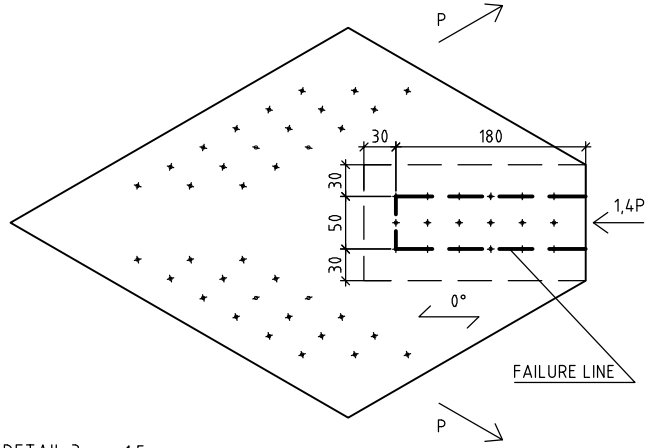

DETAIL 3 1:5

FAILURE MODE
TENSILE LOAD
DOWELED TYPE SPECIMEN
0 DEGREE ANGLE TO FACE-GRAIN

Holes were drilled with Ø6mm drill

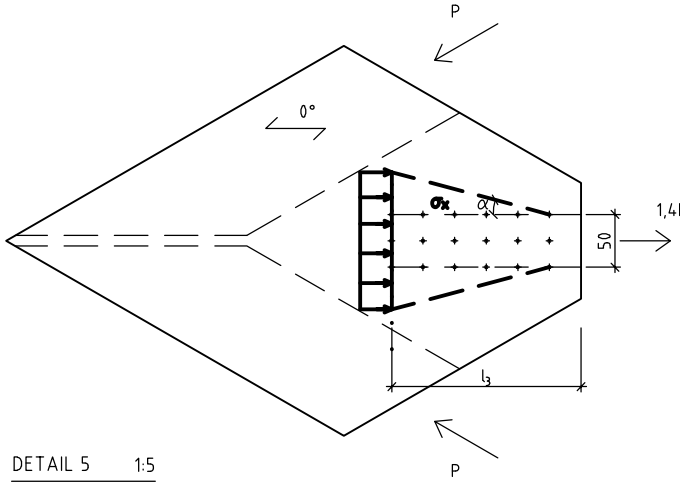

DETAIL 5 1:5

FAILURE MODE
COMPRESSIVE LOAD
DOWELLED TYPE SPECIMEN
0 DEGREE ANGLE TO FACE-GRAIN

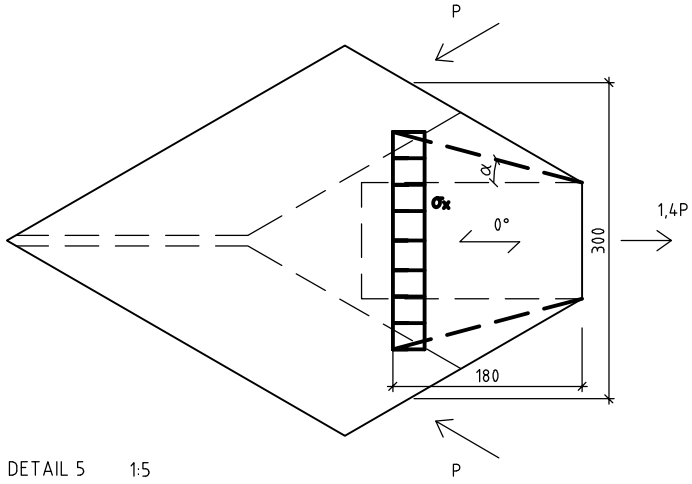

DETAIL 5 1:5

FAILURE MODE
COMPRESSIVE LOAD
GLUED TYPE SPECIMEN
0 DEGREE ANGLE TO FACE-GRAIN

-	-	K-PM04	210520	PP
BET	ANT	ÄNDRINGEN AVSER	DATUM	SIGN

CONSTRUCTION DOC.

Master thesis, KTH

	BH
	A
X	K
	V
	E
	L

UPPDRAG.NR	RITAD/KONSTR AV	HANDLÄGGARE
001	PP	PP
DATUM	ANSVARIG	
21-05-20	PH	

MSc BIRCH PLYWOOD CONNECTION
TEST SAMPLE
FAILURE MODES

SKALA	NUMMER	BET
1:5	K-20-6-1003	-

REF:

LAGER:

PL0:

PRODUCED BY AN AUTODESK STUDENT VERSION

PRODUCED BY AN AUTODESK STUDENT VERSION

PRODUCED BY AN AUTODESK STUDENT VERSION